Fachhochschule Aachen, Campus Jülich
Fachbereich 3 Chemie und Biotechnologie
Studiengang: Biotechnologie

FH AACHEN
UNIVERSITY OF APPLIED SCIENCES

Masterarbeit

Characterization of Chlorellales cell walls – Spatio-temporal refined biochemical and morphological characterization of *Chlorella sorokiniana* and *vulgaris,* and *Parachlorella kessleri*

vorgelegt von:

Stefan Robertz

3075178

Jülich, August 2021

Diese Arbeit ist von mir selbstständig angefertigt und verfasst. Es sind keine anderen als die angegebenen Quellen und Hilfsmittel benutzt worden.

_____

(Stefan Robertz)

Diese Arbeit wurde betreut von:

1. Prüferin: Prof. Dr. Ingar Janzik

2. Prüferin: Dr. Diana Reinecke-Levi

Danksagung

Ich möchte all denen danken, die mich bei diesem Masterprojekt unterstützt haben. Im Besonderen möchte ich Dr. Holger Klose für die Möglichkeit danken, dieses Projekt in der Alternative Biomasse Gruppe des IBG-2 am Forschungszentrum Jülich durchführen zu können. Außerdem möchte ich Dr. Diana Reinecke-Levi für die hervorragende Betreuung und für die Übernahme der Zweitkorrektur, sowie Prof. Dr. Ingar Janzik für die Übernahme der Erstkorrektur, danken.

Darüber hinaus möchte ich mich bei Sophie Weber für die interessanten und anregenden Diskussionen und die Hilfe bei technischen Fragen danken. Mein Dank gilt der gesamten Alternative Biomasse Gruppe für die Unterstützung und die angenehme Atmosphäre während meiner Masterarbeit. Außerdem bedanke ich mich ausdrücklich bei Prof. Dr. Gerhard Dikta für seine Expertise bei statistischen Fragen und seine Hilfsbereitschaft bei der statistischen Auswertung.

Abstract

Microalgae of the family *Chlorellaceae* are of special interest to the food, feed, and nutraceutical industry, due to their high content of valuable nutrients. However, the bioaccessibility is limited by the rigid and polymorph cell wall of these species. This work aimed to characterize the cell walls of three *Chlorellaceae* strains *in-vivo* and *in-vitro* under industry-related culturing conditions. Histochemical staining and detailed analyses of cell wall monosaccharide composition identified changes in the composition during cell maturation in *Chlorella sorokiniana* SAG 211-8k, *Chlorella vulgaris* SAG 211-11b and *Parachlorella kessleri* SAG 211-11g. The cell walls of *C. sorokiniana* and *P. kessleri* developed a higher hemicellulose content (defined as susceptible to 2 mol/L trifluoroacetic acid hydrolysis) with stable amounts of the recalcitrance components (susceptible to 6 mol/L HCl). In contrast, the cell wall of *C. vulgaris* incorporated increasingly recalcitrance components and developed higher robustness.

Additionally, a novel endogenous cell-wall-lytic enzyme (autologous Autolysin) was extracted from *C. sorokiniana* and *P. kessleri*. It showed endo-β-1,3-Glucanase activity, and partial autologous cell wall degradation in both strains. Thus, presenting a first step towards more effective methods for increased bioaccessibility, protoplast formation and genetic manipulation of *Chlorellaceae* strains.

Kurzfassung

Mikroalgen der *Chlorellaceae* sind aufgrund ihres hohen Gehalts an wertvollen Nährstoffen von besonderem Interesse für die Lebensmittel-, Futtermittel- und Nahrungsergänzungsmittelindustrie. Die Bioverfügbarkeit wird jedoch durch die starre und polymorphe Zellwand der Algen eingeschränkt. Ziel dieser Arbeit war es, die Zellwände von drei *Chlorellaceae*-Stämmen *in-vivo* und *in-vitro* unter industrienahen Kultivierungsbedingungen zu analysieren. Durch histochemische Färbungen und detaillierte Analysen der Monosaccharid Zusammensetzung wurden Veränderungen in der Zellwandzusammensetzung während der Reifung von *Chlorella sorokiniana* SAG 211-8k, *Chlorella vulgaris* SAG 211-11b und *Parachlorella kessleri* SAG 211-11g festgestellt. Die Zellwände von *C. sorokiniana* und *P. kessleri* entwickelten während der Reifung einen höheren Gehalt an Hemizellulose (definiert als hydrolysierbar durch 2 mol/L Trifluoressigsäure) mit konstanten Mengen an starrer Zellwandfraktion (anfällig für 6 mol/L HCl). Im Gegensatz enthielt die Zellwand von *C. vulgaris* zunehmend resistentere Komponenten und entwickelte eine höhere Robustheit.

Zusätzlich wurde ein neuartiges, endogenes, zellwanddegradierendes Enzym (autologes Autolysin) aus *C. sorokiniana* und *P. kessleri* extrahiert. Es zeigte endo-β-1,3-Glucanase-Aktivität und einen teilweisen autologen Zellwandabbau in beiden Stämmen. Damit wurde ein erster Schritt in Richtung effektiverer Methoden zur Verbesserung der Biozugänglichkeit, Protoplastenbildung und genetischen Manipulation von *Chlorellaceae*-Stämmen getan.

Contents

Abbreviations

AB	*Astra Blue*
AIR	*Alcohol insoluble residues*
Ara	*Arabinose*
CFW	*Calcofluor White*
dAIR	*De-starched alcohol insoluble residues*
dest. H2O	*Distilled water*
EB	*Evans Blue*
Fuc	*Fucose*
Gal	*Galactose*
GalA	*Galacturonic acid*
Glc	*Glucose*
GlcA	*Glucuronic acid*
GlcN	*Glucosamine*
HCl	*Hydrochloric acid*
HPAEC-PAD	*High-performance anion exchange chromatography with pulsed amperometric detection*
Man	*Mannose*
Rha	*Rhamnose*
RR	*Ruthenium Red*
RT	*Room temperature (21 °C)*
S	*Safranin*
TFA	*Trifluoroacetic acid*
TLS	*Trilaminar layer*
UP-H2O	*Ultrapure water*
Xyl	*Xylose*

1 Introduction

Microalgae are a promising feedstock for value-added products. They grow in various environments, exhibit rapid growth rates and do not compete with food crops for arable land (Daroch, Geng and Wang, 2013; Alhattab, Kermanshahi-Pour and Brooks, 2019). Especially, species from the genus *Chlorella* exhibit a large economic potential (Safi *et al.*, 2014). The green microalga *Chlorella vulgaris* was first discovered and described by M. W. Beijerinck, in 1890 (Safi *et al.*, 2014). Since then, hundreds of different strains were identified, described, and classified as *Chlorella sp.*, based on similarities in their appearance (Baudelet *et al.*, 2017). In 2017, the genus *Chlorella* contained forty-two taxonomical accepted species (Baudelet *et al.*, 2017). Currently, 31 species are accepted based on the comprehensive, yet unfinished, phylogenetic revision (Guiry and Guiry, 2021).

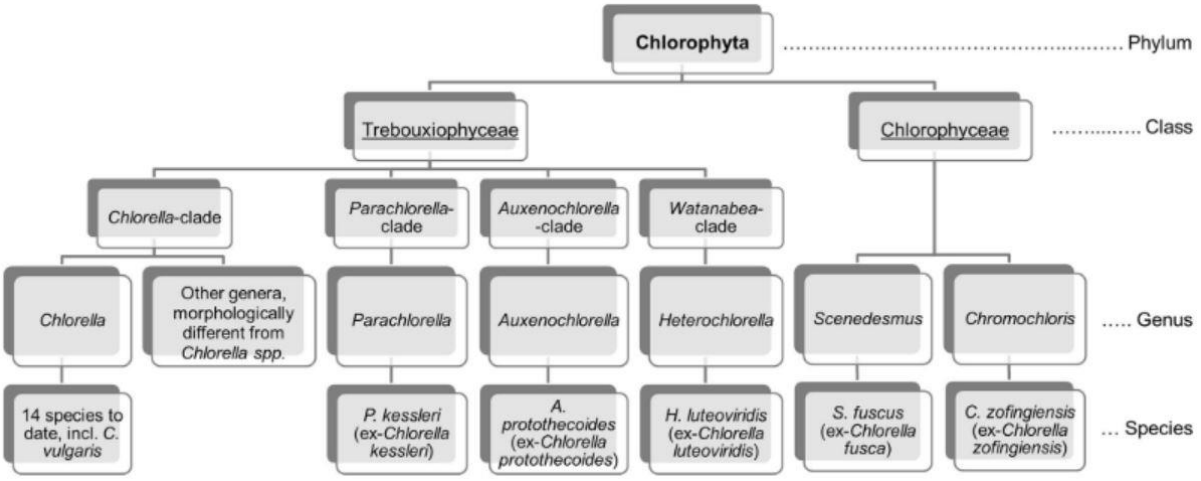

Figure 1: Taxonomic tree of the polyphyletic Chlorella group showing the independent two sister classes of Trebouxiophyceae and Chlorophyceae with their major genera, such as Chlorella and Parachlorella. (Champenois, Marfaing and Pierre, 2014).

Introduced by Otto Warburg in 1919, *Chlorella* became an important species in photosynthesis research, due to easy cultivation, easy handling, and the lack of gas diffusion by stomata opening (Bachmann, 1921; Huzisige and Ke, 1993; Nickelsen, 2007). Since the 1940s, *Chlorella* strains have been

intensively studied as a feedstock for the bioeconomy and biofuel production due to their high cellular lipid contents, growth rates and biomass yield, as well as simple cultivation (Gerken, Donohoe and Knoshaug, 2013; Safi *et al.*, 2014). To achieve economic efficiency, compared to other plant alternatives, such as maize or canola, more research is needed. Especially, to lower the costs and product-degradation of the cell wall disruption (Gerken, Donohoe and Knoshaug, 2013).

The main market of *Chlorella* biomass and its products is the food and nutraceutical sector, with a global biomass production of 6600 t dry weight per year (Muys *et al.*, 2019). The biomass is dried and sold as powder, tablets or capsules (Görs *et al.*, 2010). Several benefits are attributed to *Chlorella*, due to its richness in cellular proteins, vitamins, polysaccharides, polyunsaturated fatty acids and microelements (Görs *et al.*, 2010). Another application is the use of *Chlorella* in wastewater treatment, for its remarkable high carbon dioxide, nitrogen and phosphorus fixation rates (Safi *et al.*, 2014). This minimizes the need of fresh water during cultivation and increases the quality of the wastewater (Safi *et al.*, 2014).

However, after a century of research, the rigidity and complexity of the *Chlorella* cell wall remains a major obstacle (Gerken, Donohoe and Knoshaug, 2013; Safi *et al.*, 2013, 2014; Baudelet *et al.*, 2017; Echeverri *et al.*, 2019; Zuorro *et al.*, 2019). On the one hand, the rigid cell wall prevents a reliable and economical cell disruption. On the other hand, it hinders effective gene editing of *Chlorella sp*. (Gerken, Donohoe and Knoshaug, 2013).

1.1 Cell wall

The cell walls of green algae (Chlorophyta) are largely constituted of various polysaccharides, smaller amounts of lipids and proteins, and an inorganic fraction (Figure 2) (Canelli, Murciano Martínez, Austin, *et al.*, 2021). The polysaccharides and their monosaccharide composition have been studied for many decades with thousands of publications. Atkinson and co-workers

worked on the protoplast formation of *Chlorella* species by applying various enzymatic mixtures (Atkinson, Gunning and John, 1972). Due to the inability to obtain protoplasts from some of their species, they analyzed the cell walls and identified a polysaccharide similar to sporopollenin, now known as algaenan (Atkinson, Gunning and John, 1972; Gerken, Donohoe and Knoshaug, 2013). A highly resistant heteropolymer, first described in pollen grains of herbaceous plants and other spores (Shaw, 1971). Conte and Pore on the other hand analyzed the cell walls of different green algal species for the purpose of comparison and taxonomical classification (Conte and Pore, 1973).

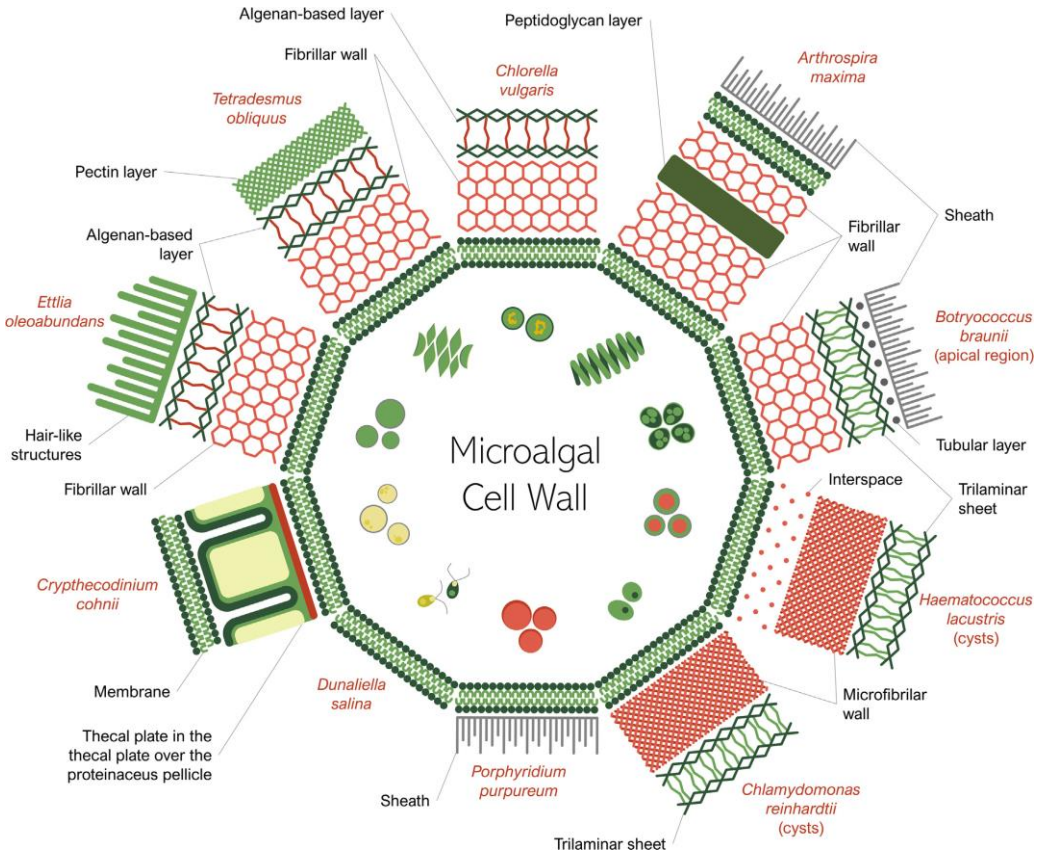

Figure 2: Cell wall structure of 10 important microalgae illustrating the main components and the diversity of structure. Layers are not to scale – the cell wall is 10 to 100 times thicker than the cell membrane; (de Carvalho *et al.*, 2020).

In 1981, Yamada and Sakaguchi described for the induction of protoplasts the cell walls of twelve different species of *Chlorella* species. They found three different types of structures among the species: Type 1 cell walls are composed of two layers, an inner electron-transparent layer and an outer trilaminar layer (TLS). Type 2 cell walls consist of two layers as well, but the outer layer is not a TLS, and type 3 walls are only one microfibrillar layer (Yamada and Sakaguchi, 1981, 1982). Blumreisinger and co-workers described two major groups of neutral cell wall sugars for chlorococcal algae (Chlorococcales, Chlorophyta), the rhamnose/galactose (Rha/Gal) and the mannose/glucose (Man/Glc) groups, respectively (Blumreisinger, Meindl and Loos, 1983).

When comparing the results of the different authors, several things have to be considered. Firstly, *Chlorellaceae* strains have been reassigned to other phylogenetic groups. For example, the former strain *Chlorella vulgaris* 15-2075 shows more homologies to *Parachlorella kessleri* than to *Chlorella vulgaris* (Conte and Pore, 1973; Müller *et al.*, 2005). Secondly, the physiology, morphology and composition of *Chlorella* cells and their cell walls change under the different culture conditions and throughout their life cycle (Liang, Sarkany and Cui, 2009; Safi *et al.*, 2014). For instance, Atkinson cultured its strains synchronous and non-synchronous in 2.5 L systems, at 25 °C with a 15 : 9 h light:dark regimen (Atkinson, Gunning and John, 1972; McCullough and John, 1972). Whereas, Conte and Pore cultivated their strains in 1 L flasks, at 30 °C in the dark (Conte and Pore, 1973). Further, Yamada and Sakaguchi cultivated in flasks on a reciprocal shaker with 16 : 8 h light:dark regimen (Yamada and Sakaguchi, 1982). And Blumreisinger cultured its strains in 1 L tubes (6.5 cm diameter), at 28 °C, with constant aeration of 2 % CO_2/air-mixture and 24 h light phase (Loos and Meindl, 1982; Blumreisinger, Meindl and Loos, 1983). Thirdly, the applied cell wall analysis methods differed between the authors. Atkinson used acetolysis and electron microscopy to identify different cell wall components (Atkinson, Gunning and John, 1972). Conte and Pore isolated four different fractions after stepwise degradation of the cell walls with 2 mol/L NaOH and 0.5 mol/L sulfuric acid (Conte and Pore,

1973). Further, Yamada and Sakaguchi used histochemistry and electron microscopy to identify different cell wall parts (Yamada and Sakaguchi, 1982) and Blumreisinger and co-workers used Seaman-hydrolysis followed by 6 mol/L HCl hydrolysis to fractionate the cell wall monosaccharides (Blumreisinger, Meindl and Loos, 1983).

Despite the difficulties of comparing these findings by the various authors, some general aspects of the *Chlorellaceae* cell walls were found by all authors and remained consistent until today. The following two paragraphs will summarize the existing literature for the three *Chlorellaceae* species studied in this work.

1.1.1 *Chlorella vulgaris* and *Chlorella sorokiniana*

According to the results of Yamada and Sakaguchi, the cell walls of both species *Chlorella vulgaris* and *Chlorella sorokiniana* are of type 3 (microfibrillar single layered) (Yamada and Sakaguchi, 1982). In *C. vulgaris* this single layer was identified as a single layered cell wall at the beginning of the growth phase, with an average thickness of 17 – 20 nm. Shortly after release, it developed into the three layered structure of i) a thick outer layer (coenobial cell wall), ii) thin inner layer (daughter cell wall) and iii) electron translucent interspace (Němcová and Kalina, 2000; Yamamoto *et al.*, 2004; Baudelet *et al.*, 2017).

The de-novo cell wall synthesis begins on the outer surface of the plasma membrane (Figure 3a/b).

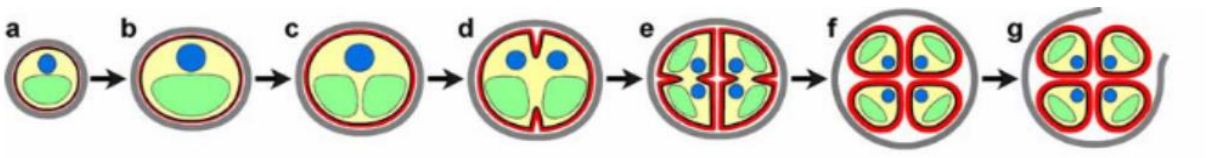

Figure 3: Schematic representation of the early autospore cell wall synthesis of Chlorellaceae. (Yamamoto, Kurihara and Kawano, 2005).

During protoplast division, the newly formed cell wall expands by invagination and increases in thickness to form autospore cell walls (Figure 3c-f). During release (Figure 3g), the coenobial wall bursts and releases 2 – 4 autospores with readily formed cell walls (Yamamoto *et al.*, 2004). This type of cell wall synthesis was named "Early Synthesis Type" and was described in *C. vulgaris* and *sorokiniana* (Yamamoto, Kurihara and Kawano, 2005).

Moreover, it is generally accepted that the cell walls of *Chlorellaceae* contain two distinct fractions, a hemicellulose or alkali-soluble fraction and a recalcitrance part, respectively (Figure 2) (Baudelet *et al.*, 2017; de Carvalho *et al.*, 2020). The first is susceptible to hydrolysis with trifluoracetic acid or sulfuric acid (Loos and Meindl, 1982; Blumreisinger, Meindl and Loos, 1983). The latter is susceptible to 6 mol/L hydrochloric acid (Takeda, 1988b). Based on this fractionation, Takeda studied the monosaccharide composition of both cell wall fractions in various algal species, such as *C. vulgaris* SAG 211-11b and *C. sorokiniana* SAG 211-8k (Takeda, 1988b, 1988a, 1991).

According to his findings, the hemicellulose fraction of *C. vulgaris* 211-11b consists of Glc (45 %), Rha (20 %), Gal (10%), xylose (Xyl, 10 %), and minor parts of Man and arabinose (Ara). The rigid cell wall fraction contained mainly glucosamine (Takeda, 1991). In contrast, *C. sorokiniana* 211-8k showed a different hemicellulose fraction. Its main sugars were Gal and Rha (30 % each), an unknown component (13 %), and smaller amounts of Xyl (10 %), Man (10%), Ara (5 %) and Glc (2 %) (Takeda, 1988a). To my best knowledge, the monosaccharide composition of those strains, or the duplicates in other collections, has not been confirmed or disputed by any other author.

1.1.2 *Parachlorella kessleri*

In 2004, the genus *Parachlorella* was introduced, based on the comparison of the phylogenetic data of various *Chlorella* species (Figure 1) (Krienitz *et al.*, 2004). As a consequence, some strains previously known as *Chlorella* were reassigned to the genus *Parachlorella* (Baudelet *et al.*, 2017) or other taxonomic groups. For example, the cell wall of *C. vulgaris* C-209 is type 1 (two layers, with TLS), *C. vulgaris* C-208 type 2 (two layers, no TLS), and *C. vulgaris* C-150 type 3 (one layer) (Yamada and Sakaguchi, 1982). Today, all of these strains are grouped under the genus *Parachlorella* and the species *kessleri* (Baudelet *et al.*, 2017).

In other publications, the cell wall of *P. kessleri* were described as a single electron transparent layer with no outer layer (Němcová and Kalina, 2000; Yamamoto, Kurihara and Kawano, 2005). These differences might be caused by the analysis of different species, cell-cycle stages or analytical error (Baudelet *et al.*, 2017).

In 2005, Yamamoto and co-workers compared the cell walls and the autospore synthesis of *P. kessleri* IAM C-531 (similar to: SAG 211-11h/20) to those of *Chlorella* (Figure 3). The cell wall of *P. kessleri* appeared as a single, electron-transparent layer, with an average thickness of 54 – 59 nm (Yamamoto, Kurihara and Kawano, 2005). However, the cell wall was less defined than in *Chlorella* species (Yamamoto, Kurihara and Kawano, 2005; Baudelet *et al.*, 2017). The synthesis of daughter cell walls begins late during the maturation of the autospores (Figure 4g/h). In the growth phase (Figure 4a/b) and during chloroplast division phase (Figure 4c-f), the daughter cell walls were not visible (Yamamoto, Kurihara and Kawano, 2005). This implies that only the plasma membrane detaches from the cell wall (Figure 4d) and surrounds the newly formed autospores (Figure 4e/f) (Yamamoto, Kurihara and Kawano, 2005).

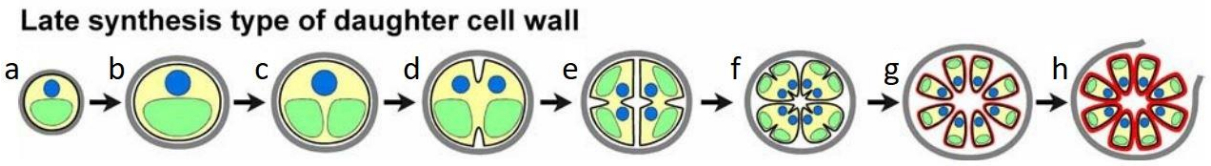

Figure 4: Schematic representation of the late autospore cell wall synthesis of Chlorellaceae. (Yamamoto, Kurihara and Kawano, 2005).

The monosaccharide composition of *P. kessleri* SAG 211-11g (Fott et Nováková), former *Chlorella kessleri*, cell walls was investigated by Takeda (Fott and Nováková, 1969; Takeda, 1991). The hemicellulose fraction held mainly Gal (40 %) and Rha (30 %) and Man, Xyl, Ara and Glc (7 % each), and fucose (Fuc, 2 %). The main component of the rigid cell wall fraction was glucosamine (Takeda, 1991). To my knowledge, this monosaccharide composition was not confirmed nor disputed by other authors.

1.2 Enzymatic cell wall degradation

The utilization of *Chlorella* is often limited by its recalcitrance cell wall, which contains glucosamine (Honjoh *et al.*, 2003; Gerken, Donohoe and Knoshaug, 2013; Burczyk *et al.*, 2014; Echeverri *et al.*, 2019). One promising approach, to overcome this hurdle is the enzymatic degradation. The following paragraph will summarize the existing literature to enzymatic cell wall degradation in *Chlorellaceae*.

Various approaches were taken to remove the cell wall by enzymes to increase the lipid yield for biofuel production. In 2013, Gerken and co-workers analyzed the effects of single and combined enzymes on the growth and cell wall development of different *Chlorella* species (Gerken, Donohoe and Knoshaug, 2013). No single enzyme effected the growth, yet a combination of chitinase, lysozyme and pectinase had the broadest effect on the growth among all strains. Additionally, chitosanase, β-glucuronidase, laminarinase, sulfatase, and trypsin showed a broad effect as well (Gerken, Donohoe and Knoshaug, 2013).

In *Chlorella vulgaris* a combination of cellulase and β-glucosidase weakened the cell wall and increased the lipid extraction yield (Cho *et al.*, 2013). A combination of exo-glucosaminidase, alginate lyase, lysozyme, and peptidoglycan N-acetylmuramic acid deacetylase effectively degraded the cell wall (Coelho *et al.*, 2019). Likewise, chitinase, rhamnohydrolase, and galactanase degraded the cell walls (Canelli, Murciano Martínez, Maude Hauser, *et al.*, 2021).

Additionally, the enzymatic degradation of the cell wall can be a tool for protoplast formation and gene editing towards strain improvement. The term "protoplast" refers to a plant and algal cell (or bacterial, fungal), without its cell wall. This can be achieved either mechanically, enzymatically or by gene editing (Echeverri *et al.*, 2019). Many attempts were made to obtain protoplasts in various *Chlorella* species (Atkinson, Gunning and John, 1972; Aach, Bartsch and Feyen, 1978; Yamada and Sakaguchi, 1981, 1982; Hatano *et al.*, 1992; Honjoh *et al.*, 2003). Only few attempts were successful in specific strains (Yamada and Sakaguchi, 1981, 1982; Hatano *et al.*, 1992; Honjoh *et al.*, 2003). In two out of twelve algaenan-negative *Chlorella* strains were protoplasts yielded after combined cellulase, macerozyme and pectinase treatment (Yamada and Sakaguchi, 1981). In *Chlorella ellipsoidea* IAM C-27 (now: *Chlorella vulgaris* Beijerinck NIES-2170) a combination of chitosanase, glycosidase and lytic enzymes containing cell-homogenate yielded protoplasts (Hatano *et al.*, 1992). In *Chlorella vulgaris* K-73122 a mix of acromopeptidase, cellulase, chitosanase, gluczyme and Uskizyme® (1,3-β-glucanase and chitinase) obtained osmotically labile cells (Honjoh *et al.*, 2003).

All the above-mentioned publications are based on commercially available enzymes in pure and admixtures. To improve the efficiency and reduce the amount of necessary different enzymes, a detailed knowledge of the cell wall under the specific cultivation conditions is mandatory (Baudelet *et al.*, 2017).

1.3 Endogenous cell-wall-lytic enzymes

The application of endogenous cell-wall-lytic enzymes can provide more insights into the cell wall composition and aid the protoplast generation. They were first described in *Chlamydomonas reinhardtii* (Schlösser, 1966; Claes, 1971; Schlösser, Sachs and Robinson, 1976; Jaenicke and Waffenschmidt, 1981), *Volvox* (Jaenicke and Waffenschmidt, 1979, 1981; Schlösser, 1981) and *Chlorella fusca* (Loos and Meindl, 1984, 1985).

In 1966, Schlösser described a lytic "factor" in the culture medium of synchronized *Chlamydomonas reinhardtii*. It was capable of degrading cell walls at specific life cycle stages (Schlösser, 1966). He postulated an enzymatic nature of this "factor", which was later supported by the results of Claes, indicating the presence of one or more enzymes involved in cell wall lysis (Schlösser, 1966; Claes, 1971). In 1981, Jaenicke and Waffenschmidt identified a lytic enzyme as serine-hydrolase, with a molecular weight of 34 kDa, comparable to the previously isolated lytic enzyme of *Volvox sp.* (Jaenicke and Waffenschmidt, 1979, 1981). Additionally, Matsuda an co-workers described a 130 kDa endogenous protease, capable of degrading sporangial cell walls of *Chlamydomonas* (Matsuda *et al.*, 1995). In 2006, molecular analysis of such enzymes in *Volvox* identified a 125 kDa subtilisin-like serine protease (Fukada, Inoue and Shiraishi, 2006), which is also true for *Chlamydomonas* (Kubo *et al.*, 2009).

Loos and Meindl identified a cell-wall degrading enzyme in *Chlorella fusca* (now: *Scenedesmus vacuolatus* SAG 211-8b) (Loos and Meindl, 1984, 1985). According to their results, the enzyme was active during autospore release (degradation of coenobial cell walls) and the activity is closely related to an endo-mannanase (Loos and Meindl, 1985). Araki and Takeda initially isolated lytic enzymes from the cell wall and the culture medium of *Chlorella elipsoidea* (now: *Pseudochlorella pringsheimii* (Darienko *et al.*, 2010)) (Araki and Takeda, 1992a). Later, isolates of twelve other *Chlorella* strains showed different lytic activities and physiological properties. Among these strains was *Chlorella sorokiniana* SAG 211-8k. Its lytic enzymes

produced oligosaccharides, when degrading the cell wall, and showed an activity-optimum at pH 6 – 8 (Araki and Takeda, 1992b).

1.4 Objectives

Although, the *Chlorellaceae* play an important role in microalgal industry and research, knowledge to their exact cell wall composition remains limited. Therefore, the cell wall composition of three species of this family, *Chlorella sorokiniana*, *Chlorella vulgaris* and *Parachlorella kessleri* were investigated in detail in this work. The algae were synchronously cultivated at diurnal light in glass tubes, with constant bubbling of ambient air, at room temperature. The cultivation conditions were chosen to mimic the industrial cultivation systems. Thus, the histochemical and biochemical results of the cell wall composition obtained in this work are more transferable to industrial cultures. Basic histochemistry methods known from studies of plant cell walls were applied. They provided insights into the *in-vivo* cell wall composition. In addition, to effectively disrupt the cell walls, different mechanical and chemical methods were tested. The most efficient was used to analyze the monosaccharide composition of the cell walls at three different life cycle stages, namely young daughters, mature cells and coenobia.

Moreover, a novel endogenous cell-wall-degrading enzyme, the autologous Autolysin, was isolated. The activity was compared to a commercially available endo-1,3-β-Glucanase and it was tested for its capability of degrading the cell walls. Efficient cell wall degradation with endogenous enzymes in the three *Chlorellaceae* species is an important step toward stable protoplast formation for effective molecular biology in *Chlorella* species.

2 Materials and methods

This chapter describes the applied chemicals and solutions, as well as the workflow and analytical methods.

2.1 Materials

The following two chapters describe the materials and devices used in this work.

2.1.1 Organisms

The three microalgal strains *Chlorella sorokiniana* 211-8k, *Chlorella vulgaris* 211-11b (*Chlorella*, Trebouxiophyceae, Chlorophyta) and *Parachlorella kessleri* 211-11g (*Parachlorella*, Trebouxiophyceae, Chlorophyta) were studied in this work (Table 1).

Table 1: Tested microalgal strains of the Chlorellaceae family studied in this work.

Organism	Gene Bank
Chlorella sorokiniana 211-8k	All ordered from Sammlung für Algen, Universität Göttingen
Chlorella vulgaris 211-11b	
Parachlorella kessleri 211-11g	

2.1.2 Chemicals and consumables

If not otherwise stated, all used chemicals are ordered from Roth (Carl Roth GmbH & Co. KG, Karlsruhe, Germany) or Sigma Aldrich (Merck KGaA, Darmstadt, Germany).

All the consumables are ordered from Sarstedt (SARSTEDT AG & Co. KG, Nürnbrecht, Germany), VWR (VWR International GmbH, Darmstadt, Germany) or Eppendorf (Eppendorf AG, Hamburg, Germany).

2.1.3 Devices

Table 2: Devices.

Device	Name/Number	Seller
High-performance anion exchange chromatography with pulsed amperometric detection	Autosampler and Thermal compartment AS50 Gradient Pump GP50 Detector ED50	Dionex
Centrifuge	5430 R	Eppendorf
Coulter Counter	Multisizer 3	Beckman Coulter
Lyophilizer	Alpha 2-4 LSCplus	Christ
Microscope	Axioplan 2 Axiophot 2 Axiocam 506 color	Zeiss
Microscope lamp	HBO 100 W(/2) HAL 100	Zeiss
Orbital shaker	DOS-20L	ELMI
Photometer	DR 5000	Hach Lange
Plate reader	Synergy 2	BioTek
Sample concentrator	Dri-Block DB-3D Sample concentrator	Techne

2.2 Methods

This chapter describes the detailed workflow, starting with algal cultivation and harvesting and the histochemistry of living cells. In addition, different cell disruption methods are shown, as well as the cell wall polysaccharide preparation and hydrolyzation, up to the analytical method for monosaccharide identification. The final chapter shows the detailed protocol for Autolysin extraction and the activity assays.

2.2.1 Cultivation and synchronization

The cultures of the three algal strains (*Chlorella sorokiniana*, *Chlorella vulgaris* and *Parachlorella kessleri*) were cultivated in 300 mL column reactors (inner diameter 36 mm, height 500 mm) at room temperature (RT, 20 – 22°C), constant bubbling with moistened ambient air, under a light dark regimen (16 h light/8 h dark) and in BG-11 medium (Table 3). The cultures were illuminated by three LED bars (8500 mm, 1100 Lumen), with 2500 mm distance to the column reactors, resulting in a light intensity of 40, 60 and 50 µmol photons m^{-2} s^{-1} at the top, middle and bottom of the reactor, respectively.

The synchronization of the cultures was achieved by different methods for the different strains. *C. sorokiniana* cultures were grown up to their stationary growth phase in BG-11 medium and transferred to starvation BG-11 medium without the addition of $NaNO_3$ (Table 3, solution 1). In the following 3 days, most of the cells reached a resting point in their life cycle and after transfer to standard BG-11 medium, almost all cells re-started their cell-cycle and showed divisions.

Table 3: Stock solutions for BG-11 medium.

	Stock solution	Per L distilled water	For 1 L media
1.	$NaNO_3$	15 g	100 mL
2.	K_2HPO_4 x 3 H_2O	4.0 g	10 mL
3.	$MgSO_4$ x 7 H_2O	7.5 g	10 mL
4.	$CaCl_2$ x 2 H_2O	3.6 g	10 mL
5.	Citric acid	0.6 g	10 mL
6.	Ferric ammonium citrate	0.6 g	10 mL
7.	EDTA	0.1 g	10 mL
8.	Na_2CO_3	2.0 g	10 mL
9.	Trace metal mixture	g/L	1 mL
	H_3BO_3	2.86 g	
	$MnCl_2$ x 4 H_2O	1.81 g	
	$ZnSO_4$ x 7 H_2O	0.222 g	
	Na_2MoO_4 x 2 H_2O	0.39 g	
	$CuSO_4$ x 5 H_2O	0.079 g	
	$Co(NO_3)_2$ x 6 H_2O	0.0494 g	

C. vulgaris and *P. kessleri* cultures were both synchronized by light deprivation and temperature reduction to 5 °C for several days without gassing. In this time, the cell division rested. After transfer to fresh BG-11 medium and standard culture conditions, almost all cells re-started their cell-cycle and showed divisions.

2.2.2 Cell wall staining

Different dyes for various components of the cell and cell wall were tested in the different life cycle stages. The detailed procedures are shown below.

Evans Blue

Evans Blue (EB) is an azo-dye that can be used for viability tests, as vital cell walls withhold the dye, while damaged cell walls are permeable (Gaff and Okong'o-ogola, 1971).

In short, 1 mL of culture were centrifuged, and the medium replaced by 0.2 mL distilled H_2O (dest. H_2O). Evans Blue solution was added to a final concentration of 0.25 % (w/v). After 10 min incubation time, 10 µL of the mixture were transferred to a microscope slide, covered with a cover slip and examined with the Axioplan 2 microscope.

Calcofluor White

Calcofluor White (CFW) binds to ß-1,3 and ß-1,4 polysaccharides in chitin, chitin-like structures or cellulose. The wavelength shows a maximum at 347 nm.

In short, 1 mL of algal culture was mixed with Calcofluor solution (concentration: 1 g/L) resulting in a final concentration of 53 µM Calcofluor White (Dunker and Wilhelm, 2018). After 10 min incubation time, 10 µL of the mixture were transferred to a microscope slide, covered with a cover slip, and examined under ultraviolet light with the Axioplan 2 microscope.

Ruthenium Red

Ruthenium Red (RR) is a hexavalent cation, that binds to a variety of different anions, including pectin (Soukup, 2014). In short, 1 mL of algal culture was centrifuged and resuspended in 200 µL MES buffer (20 mM) and

mixed with 0.025 % (w/v) Ruthenium Red, for 5 min. After washing once with MES buffer, 10 µL of the suspension were examined with the Axioplan 2 microscope.

Astra Blue (Basic Blue 140) and Safranin

Astra Blue (AB) binds to pectins, non-lignified cell walls of plants and glycosaminoglycans, which could be present in the cell walls of young algal cells. In short, 1 mL of algal culture was centrifuged and resuspended in 0.2 mL dest. H_2O. Astra Blue solution was added to a final concentration of 0.25 % (w/v). After 5 min incubation, the cells were centrifuged and washed once with 0.2 mL dest. H_2O. 10 µL of the mixture were examined with the Axioplan 2 microscope.

Safranin (S) is often used as a counter stain to AB, as it binds to lignified cell walls of plants. For the Safranin staining solution, 1 g of Safranin were dissolved in 100 mL dest. H_2O.

Following the AB staining, the cells were incubated in Safranin solution, for 5 min. Afterwards the samples were washed with 70 % EtOH for 5 min and once with HCl solution (100 mL 70 % EtOH + 0.5 mL conc. HCl). Finally, the cells were washed thoroughly with 90 % EtOH and examined with the with the Axioplan 2 microscope. Lignified cell walls appear red and cellulose or mucopolysaccharide containing walls blue (Gerlach, 1977).

2.2.3 Harvest and drying

During the cultivation, the growth rate was monitored by automated cell-counting and -sizing with the Multisizer 3 Coulter Counter and microscopic control. For the Multisizer 3 measurements, 500 µL cell suspension ($OD_{750\ nm} < 0.4$) were mixed with 9.5 mL isotone electrolyte. The Multisizer 3 counted any particle of 0.9 - 18.0 µm diameter in 100 µL of the solution.

When the cultures reached the target point in their life cycle (young daughter, mature cells, coenobia), the cultures were centrifuged (5 min, max. rpm, RT). The medium was discarded, and the pellet was stored at -20°C for lyophilization. For the lyophilization, the frozen pellet was dried at -80°C and 1 mbar for 22 hours. In a second step, the pressure was lowered to 0.001 mbar (2 hours), to remove the last moisture. Afterwards, the pellets were stored at room temperature until cell disruption.

2.2.4 Cell disruption methods

The freeze-dried algal pellets were disrupted with different methods.

Manually grinding in liquid nitrogen was performed with the addition of quartz sand (Ø 0.18 – 0.35 mm). Here 250 mg freeze-dried algal biomass was resuspended in 10 mL UP-H_2O and shock frozen with liquid nitrogen. Then the biomass was manually ground for 20 min, with frequent addition of liquid nitrogen. Afterwards, the material was resuspended in EtOH, to a final concentration of 70 % for the extraction of the cell wall polysaccharides.

Sonic degradation was performed on 60 mg of freeze-dried algal biomass resuspended in 10 mL 70 % EtOH (50 mL Falcon tubes), and sonicated at 100 % amplitude and a pulse of 10 s with 1 s break, for 5 or 30 min. The samples were kept in an ice bath during disruption to prevent heat-degradation. Afterwards, the suspension was centrifuged (5 min, max. rpm, RT), the supernatant discarded, and the pellet resuspended in 4 mL 70 % EtOH for the extraction of the cell wall polysaccharides.

Chemical degradation was tested on the algal biomass as well, based on the protocol of S. Weber (unpublished). 20 mg freeze-dried biomass were resuspended in 1.5 mL 1 mol/L NaOH and incubated at 100°C with constant shaking at 800 rpm for 60 min. Subsequently, the suspension was neutralized with 300 µL 5 M HCl and centrifuged (5 min, 10000 rpm, RT). The supernatant was transferred to a fresh tube. The pellet was washed

with 400 µL acetone and dried (50 °C), weighed and resuspended in 600 µL 70 % EtOH for extraction of the cell wall polysaccharides.

The polysaccharides of the supernatant were precipitated by the addition of nine-fold volume of 100 % EtOH (Pieper *et al.*, 2012). After 5 min of incubation at RT, the samples were centrifuged (5 min, 10000 rpm, RT) and washed with 80 % methanol (MetOH), 100 % MetOH, acetone, and dried at 50 °C. Afterwards, the polysaccharides were hydrolyzed with 2 mol/L trifluoroacetic acid (TFA), as shown in chapter 2.2.7.

2.2.5 Extraction of alcohol-insoluble-residues

After cell disruption, the extraction of alcohol-insoluble-residues (AIR) was conducted, based on the protocol of Foster and co-workers (Foster, Martin and Pauly, 2010). The samples (resuspended in 70 % EtOH, as shown above) were centrifuged for 5 min at max. rpm and RT, the supernatant was discarded and replaced with the same volume of 70 % EtOH. This process was repeated, until the supernatant was colorless. After the last washing step, the supernatant was replaced with chloroform/MetOH (1:1 [v:v]) and another three washing cycles were conducted. Finally, the samples were washed with 400 µL acetone once and dried at 50 °C.

2.2.6 Starch digestion and glucose determination

For both, starch digestion and glucose determination, the procedure was based on the protocol of Foster et al. (Foster, Martin and Pauly, 2010). For the initial starch digestion, the AIR material was resuspended in 750 µL 0.1 M sodium acetate buffer (pH 5.5) and heated at 80°C with constant shaking at 1400 rpm for 20 min. After cooling on ice, 750 µL of enzyme mixture, containing 739.5 µL sodium acetate buffer (pH 5.5), 1.5 µL amyloglucosidase (3260 U/mL, Megazyme®) and 9 µL α-amylase (1000 U/mL, Megazyme®) were added to each sample, thoroughly vortexed and incubated at 37 °C and constant shaking at 300 rpm for 8 days with

one enzyme change at day 4. At day 8, the starch digestion was terminated by heating the samples at 100 °C for 10 min, followed by four washing steps with dest. H_2O. After a final washing step with acetone, the pellets were dried at 50 °C and weighed prior hydrolyzation (chapter 2.2.7).

The released glucose was measured by the method shown in Foster (Foster, Martin and Pauly, 2010). 50 µL of the de-starched supernatant, or a glucose standard curve (0, 1, 2, 5, 10, 25, 50 µL of a 1 mg/mL glucose solution in distilled water with a final volume of 50 µL), were mixed with 139 µL HEPES buffer (pH 7), 5 µL 100mM ATP, 5 µL 45 mM NADP and 1 µL glucose-6-phosphat dehydrogenase in a 96-well plate. The kinetics were photometrically monitored at 340 nm for 10 min with a Synergy 2 plate reader. Afterwards, 2 µL hexokinase (1250 U/mL, Megazyme®) was added to each well and the kinetics measured for another 20 min. The difference between the average minimum and maximum were calculated for each sample and the amount of detected glucose was determined by the Glc-standard curve.

2.2.7 Detection of the monosaccharide composition

To detect the exact monosaccharide composition of the algal cell walls, the destarched-AIR (dAIR) material was hydrolyzed, and the resulting monosaccharides were analyzed by high pressure anion exchange chromatography.

Two different hydrolyzation methods of the cell walls were combined. In a first step, the 2 mol/L TFA hydrolysis to the matrix fraction and afterwards the 6 mol/L HCl hydrolysis to the rigid fraction.

For TFA hydrolysis, approximately 2 – 3 mg dAIR were weighed in a pre-weight screw cap tube. 250 µL 2 mol/L TFA were added and the samples were incubated at 100°C and constant shaking at 800 rpm for 90 min. Afterwards, the tubes were cooled down and centrifuged at RT and max. rpm for 5 min. 100 µL of this supernatant were transferred to a new tube and evaporated with a sample concentrator, resuspended in

400 µL ultrapure water (UP-H_2O) and stored at -20°C, whereas the pellet was washed three times with 1 mL of dest. H_2O and once with 400 µL acetone, before dried overnight.

After drying, the tubes were weighed again to determine the loss of dAIR. Then, 1 mL of 6 mol/L HCl was added to each tube and incubated at 100°C and constant shaking at 800 rpm for 20 hours. After cooling down, 900 µL of the solution was filtered with a syringe filter (diameter: 17 mm; area: 1.33 cm^2; pore diameter: 0.45 µm; material: polytetrafluoroethylene). 400 µL of the filtrate were transferred to a new tube and evaporated with the sample concentrator, resuspended in 400 µL UP-H_2O and stored at -20°C.

The High-performance anion exchange chromatography with pulsed amperometric detection (HPAEC-PAD) was run with a CarboPac PA20 column (Thermo Fisher®), variable NaOH concentrations as eluent and a constant flow rate of 0.5 ml/min at 25 °C.

For measurements, an appropriate dilution with a total volume of 200 µL was prepared. For calibration, 200 µL of standard mixtures with 5, 10, 25, 50, 75, 100 mmol/L of fucose, rhamnose, arabinose, glucosamine, galactose, xylose, glucose, mannose, galacturonic acid and glucuronic acid in UP-H_2O were used. 1 µL 2-Deoxy-D-glucose per 100 µL sample was added to each tube as an internal standard.

In the first 10 min, the column was washed and conditioned with 2 mmol/L NaOH. After 10 min, 10 µL of the sample were injected on the column. For 20 min, the conditions were kept at 2 mmol/L NaOH, to eluate the nonpolar monosaccharides. Afterwards the concentration was raised to 0.8 mol/L NaOH, to eluate the carbon acids and all sample residues. After 54 min total run time, the program started again with the next sample and 10 min column recovery and preparation with 2 mmol/L NaOH.

The results are calculated in %, based on g (monosaccharide) / g (biomass pre-hydrolyzation).

2.2.8 Extraction of Autolysin

Based on the extraction method by D. Reinecke-Levi *(in press)* autologous autolysin was isolated from all three algal strains.

In short, a five-day-old culture in the stationary growth phase was washed and resuspended in fresh BG-11 media to initiate the formation of sporangial cells. After 24 – 48 h, depending on the growth rate of the culture, the cells were centrifuged (10 min, 5000 rpm, RT) and ten-fold concentrated in dest. H_2O. On the following day, the daughter cells and the sporangial exudate were released. To amplify the release, the culture was thoroughly vortexed (10 min, max. speed). Following centrifugation (10 min, 5000 rpm, RT), the supernatant (containing the sporangial exudate) was further concentrated by size-filtration Centriprep® 10K Filter devices, according to the manufacturers instruction (Merck Millipore).

The resulting concentrated sporangial exudate (autolysin) was used in the permeability test on different algal populations, as well as in the endo-1,3-β-Glucanase activity assay.

2.2.9 Endo-1,3-β-Glucanase activity assay

The activity test was performed with slight modifications according to manufacturer's instructions (T-PAZ-200T, Megazyme®). A standard curve of the endo-1,3-β-Glucanase (E-Lams, Megazyme®) was prepared in 200 mM sodium acetate buffer (pH 4.5) with the following concentrations: 6.25, 12.5, 25, 50, 100 mU. In addition, the sporangial exudate and a blank (only buffer, without enzyme) were tested in each run. Following the instructions, the 0.5 mL samples were tempered to 30°C for 5 min and one 1,3-β-Glucazyme tablet (substrate) was added to each sample. After exactly 10 min incubation, the reaction was terminated with the addition of 10 mL Tris Buffer Salt Solution (2% w/v, pH ~ 10) and thoroughly vortexing. After another 5 min of incubation at RT, the samples were vortexed again and 2 mL were transferred to epi tubes and centrifuged (5 min, max rpm, RT). 1 mL of the supernatant were transferred to cuvettes

and the absorbance at 590 nm was measured with the DR 5000 photometer (Hach Lange) against the substrate blank. The activity of the sporangial exudate was later calculated with the standard curve.

2.2.10 Permeability assay

For the permeability assay were cells of defined populations (daughter cells, mature cells, coenobia) ten-fold concentrated in MES buffer (20 mmol/L) and 1:1 diluted with coenobial exudate. The test was performed for all three algal strains, at room temperature with constant shaking at 120 rpm. Within the next four hours, the cell number was counted every hour. In addition, the samples were microscopically examined for cell wall perforations, leakages, or degradations with the Axioplan 2 microscope. After 24 h, the cells were counted again and centrifugated. The supernatant was stored at -20 °C for monosaccharide analysis with the HPAEC-PAD.

2.2.11 Statistics

The results of the HPAEC-PAD were statistically analyzed in Microsoft Excel, GraphPad Prism and R. The Kruskal-Wallis test for independent samples was used (if the number of individual samples per group was ≥ 3) to test whether the central tendencies of the monosaccharides differ between the life cycle stages. If so, and the number of individual samples per group was ≥ 6, pairwise Wilcoxon rank sum Test, with an adjusted p-value according to the Bonferroni method, was used to identify significant differences between specific life cycle stages.

3 Results

This chapter describes the results of the performed experiments in detail.

3.1 Growth experiments

As described in chapter 2.2.1, the algae were harvested at specific points during their life cycle. Therefore, a detailed knowledge to the synchronization and the growth rate under the specific conditions was essential. The following chapters present the results of the Neubauer counting chamber and the automated cell-counting and -sizing for each strain and its populations.

Chlorella sorokiniana 211-8k

The culture of *C. sorokiniana* 211-8k was inoculated at a cell number of 3.4 x 10^7 cells/mL and characterized for 3 days (Figure 5). The culture initially consisted to 91 % of mature cells, with an average cell-diameter of 3.8 µm, and 9 % coenobia. After 42 h, the coenobia population increased to 35 % and the average cell-diameter to 4.1 µm (Figure 5). The coenobia maximum was reached with 57 %, after 44.5 h. At 46 h, the coenobia released their daughter cells. The population assembly shifted to 82 and 18 % daughter cells and coenobia, respectively. The total cell-count increased to 5.0 x 10^7 cells/mL (150 %).

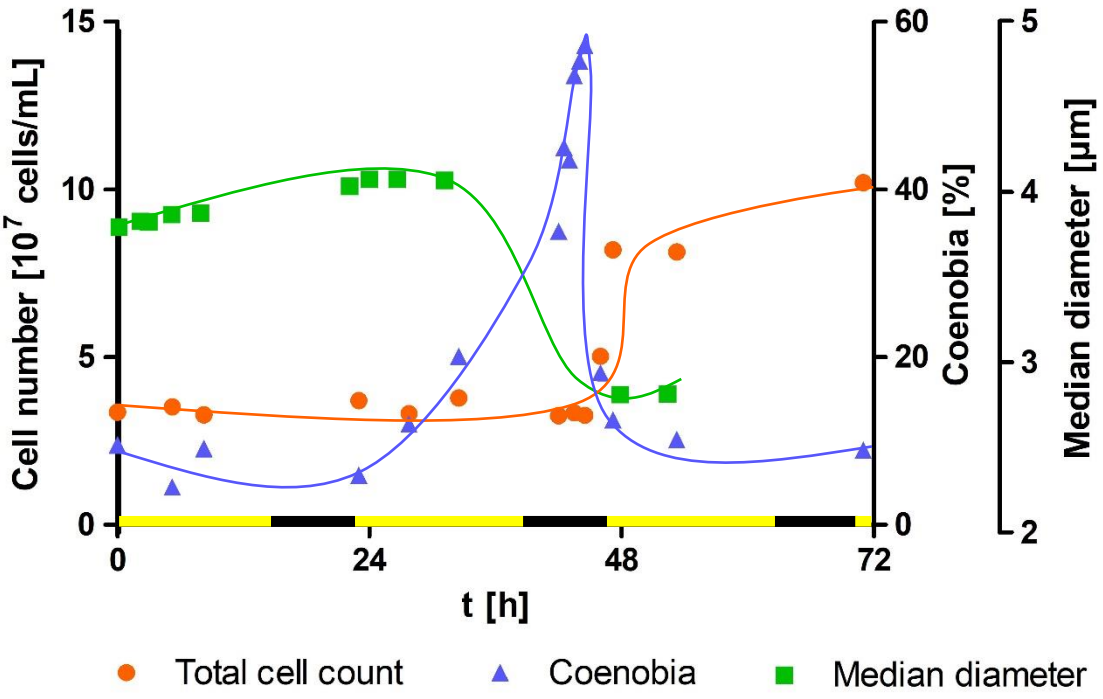

Figure 5: Growth curve of Chlorella sorokiniana 211-8k. Cell number (●), percentage of coenobia (▲) and average cell diameter (■) of C. sorokiniana 211-8k grown in a column reactor with constant gassing of moistened ambient air and 16 to 8 hours light-dark regimen (indicated by the yellow and black bars); T = 21°C; cell number counted with Neubauer counting chamber (improved); x-axis: time in hours; y-axis left: cell number in 10^7 cells/mL; 1st y-axis right: proportion of coenobia of the total cell number in percentage, 2nd y-axis right: average diameter of particles between 2.062 µm and 6.001 µm measured with the Coulter Counter in µm.

After 47 h, the culture consisted of 88 and 12 % daughter cells and coenobia, respectively with a total cell-count of 8.2 x 10^7 cells/mL (240 %), while the average cell-diameter decreased to 2.8 µm (68 %). Over the last 24 h, the daughter cell release continued, the cell number increased to 10.1 x 10^7 cells/mL (297 %), the cell-diameter remained stable (2.8 µm), and the coenobia population decreased back to 8 %. These results indicate the daughter cell release and optimum time-point for the autolysin-harvest in the second dark-phase between 44.5 to 46 h (Figure 5).

Chlorella vulgaris 211-11b

The culture of *C. vulgaris* 211-11b was inoculated with 4.3 x 10^7 cells/mL and characterized for 9 days (Figure 6). The initial population consisted to 99 and 1 % of daughter cells and coenobia, respectively, with an average cell diameter of 3.2 µm. Within the next 48 h, the daughter cells matured to cells with an average diameter of 4.0 µm (125 %). After 72 h, the culture consisted to 89 and 11 % of mature cells and coenobia, respectively, but the cell number remained at 4.5 x 10^7 cells/mL (Figure 6). At 120 h, the beginning of the sixth dark phase, the coenobia population peaked at 47 % and the average diameter increased to 4.5 µm (140 %).

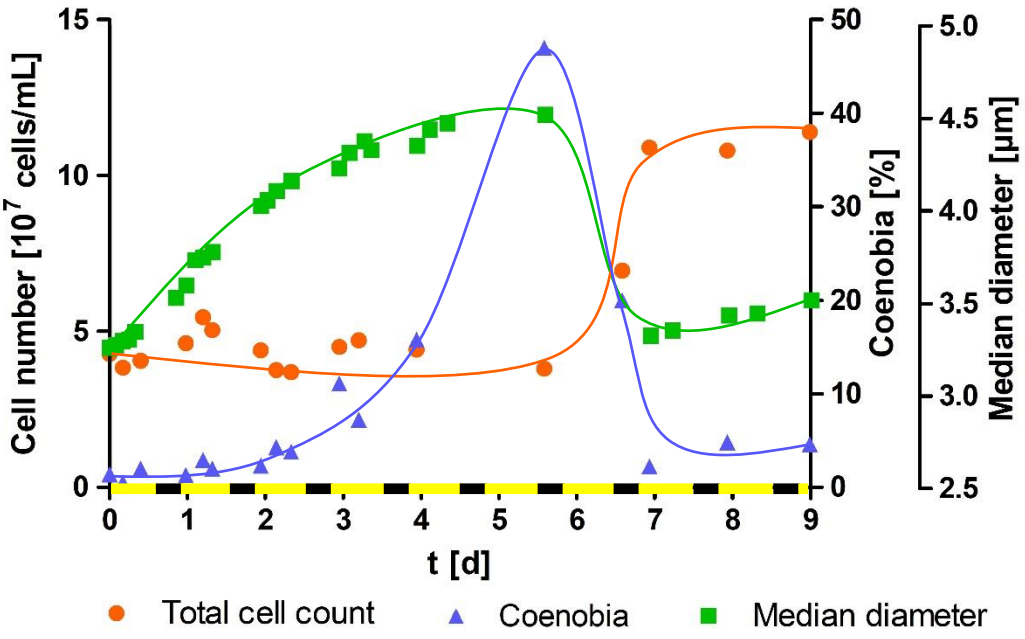

Figure 6: Growth curve of Chlorella vulgaris 211-11b. Cell number (●), percentage of coenobia (▲) and average cell diameter (■) of C. vulgaris 211-11b grown in a column reactor with constant gassing of moistened ambient air and 16 to 8 hours light-dark regimen (indicated by the yellow and black bars); T = 21°C; cell number counted with Neubauer counting chamber (improved); x-axis: time in days; y-axis left: cell number in 10^7 cells/mL; 1st y-axis right: proportion of coenobia of the total cell number in percentage, 2nd y-axis right: average diameter of particles between 2.062 and 7.001 µm measured with the Coulter Counter in µm.

Over the next 48 h, the coenobia released their daughter cells (Figure 6). The cell number increased to 10.9 x 10^7 cells/mL (253 %), holding 98 % daughter cells, and the average cell diameter dropped back to 3.3 µm (103 %). The coenobia population decreased to 2 %. Over the next 48 h, the cell number further increased to 11.4 x 10^7 cells/mL (265 %), while the daughter cells began to mature to an average cell diameter of 3.5 µm.

Parachlorella kessleri 211-11g

The culture of *P. kessleri* 211-11g was inoculated with a cell number of 6.4 x10^7 cells/mL and characterized for 240 h (Figure 7). The population consisted to 98 and 2 % of daughter cells and coenobia, respectively, with an average cell diameter of 4.4 µm (Figure 7). Within the first 72 h, the daughter cells matured to a mean diameter of 5.8 µm (131 %) without changes in the cell number, or the percentage of coenobia. 24 h later, the culture consisted to 85 and 15 % of mature cells and coenobia, respectively. After 144 h, at the beginning of the sixth dark phase, the coenobia population peaked at 47 % and the average diameter further increased to 6.0 µm (136 %).

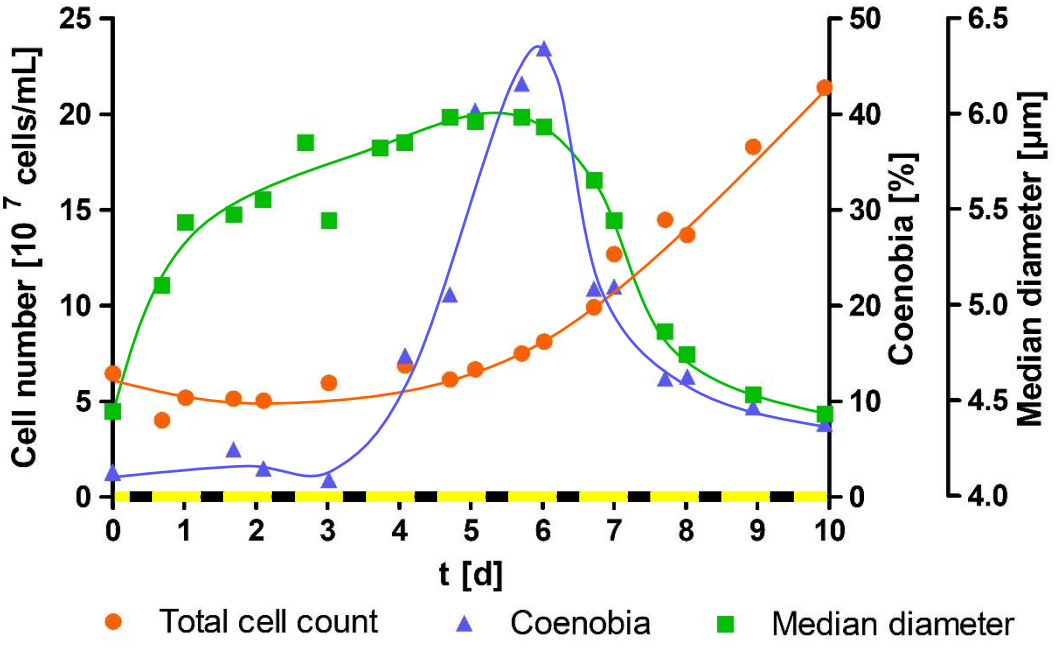

Figure 7:Growth curve of Parachlorella kessleri 211-11g. Cell number (●), percentage of coenobia (▲) and average cell diameter (■) of P. kessleri 211-11g grown in a column reactor with constant gassing of moistened ambient air and 16 to 8 hours light-dark regimen (indicated by the yellow and black bars); T = 21°C; cell number counted with Neubauer counting chamber (improved); x-axis: time in days; y-axis left: cell number in 10^7 cells/mL; 1st y-axis right: proportion of coenobia of the total cell number in percentage, 2nd y-axis right: average diameter of particles between 3.013 and 9.001 µm measured with the Coulter Counter in µm.

Over the next 48 h, the coenobia released their daughter cells, and the total cell number increased to 12.7 x 10^7 cells/mL (198 %). The percentage of coenobia decreased to 22 % and the average diameter decreased to 5.65 µm (128 %). After 192 h, the total cell number further increased to 14.5 x 10^7 cells/mL (226 %), and the population consisted to 88 and 12 % of daughter cells and coenobia, respectively, with an average diameter of 4.86 µm (110 %). Over the next 48 h the cell number further increased to 21.4 x 10^7 cells/mL (334 %), with 93 % daughter cells, 7 % coenobia and an average diameter of 4.4 µm (100 %).

3.2 Histochemistry

Different histochemical methods were tested for all three microalgae, as shown in chapter 2.2.2. This chapter will present these results in detail, for the individual populations in the life cycle of each microalga. An overview is given in Table 4.

Table 4: Results of the different staining methods applied to the algae at different life cycle stages.

Strain	Population	Dye				
		Evans Blue	Calcofluor White	Ruthenium Red	Astra Blue	Safranin
C. sorokiniana	Daughter	+	+	+	+	-
	Mature	-	+	+	+	-
	Coenobia	-	+	+	+	-
	Dead cells	+	-	+	+	-
	Debris	+	+	+	+	-
C. vulgaris	Daughter	-	+	+	+	- *
	Mature	-	+	+	+	- *
	Coenobia	-	+	+	+	- *
	Dead cells	+	-	+	+	- *
	Debris	+	+	+	+	- *
P. kessleri	Daughter	-	+	-	+	- *
	Mature	-	-	-	+	- *
	Coenobia	-	-	-	+	- *
	Dead cells	-	-	-	+	- *
	Debris	-	+	-	+	- *

*Positive staining results are indicated by "+", negative results by "-"; *Safranin results differ with different procedures applied to the alga.*

Evans Blue

Evans Blue (EB) is a widely used bis-azo dye for histochemical staining of blood cells, as it has a high affinity to serum albumin (Yao *et al.*, 2018). Additionally, it was shown that it can be used as a viability stain in plant cells (Gaff and Okong'o-ogola, 1971). Thus, we tested the suitability of EB dye on our algal strains to indicate the cell-wall integrity of the different populations and the cells after autolysin treatment (chapter 3.5). In line with plant cells, dead cells of *C. sorokiniana* and *C. vulgaris* were EB positive at any cell-cycle stage (Table 4). Dead cells were intensively stained by EB (Figure 8, orange arrows).

Strikingly, the cell walls of vital daughter cells of *C. sorokiniana* were EB positive (Figure 8, blue arrows), while the cell walls of mature cells remained negative (Figure 8, red arrow). This could indicate the presence or accessibility of a proteinous target for EB in the cell walls of daughter cells, which is absent during other cell-cycle stages.

In contrast, dead cells of *Parachlorella kessleri* populations remained EB negative throughout.

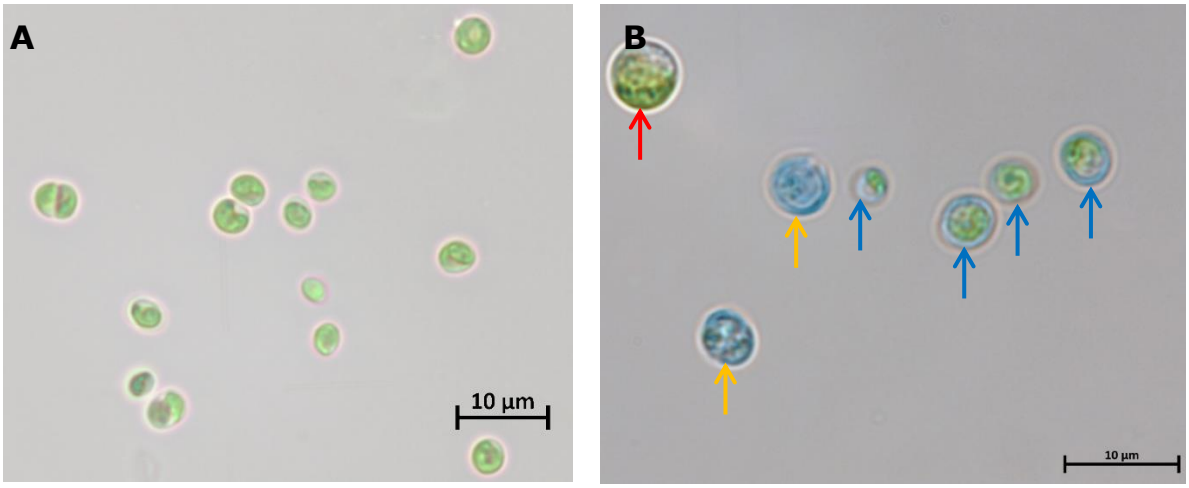

Figure 8: Chlorella sorokiniana 211-8k stained with Evans Blue. Control (A) and stained (B) as shown in chapter 2.2.2. Observed with Axioplan 2 microscope and HAL 100 lamp, with 100x magnification (A) and 157x magnification (B); mature cell (↑); dead cells (↑); daughter cells (↑).

Calcofluor White

Calcofluor White (CFW) is a fluorescent dye that stains β-glucans in cell walls (Voiniciuc *et al.*, 2019). Its selectivity is considered to be related to the 1-3-β- and 1-4-β-chains of polysaccharides (Wood, Fulcher and Stone, 1983; Soukup, 2014). Previous works have confirmed its suitability for cell wall studies in microalgal species (Kloareg, Quatrano and Marine, 1987; Reinecke *et al.*, 2018). In line, the cell walls of our *Chlorella* strains were positively stained at all cell-cycle stages (Table 4). Again, *P. kessleri* populations showed different staining patterns (Figure 9).

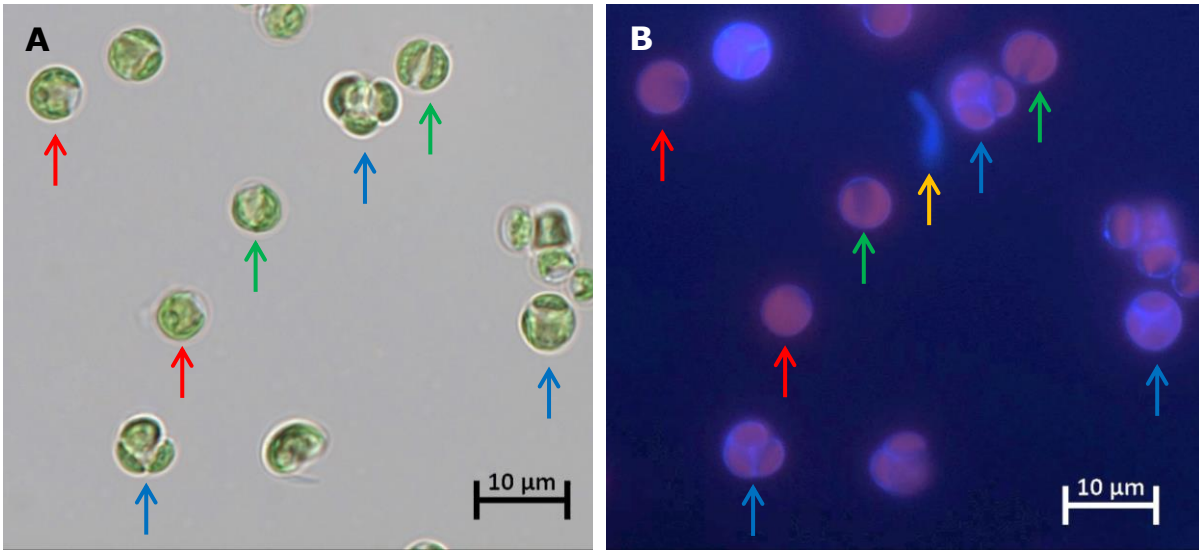

Figure 9: Parachlorella kessleri 211-11g stained with Calcofluor White. Bright field image (A) examined with Axioplan 2 microscope and HAL 100 lamp and ultraviolet image (B) with Axioplan 2 microscope and HBO 100 W/2 lamp both at 63x magnification; stained as shown in chapter 2.2.2; mature cells (↑); daughter cells with an cell wall (↑); coenobial cells before daughter cell wall formation (↑); cell wall debris (↑).

The cell walls of mature cells were CFW negative (Figure 9, red arrows) Likewise, the cell walls of immature daughter cells inside the coenobia were CFW negative (Figure 9 green arrows). Yet, the cell walls of fully developed daughter cells, even within coenobia, were CFW positive (Figure 9, blue arrows). Moreover, coenobial cell wall debris was intensively CFW positive (Figure 9, orange arrow). These findings indicate the presence of 1-3-β- or 1-4-β-linked polysaccharides in the cell wall of daughter cells. While in

mature cells with fully developed cell walls these polysaccharides are not accessible for CFW. And the dividing intra-coenobial autospores lack initially the β-linked polysaccharides in their developing cell wall.

Ruthenium Red

Ruthenium Red (RR) is known for its high affinity to pectin in plant cell walls (Soukup, 2014). Additionally, it can bind to a variety of other polyanions, due to its hexavalent cation (Pieper *et al.*, 2012; Soukup, 2014). Possible targets in algal cell walls might be the uronic acids (galacturonic acid and glucuronic acid) (Pieper *et al.*, 2012; Reinecke *et al.*, 2018). The cell walls of our *Chlorella* strains were positively stained at all cell-cycle stages (Table 4 and Figure 10). Once more, *P. kessleri* populations showed a different staining pattern (Table 4).

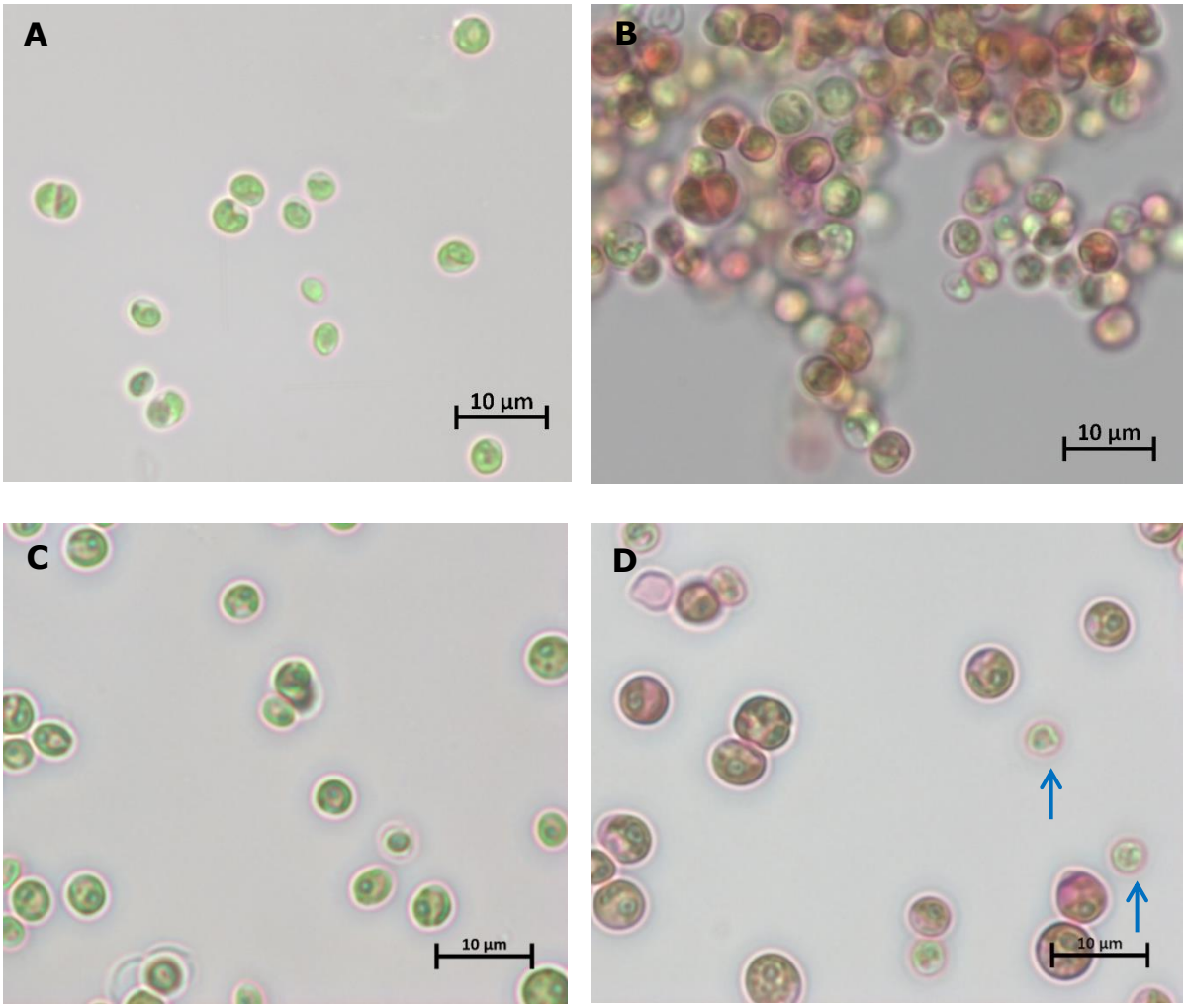

Figure 10: Chlorella sorokiniana 211-8k and Chlorella vulgaris 211-11b stained with Ruthenium Red. Control (A) and stained cells of C. sorokiniana (B); control (C) and stained cells of C. vulgaris (D); procedure shown in chapter 2.2.2; examined with Axioplan 2 microscope; 100x magnification; daughter cells (↑).

C. sorokiniana cells immediately started clustering regardless of the life cycle stage, after contact with RR, (Figure 10, B). The cells were completely permeable for RR and showed a RR positive cytoplasm (Figure 10, B). Contrasting, *C. vulgaris* cells did not cluster and daughter cells were not permeabilized by RR (Figure 10, D, blue arrows). Whereas the coenobia and mature cells were completely permeable for RR and showed a RR positive cytoplasm (Figure 10, D).

P. kessleri cells clustered after contact with RR, but the dye was almost completely washed out (Figure 11). In line with previous reported results for *P. kessleri*, its cell wall is RR negative (Yamamoto, Kurihara and Kawano, 2005). However, a weak RR positive staining might indicate low amounts of pectineus substances or uronic acids in the cell walls of our *P. kessleri* strain.

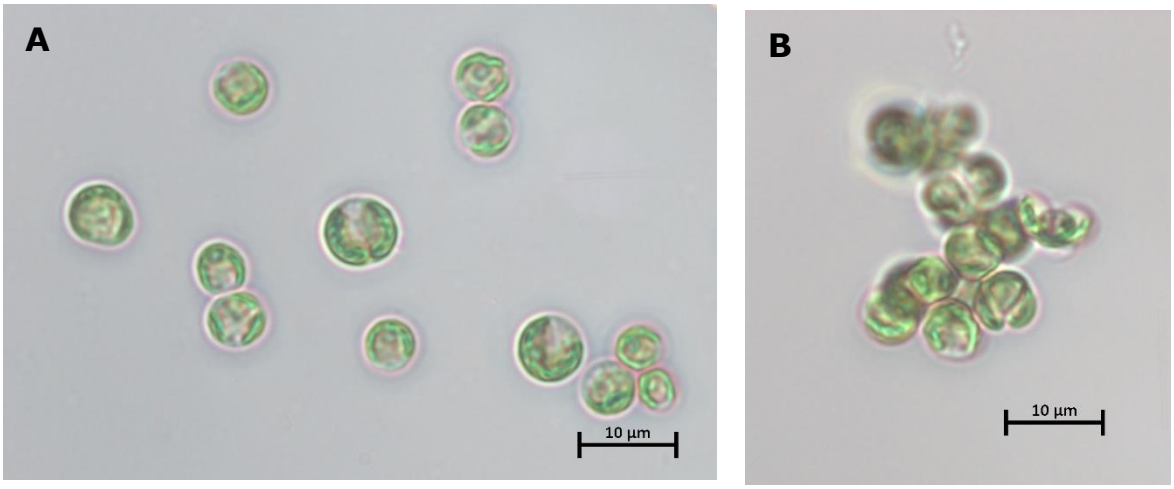

Figure 11: Parachlorella kessleri 211-11g stained with Ruthenium Red. Untreated (A) and stained with Ruthenium Red (B), as shown in chapter 2.2.2; examined with Axioplan 2 microscope and HAL 100; 100x magnification.

Astra Blue

Astra Blue is a widely used dye in plant histochemistry for lignin staining (Kraus *et al.*, 1998; Vazquez-Cooz and Meyer, 2002; Montiel *et al.*, 2007). Additionally, it was shown that it stains glycosaminoglycans (GAGs) of mast cell granules (Blaies and Williams, 1981). The presence of GAGs was also reported for *Chlorella* cell walls (Mercola and Klinghardt, 2001). Thus, we tested AB on our algal strains.

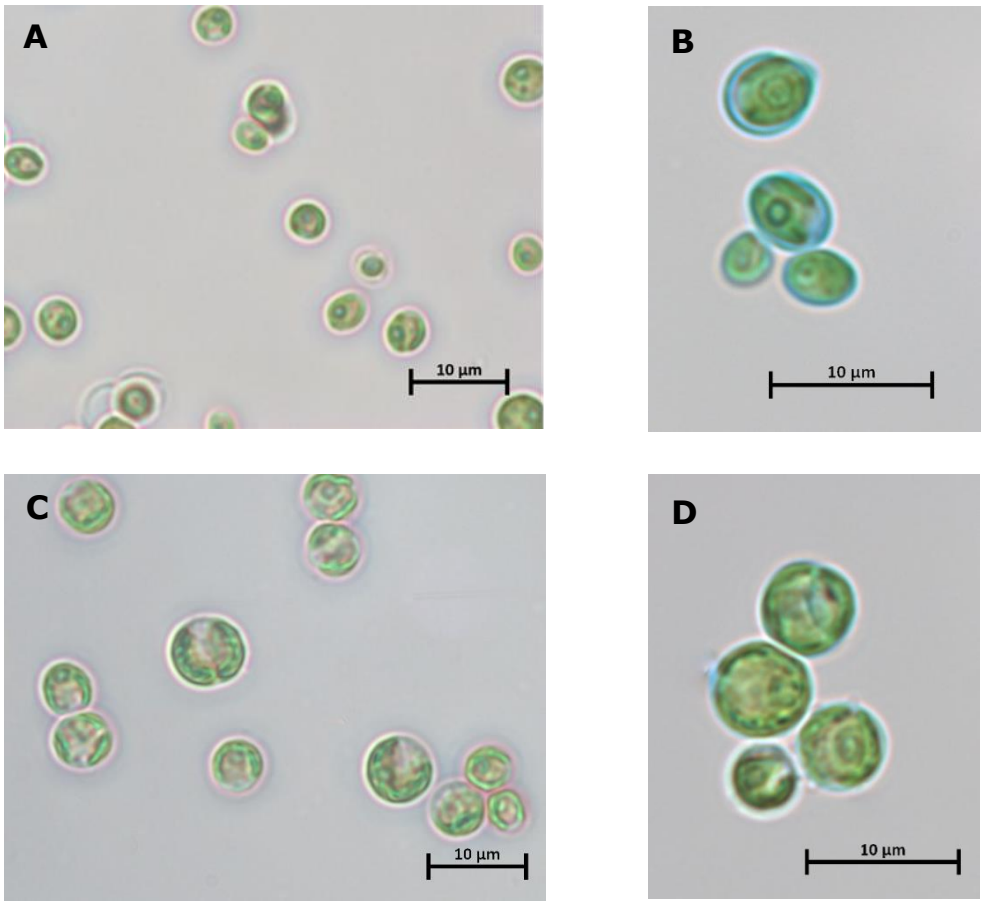

Figure 12: Cells of Chlorella vulgaris 211-11b and Parachlorella kessleri 211-11g stained with Astra Blue. Control (A) and stained cells of C. vulgaris (B); control (C) and stained cells of P. kessleri (D); procedure shown in chapter 2.2.2; examined with Axioplan 2 microscope and HAL 100; 100x magnification for A/C; 157x magnification for B/D.

The cell walls of all our *Chlorellaceae* were stained throughout all cell-cycle stages (Table 4). However, compared to *C. vulgaris* the walls of *P. kessleri* were less intensively stained (Figure 12). This could indicate the presence or accessibility of more GAGs in the cell wall of *C. vulgaris* rather than in *P. kessleri*.

Safranin

Safranin dye is used as a counterstain to AB, as it indicates lignin in plant cell walls (Vazquez-Cooz and Meyer, 2002). Nevertheless, in a first approach, we tested S without previous AB staining (chapter 2.2.2, Figure 13).

The cells of *C. sorokiniana* immediately clustered regardless of the cell-cycle stage, after contact with S, (Figure 13B). A slight red shimmer surrounding the cells, also visible in the control, is a microscopic artefact (Figure 13A).

The cells of *C. vulgaris* slightly clustered after staining (Figure 13D). However, the cells remained S negative throughout all life cycle stages (Table 4). Interestingly, the cells of *P. kessleri* were bleached by the staining procedure (Figure 13F) but remained S negative.

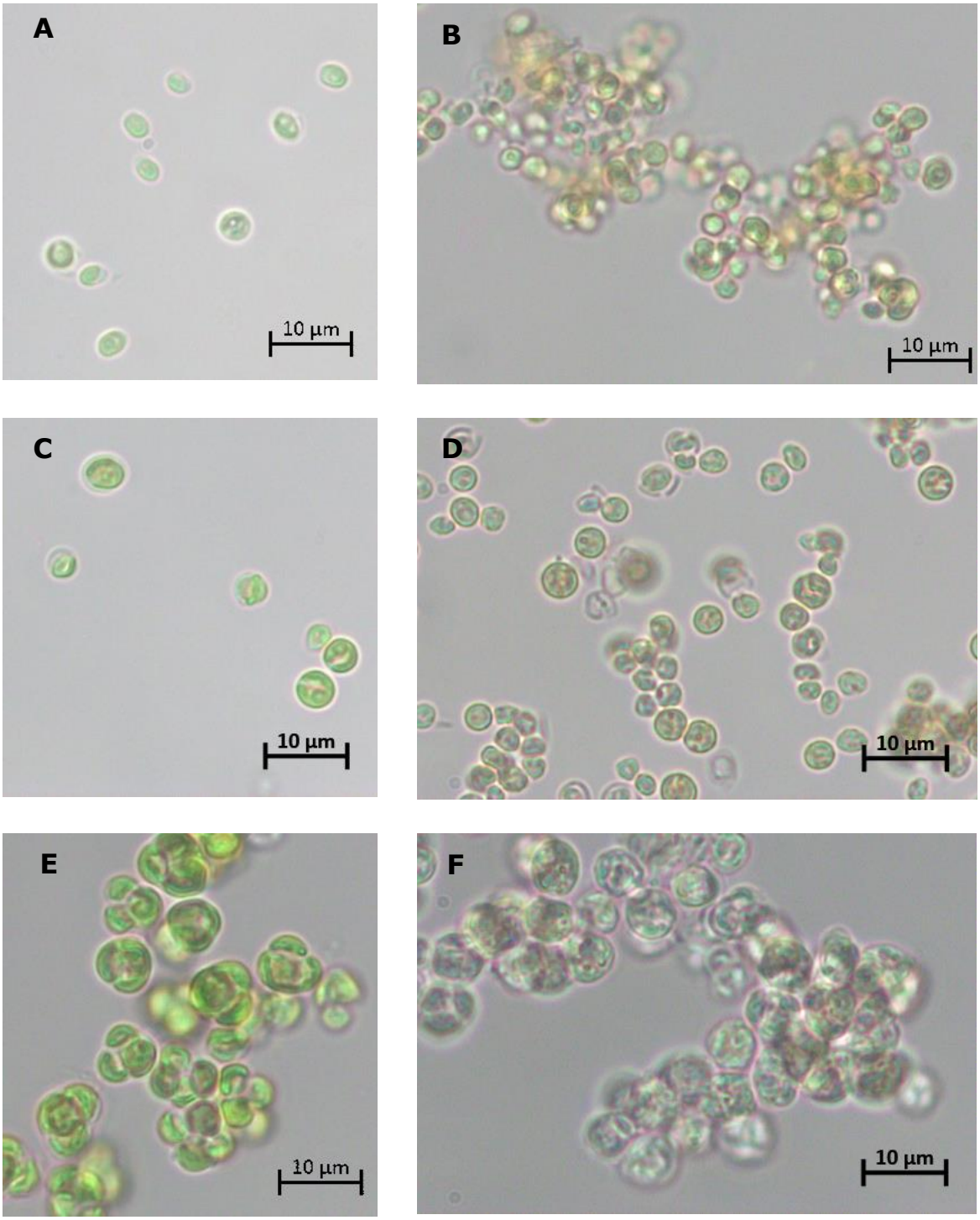

Figure 13: Staining results of Safranin for the three different Chlorellaceae. Control (A) and stained C. sorokiniana 211-8k (B); control (C) and stained C. vulgaris 211-11b (D); control (E) and stained P. kessleri 211-11g (F); procedure shown in chapter 2.2.2; examined with Axioplan 2 microscope and HAL 100; 100x magnification.

To prevent cell bleaching, the staining was repeated, but without the ethanol washing. Instead, the cells were washed three times with dH_2O (Figure 14).

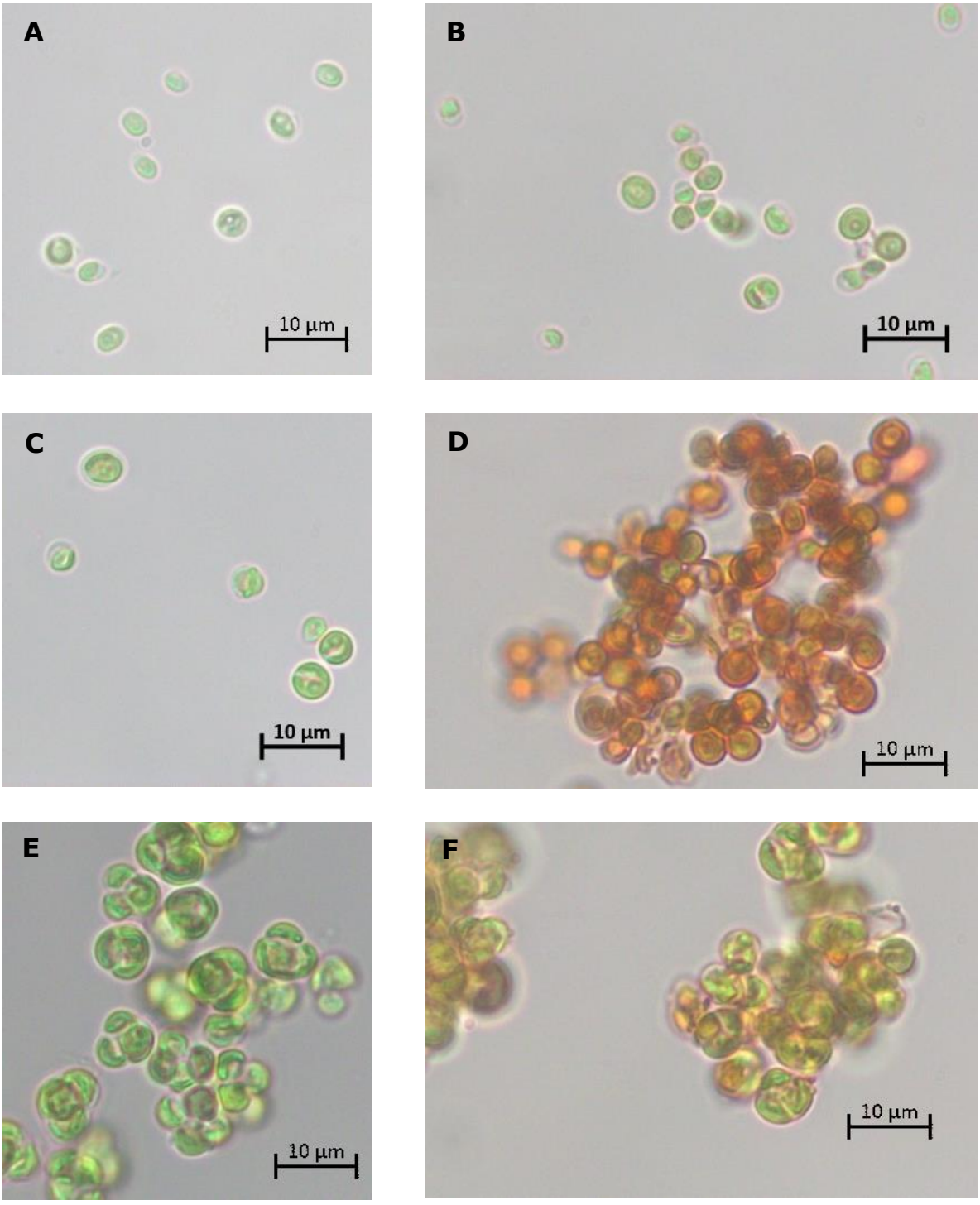

Figure 14: Results of modified Safranin staining for the three different Chlorellaceae. Control (A) and stained C. sorokiniana 211-8k (B); control (C) and stained C. vulgaris 211-11b (D); control (E) and stained P. kessleri 211-11g (F); procedure shown in chapter 2.2.2, modified: washing-step in water, instead of ethanol and HCl; examined with Axioplan 2 microscope and HAL 100; 100x magnification.

According to Soukup, the affinity of S to cell walls is highly depending on particular conditions (e.g. pH-value, polarity of solvent, temperature, time of dyeing) (Soukup, 2014). In line with this, the S staining results differ to the previous results (Figure 13). The cells of *C. sorokiniana* clustered less (Figure 14B) but remained S negative throughout.

Differing with this dyeing procedure, the *C. vulgaris* cells clustered and showed intensively stained cell walls and content (Figure 14D). Likewise, *P. kessleri* cells were not bleached but slightly stained. Especially, readily formed daughter cells inside the coenobia (Figure 14F).

Combined Astra Blue and Safranin staining

As mentioned above, AB and S are often combined to differentiate cell wall components. Thus, we tested both as described in chapter 2.2.2 (Figure 15). The cells of *C. sorokiniana* clustered after staining with AB and S (Figure 15B). However, *C. sorokiniana* was negative for both dyes, even though it showed positive results for AB before. This indicates that the binding of AB to the cell walls of *C. sorokiniana* is not strong enough to resist the harsh washing procedure.

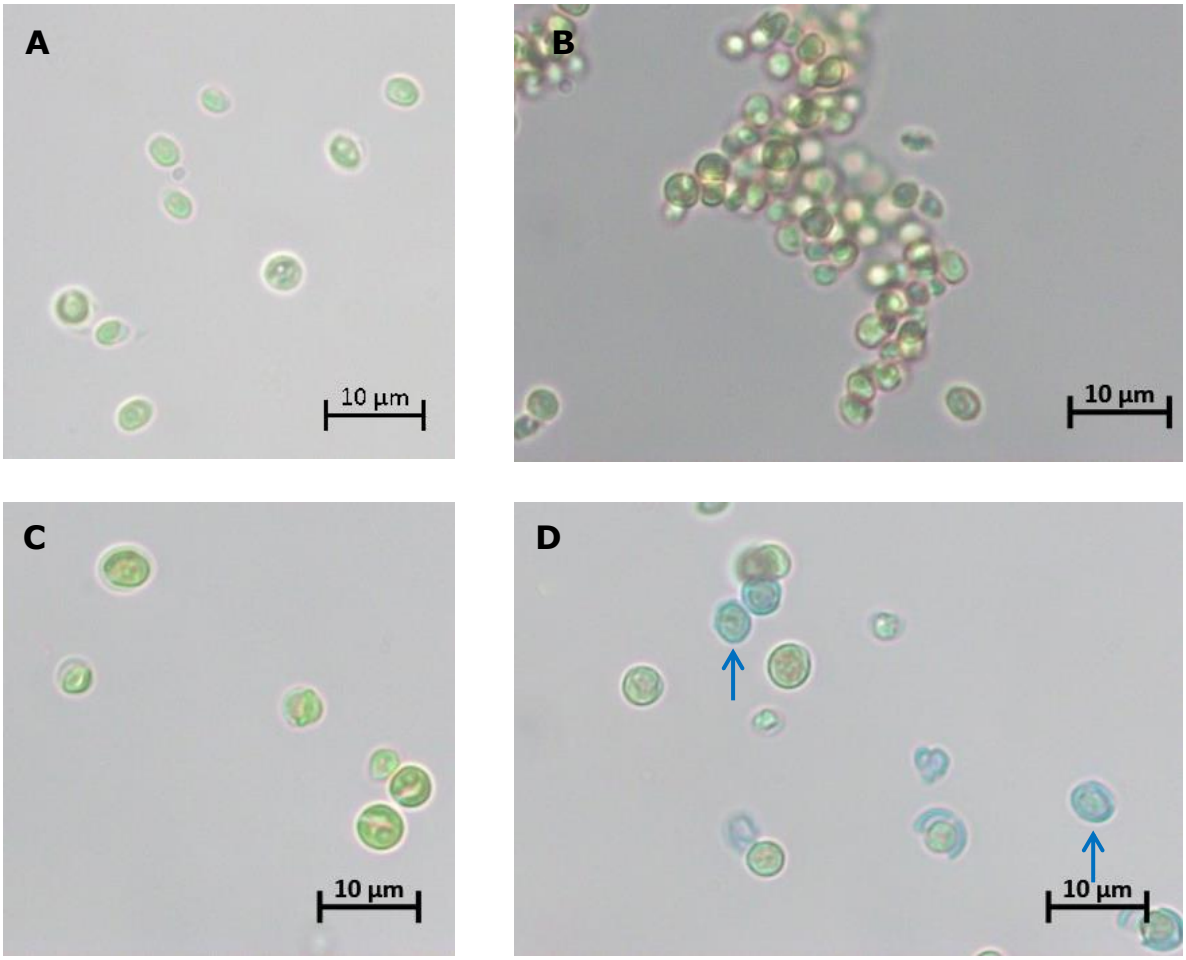

Figure 15: Staining results of Astra Blue and Safranin for the three different Chlorellaceae. Control (A) and stained C. sorokiniana 211-8k (B); control (C) and stained C. vulgaris 211-11b (D) daughter cells (↑); procedure shown in chapter 2.2.2; examined with Axioplan 2 microscope and HAL 100; 100x magnification.

Contrasting, cell wall debris and young daughter cells of *C. vulgaris* were intensively stained by AB, but not by S (Figure 15D, blue arrows). The GAGs stained by AB might be especially present in the cell walls of young daughter cells, and in the inner side of mature cells and coenobia. This could explain the positive staining of cell wall debris, but the negative result of mature cells (Figure 15D). However, as shown before, AB alone is not washed out from mature cell walls by water (Figure 12).

In line with our previous results, cells of *P. kessleri* were bleached in the washing procedure (not shown). Thus, we tested the combined staining of AB and S without ethanol washing, but with water (Figure 16).

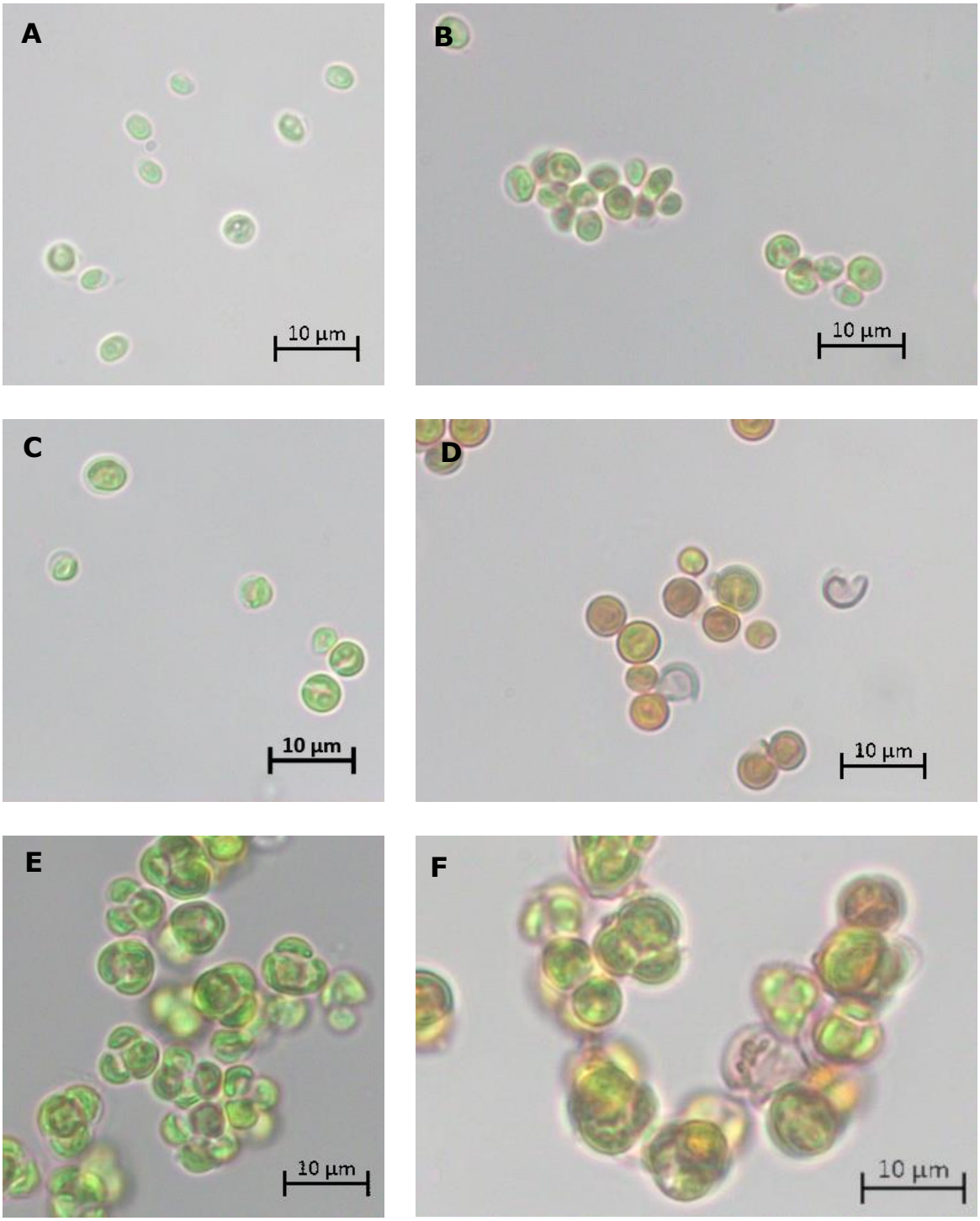

Figure 16: Staining results of Astra Blue and Safranin for the three different Chlorellaceae. Control (A) and stained C. sorokiniana 211-8k (B); control (C) and stained C. vulgaris 211-11b (D); control (E) and stained P. kessleri 211-11g (F); procedure shown in chapter 2.2.2, water used for washing, instead of ethanol and HCl; examined with Axioplan 2 microscope and HAL 100; 100x magnification.

The results for *C. sorokiniana* (Figure 16B) are comparable to the results after staining with S (Figure 14B). The clusters were smaller compared to

the ethanol washing (Figure 15B), however no positive staining results were found for both, AB and S.

C. vulgaris cells were S positive (Figure 16D). Interestingly, cell wall debris showed a purple color, which indicates that AB and S are overlapping. Additionally, the cells clustered less compared to S staining alone (Figure 14D).

In *P. kessleri* AB staining remained negative (Figure 16F) and was comparable to S alone (Figure 14F).

3.3 Disruption techniques

In *C. sorokiniana* several disruption techniques (chapter 2.2.4) were tested and evaluated by microscopy, Coulter Counter and by cell wall related monosaccharide release.

Sonication

The efficiency of 5 and 30 min sonication, respectively, was compared by automated cell-counting and -sizing (Figure 17).

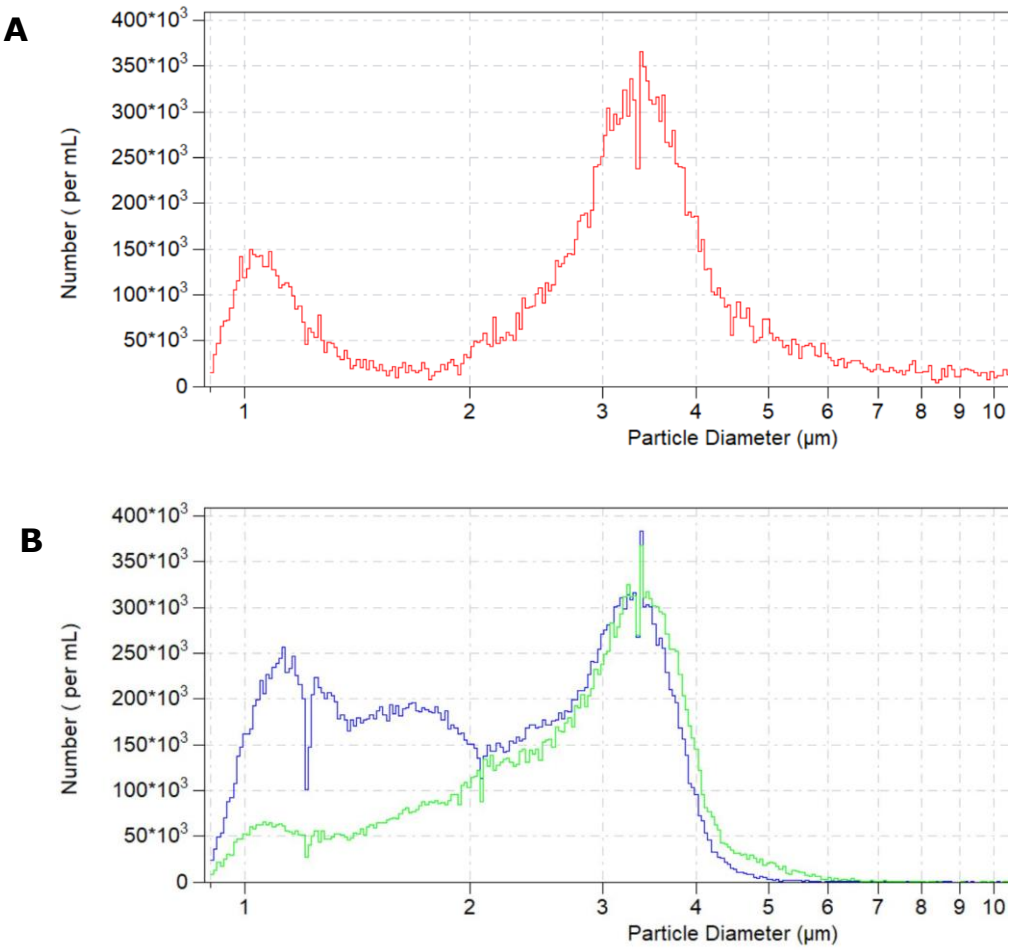

Figure 17: Comparison of cell size and number of Chlorella sorokiniana. Before sonication (A, red), after 5 min (B, green) and 30 min (B, blue) of sonication; measured with the Multisizer 3 Coulter Counter.

Before sonication, the culture of mature cells showed one peak of cell wall debris at 0.9 – 2 µm with a total of 4.6 x 10^6 particles/mL (maximum at 1.0 µm with 156 x 10^3 particles/mL) (Figure 17 A). And a second peak of intact cells at 2 – 5 µm with a total of 15.1 x 10^6 particles/mL (maximum at 3.3 µm with 381 x 10^3 particles/mL, median 3.3 µm) (Figure 17 A).

After 5 min of sonication, the amount of cell debris increased at 0.9 – 2 µm to 4.8 x 10^6 particles/mL (105 %), especially between 1.5 – 2 µm with 2.3 x 10^6 particles/mL (Figure 17 B, green). The second peak slightly decreased to 15.0 x 10^6 particles/mL (99 %) (maximum at 3.3 µm with 367 x 10^3 particles/mL, median 3.1 µm). Indicating the destruction of formerly large cells. The reduction of the first peak could be explained by de-clumping of cell debris, following the freeze-drying process, or disintegration below the detection limit of 0.9 µm.

After 30 min of sonication, the amount of cell debris increased to 14.1 x 10^6 particles/mL (306 %) (maximum at 1.1 µm with 256 x 10^3 particles/mL) (Figure 17 B, blue). The second peak slightly decreased again to 14.9 x 10^6 particles/mL (98 %) (maximum at 3.3 µm with 383 x 10^3 particles/mL, median 3.0 µm).

Interestingly, even though the amount of cell debris increased in both samples, the number of particles within the range of 2 – 5 µm only changed slightly. To check, whether the cell walls were permeabilized after the sonication, a viability staining with Evans Blue Dye was performed (chapter 2.2.2, Figure 18).

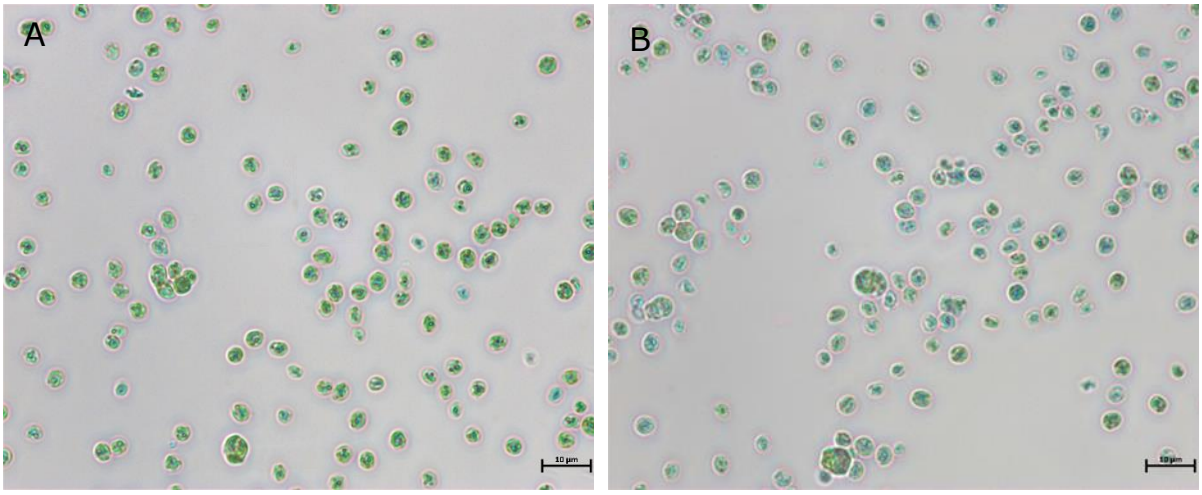

Figure 18: Cells of Chlorella sorokiniana 211-8k after sonication in 70 % EtOH. Procedure shown in chapter 2.2.4; after 5 min (A) and 30 min (B) of sonication; cell suspension washed with water once and stained with Evans Blue (chapter 2.2.2) and examined with Axioplan 2 microscope with HAL 100 lamp and 100x magnification.

Microscopic cell count confirmed 17 % ± 2% and 89 % ± 2 % positively stained cells after 5 and 30 min sonication, respectively (Figure 18).

Grinding

The efficiency of manually grinding of *C. sorokiniana* cells in liquid nitrogen (chapter 2.2.4) was checked with the Axioplan 2 microscope (Figure 19). Due to the addition of quartz sand, no automated cell-counting and -sizing was performed.

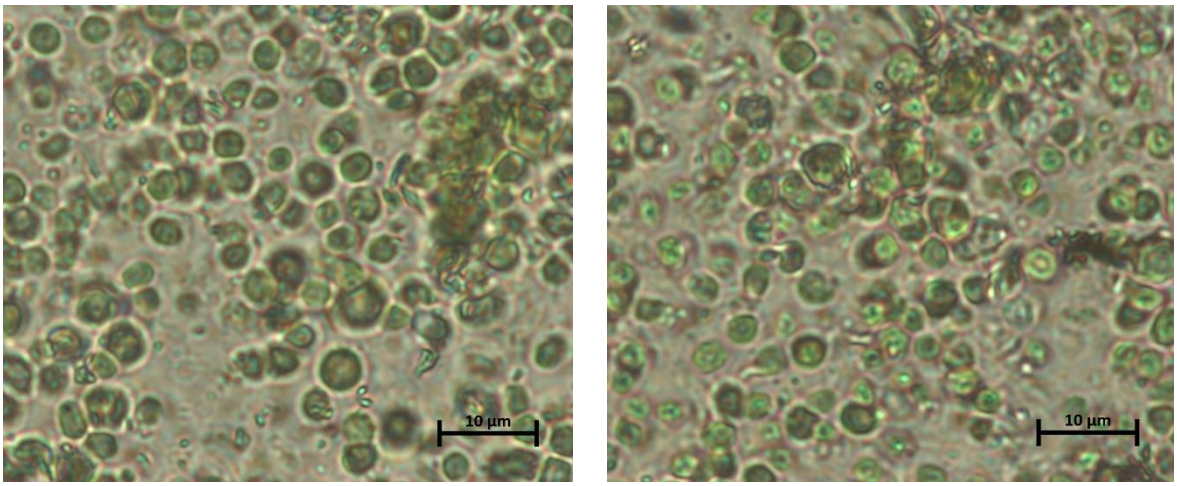

Figure 19: Chlorella sorokiniana 211-8k manually ground in liquid nitrogen. Examined with Axioplan 2 microscope with HAL 100 lamp and 100x magnification

Microscopic observations found damaged cells and aggregates of cell debris (Figure 19).

Chemical-based cell disruption

The efficiency of NaOH-based cell disruption (chapter 2.2.4) was evaluated by automated cell-count and -sizing via Coulter Counter.

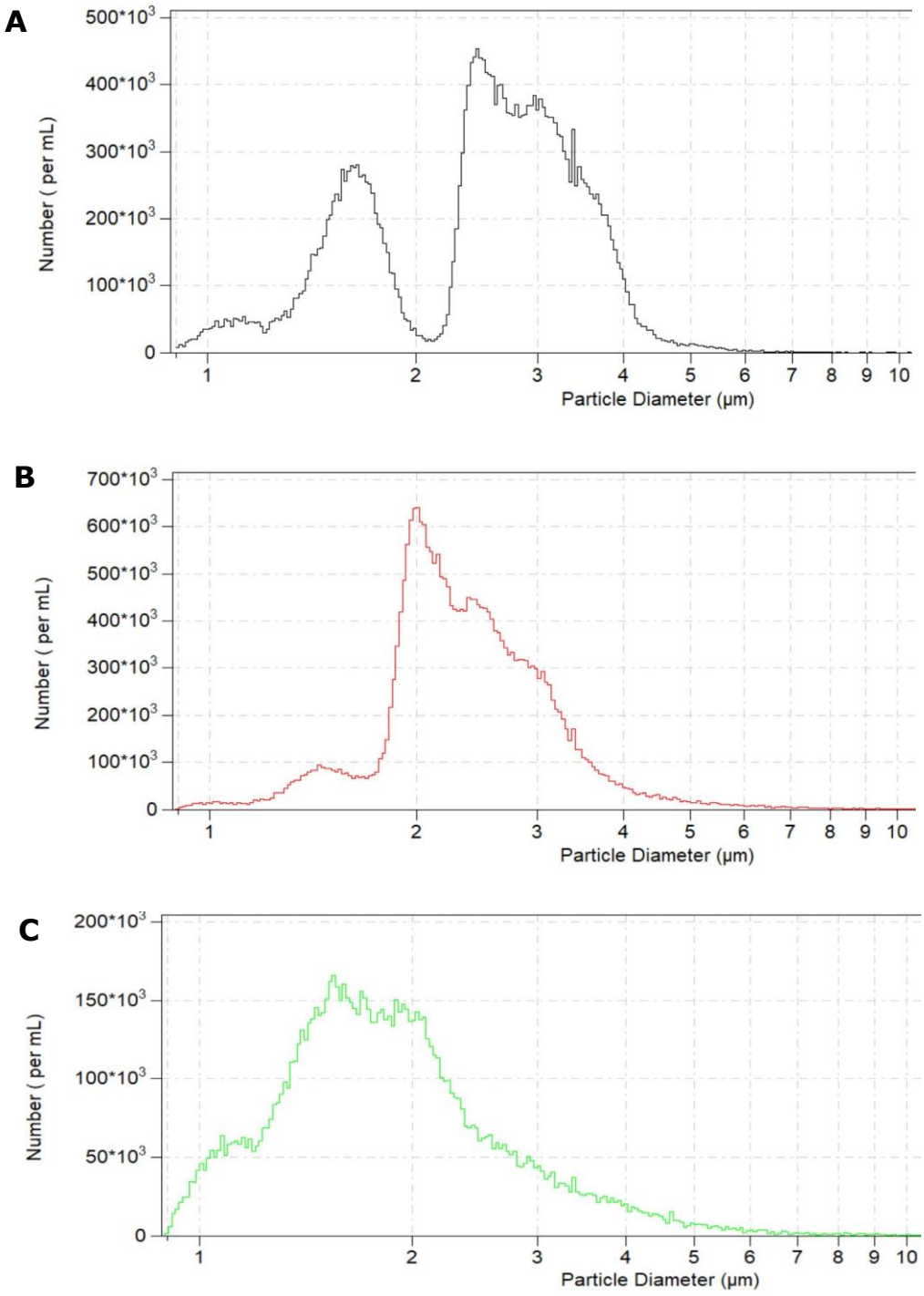

Figure 20: Cell size and number of Chlorella sorokiniana 211-8k determined by Coulter Counter. After harvest (A); after freeze-drying (B); after freeze-drying and 1 mol/L NaOH treatment (C).

After harvest, the culture showed one peak of cell wall debris between 0.9 – 2 µm with a total of 8.4 x 10^6 particles/mL (maximum at 1.6 µm with 280 x 10^3 particles/mL) (Figure 20A). The second peak of daughter and mature cells between 2 – 5 µm showed a total of 19.1 x 10^6 particles/mL (maximum at 2.4 µm with 454 x 10^3 particles/mL, median 2.9 µm) (Figure 20A).

After freeze-drying, the peak of debris decreased to 7.1 x 10^6 particles/mL (84 %, maximum at 2.0 µm with 640 x 10^3 particles/mL) (Figure 20B). The cell peak increased to 19.5 x 10^6 particles/mL (102 %, maximum at 2.0 µm with 640 x 10^3 particles/mL, median 2.5 µm) (Figure 20B). This can be explained by clumping of cell wall debris, due to lyophilization.

After 1 mol/L NaOH treatment, the debris peak remained at 6.9 x 10^6 particles/mL (82 %, maximum at 1.5 µm with 165 x 10^3 particles/mL) (Figure 20C). In contrast, the cell peak sharply decreased to 3.8 x 10^6 particles/mL (19 %, maximum at 2.0 µm with 142 x 10^3 particles/mL) (Figure 20C). The decrease in the total amount of overall particles can be explained by hydrolyzation of the cells and cell debris to a smaller diameter than the Coulter Counter threshold. To confirm the successful cell disruption, the cells were checked microscopically (Figure 21).

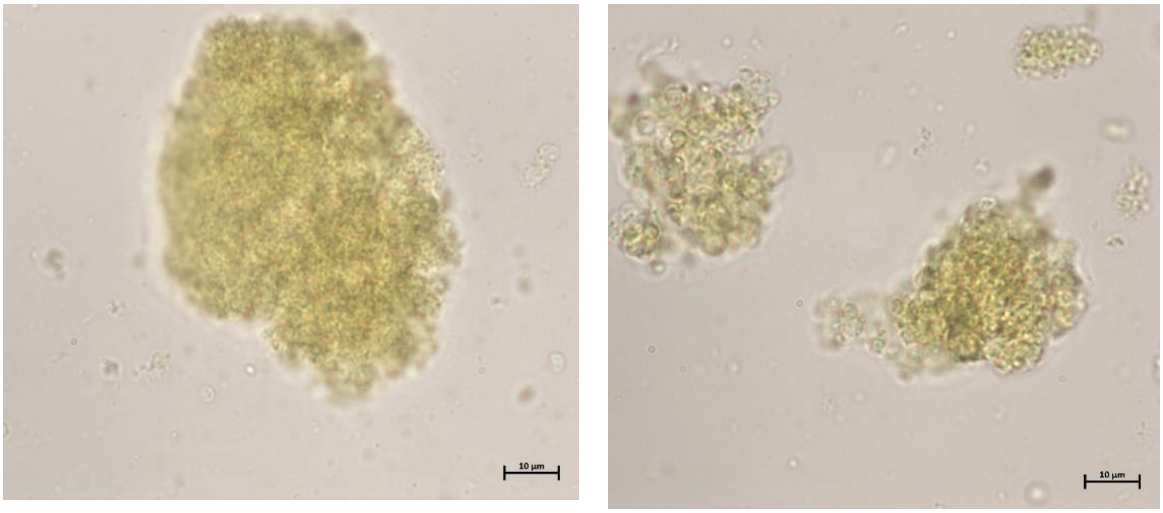

Figure 21: Chlorella sorokiniana 211-8k after hydrolysis with 1 mol/L NaOH. Procedure shown in chapter 2.2.4.; examined with Axioplan 2 microscope with HAL 100 lamp and 100x magnification.

After hydrolysis, only aggregates of cell wall debris and cell residues were visible (Figure 21). No intact cells were found in the sample (Figure 21). The second peak in Figure 20C can be caused by clumping of cell residues and not by intact cells left in the sample.

Cell wall related monosaccharide release

In a second step, the efficiencies of the three different disruption methods (chapter 2.2.4), were compared for the amount of released cell wall sugars in *Chlorella sorokiniana* (chapters 2.2.5 - 2.2.7). The comparison of the total amount of released cell wall sugars is shown below (Figure 22).

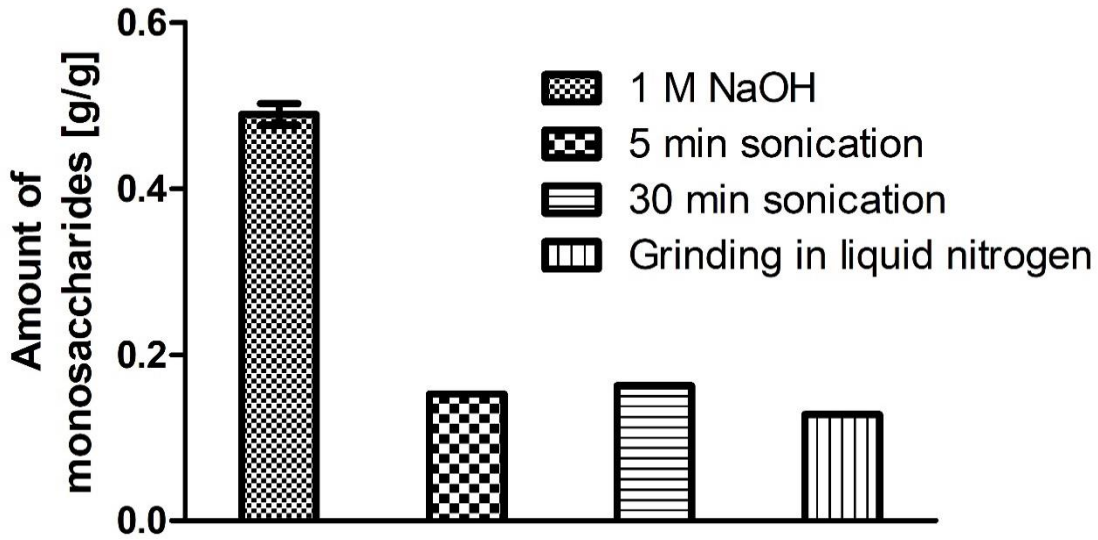

Figure 22: Comparison of the total amount of monosaccharides detected after disruption of Chlorella sorokiniana 211-8k. Procedures are explained in chapter 2.2.4; cell wall monosaccharides were isolated as described in chapters 2.2.5 - 2.2.7; 1 mol/L NaOH ( ): small squares; 5 min Sonication ( ): big squares; 30 min Sonication ( ): horizontal lines; grinding in liquid nitrogen ( ): vertical lines; n = 2 for 1 mol/L NaOH, error bar indicates standard deviation; n = 1 for sonication (5/30) and grinding in liquid nitrogen; Glc is not considered as a cell wall related monosaccharide.

The NaOH-based cell disruption released nearly three-fold more (~ 296 %) detectable monosaccharides than the mechanical methods. Strikingly, only minor differences were found between the 5 and 30 min sonication. This indicates that, despite the five-fold increase in broken EB-positive cells after 30 min sonication, the cell wall ruptured but sugars remained chemically bond. The grinding in liquid nitrogen showed the lowest monosaccharide release.

For the in-depth analysis of the cell wall monosaccharide composition the alkali catalyzed hydrolysis was chosen. The following chapter describes the results in closer detail.

3.4 Monosaccharide composition

The results for the monosaccharide composition will be shown for two different fractions as well as for each algal specie at three life cycle stages. The two fractions are distinguished according to their hydrolyzation medium in the i) hemicellulose fraction susceptible to hydrolysis with 2 mol/L trifluoroacetic acid, and ii) the recalcitrance fraction susceptible to 6 mol/L HCl.

Data for glucose are not shown, because it was not possible to distinguish between the storage and structural Glc originating from starch and cell wall polysaccharides, respectively. Due to technical problems at the HPAEC-PAD, the presented data contain an unbalanced number of repetitions and need to be evaluated as tentative. Conclusive data will be presented in Robertz et al., 2022 (in progress).

Chlorella sorokiniana 211-8k

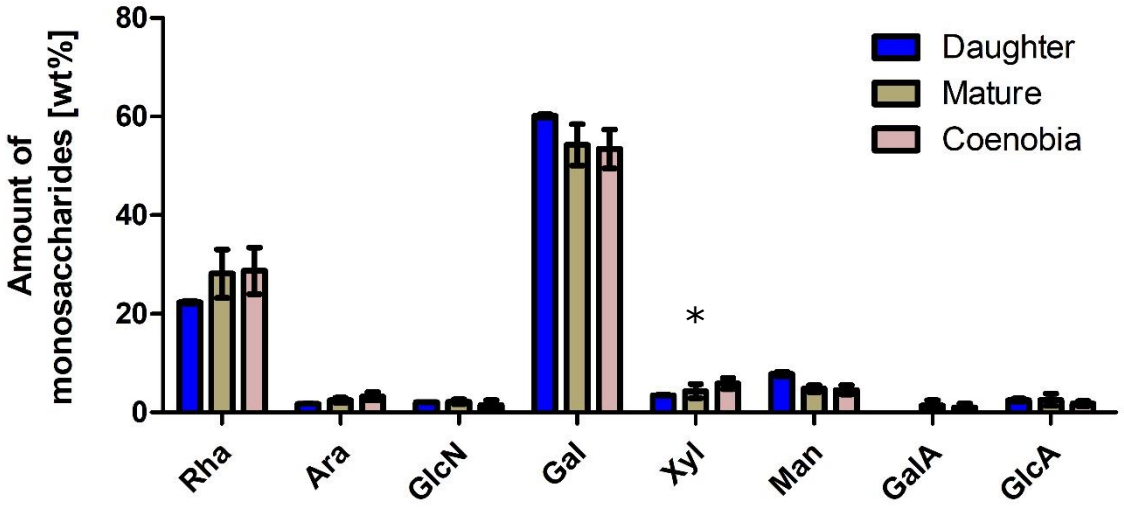

*Figure 23: Cell wall monosaccharides of the hemicellulose fraction of Chlorella sorokiniana 211-8k at three cell-cycle stages. Cell population of daughter (■), mature (■) and coenobia (■); amount of individual monosaccharides in wt% relative to the total amount of detected monosaccharides; procedure shown in chapter 2.2.7; n = 2 for daughter, n = 8 for mature, n = 6 for coenobia; error bars indicate standard deviation; Kruskal-Wallis test: * = 0.05 > p > 0.01; not significant differences are not indicated.*

The hemicellulose fraction of *C. sorokiniana* daughter cells held 60 ± 0.2 and 22 ± 0.2 % of galactose and rhamnose, respectively (Figure 23). Low amounts of mannose (7.7 ± 0.3 %) and arabinose, glucosamine, xylose, and glucuronic acid (< 4 %, each) were detected.

Cell walls of mature cells contained 54 ± 3.7 and 28 ± 4.3 % Gal and Rha, respectively. Coenobia cell walls contained 53 ± 3.3 and 28 ± 4.0 % Gal and Rha, respectively. The decrease in Gal and increase of Rha, compared to daughter cells, could indicate modification of the cell wall during the maturation. Yet, no significant difference could be found between the three life cycle stages. Interestingly, traces of galacturonic acid were not found in daughters, but in mature (1.4 ± 1 %) and coenobia (1 ± 0.7 %) cell walls.

The Kruskal-Wallis-Test indicated significant differences between the life cycle stages only for Xyl ($p = 0.028$) (daughter 3.5 ± 0.3 %; mature 4.3 ± 1.3 %; coenobia 5.9 ± 1 %). Due to the low number of replicates no multiple comparison test was performed.

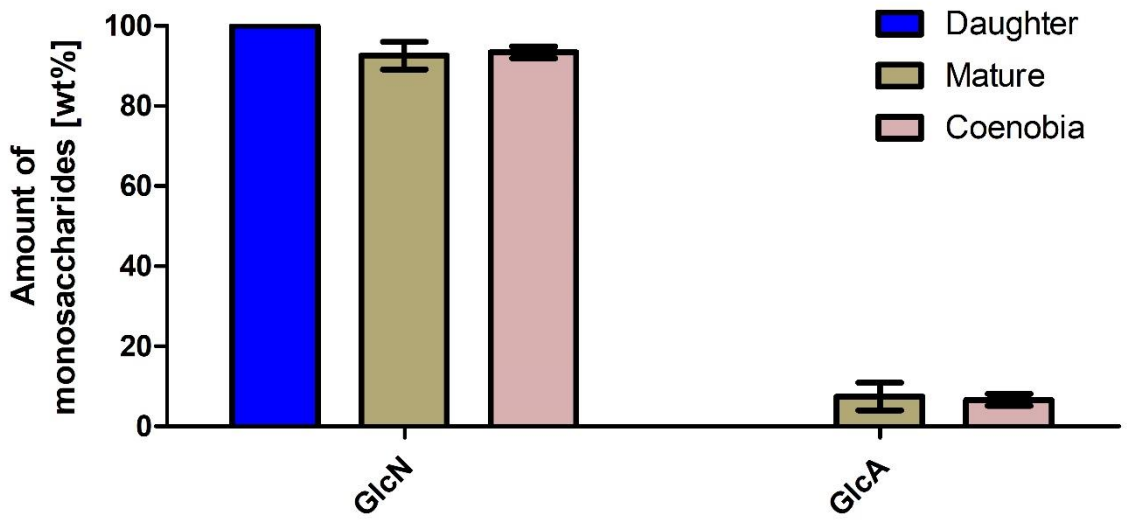

Figure 24: Cell wall monosaccharides of the recalcitrance fraction of Chlorella sorokiniana 211-8k. Cell population of daughter (■), mature (■) and coenobia (■); amount of individual monosaccharides in wt% relative to the total amount of detected monosaccharides; procedure shown in chapter 2.2.7; n = 2 for daughter, n = 3 for mature, n = 2 for coenobia; error bars indicate standard deviation.

The recalcitrance cell wall fraction of daughter cells was only composed of GlcN, while the other life cycle stages contained GlcN and GlcA (Figure 24). Mature cell walls contained 92 ± 2.8 % 7.5 ± 2.8 % GlcN and GlcA, respectively. The recalcitrance fraction of coenobia contained 93 ± 1 % and 6.6 ± 1 % GlcN and GlcA, respectively.

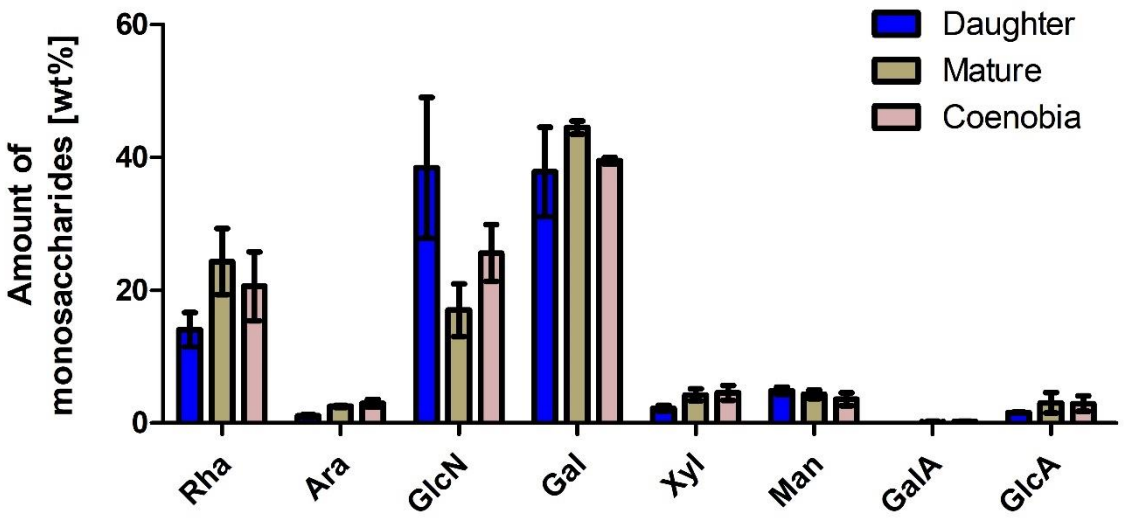

Figure 25: Monosaccharide composition of the cell walls of Chlorella sorokiniana 211-8k. Cell population of daughter (■), mature (■) and coenobia (■); amount of individual monosaccharides in wt% relative to the total amount of detected monosaccharides; procedure shown in chapter 2.2.7; n = 2 for daughter, n = 3 for mature, n = 2 for coenobia; error bars indicate standard deviation.

The overall cell wall monosaccharide composition of *C. sorokiniana* changed throughout its life cycle (Figure 25). The daughter cell walls consisted to 38 ± 7.4 %, 38 ± 4.7 % and 14 ± 1.8 % of GlcN, Gal and Rha, respectively. In contrast, mature cells held 17 ± 2.8 %, 44 ± 0.7 % and 24 ± 3.5 % GlcN, Gal and Rha, respectively (Figure 25). Similar, coenobia held 25 ± 2.5 %, 39 ± 0.3 % and 20 ± 3 % GlcN, Gal and Rha, respectively (Figure 25). Additionally, daughter cell walls contained Man (4.8 ± 0.3 %), GlcA (1.6 ± 0.05 %), Xyl (2.2 ± 0.3 %) and Ara (1 ± 0.14 %). Apart from Man, the proportions of the individual monosaccharides were lower in daughter cell walls, compared to the other two life cycle stages. This and the changes in the amounts of Rha and Gal indicate an increase in the hemicellulose fraction during cell maturation.

Chlorella vulgaris 211-11b

The monosaccharide composition of the hemicellulose fraction of *C. vulgaris* is shown below.

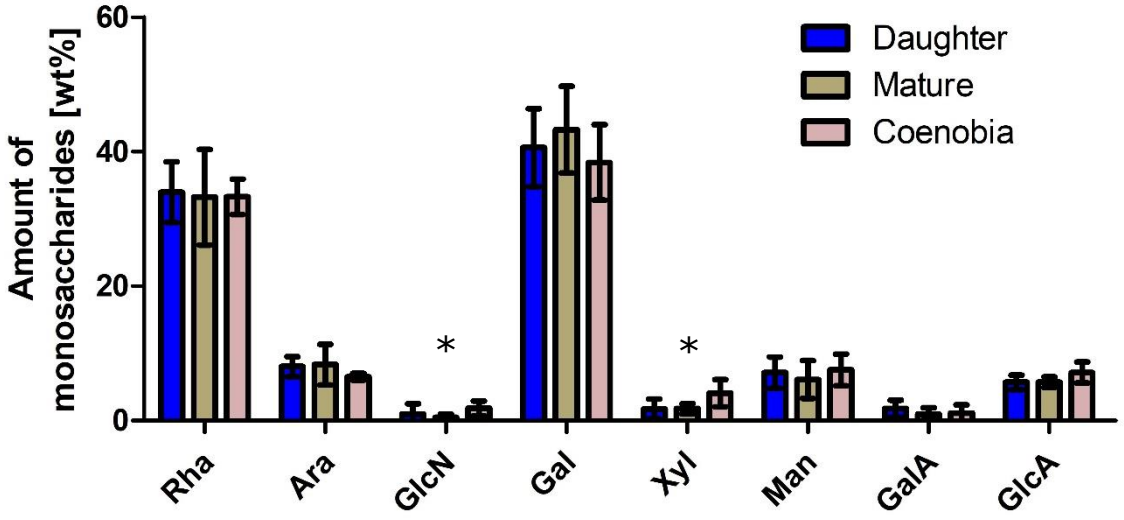

*Figure 26: Cell wall monosaccharides of the hemicellulose fraction of Chlorella vulgaris 211-11b. Cell population of daughter (■), mature (■) and coenobia (■); amount of individual monosaccharides in wt% relative to the total amount of detected monosaccharides; procedure shown in chapter 2.2.7; n = 9 for daughter, n = 8 for mature, n = 6 for coenobia; error bars indicate standard deviation; Kruskal-Wallis test: not significant differences are not indicated; if * = 0.05 ≥ p ≥ 0.01, pairwise Wilcoxon Test was conducted with adjusted p according to Bonferroni: ns: p > 0.0167.*

The hemicellulose fraction of daughter cell walls of *C. vulgaris* consisted mainly of Rha and Gal, 34 ± 4.3 % and 40 ± 5.5 %, respectively (Figure 26). Smaller amounts of Ara (8.5 ± 0.7 %), Man (7.4 ± 1.9 %) and GlcA (5.6 ± 1.0 %) were detected. Additionally, 1.7 ± 1.3 %, 0.7 ± 0.7 % and 1.9 ± 1.3 % of Xyl, GlcN and GalA, respectively, were found (Figure 26).

Mature cells consisted of 33 ± 6.6 % and 43 ± 6.1 % Rha and Gal, respectively (Figure 26). Coenobia cell walls contained 33 ± 2.4 % and 38 ± 5.1 % Rha and Gal, respectively.

The Kruskal-Wallis Test indicated significant differences for the Xyl and GlcN proportion, however the Wilcoxon test with adjusted p showed no significant differences between the individual groups.

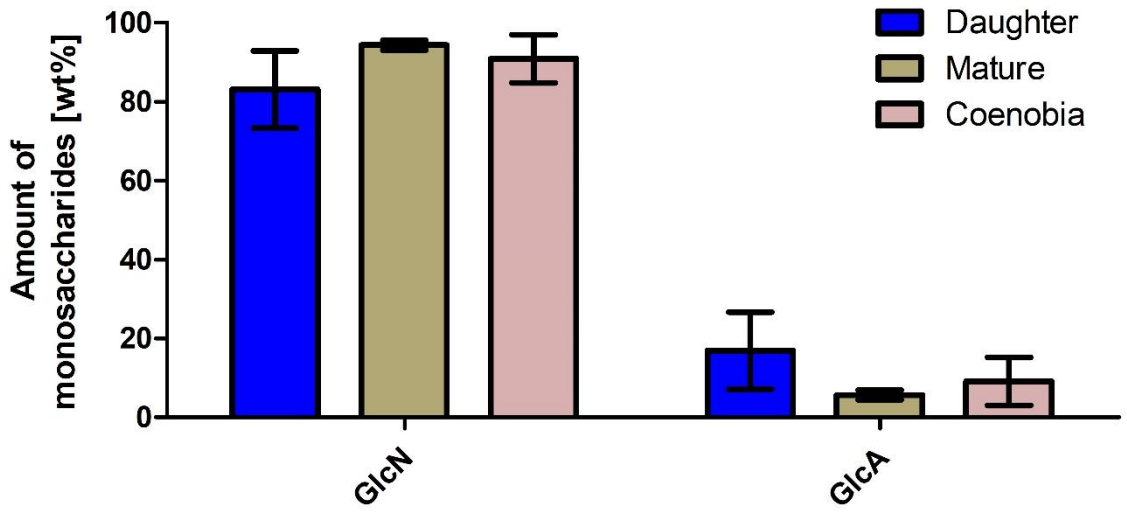

Figure 27: Cell wall monosaccharides of the recalcitrance fraction of Chlorella vulgaris 211-11b. Cell population of daughter (■), mature (■) and coenobia (■); amount of individual monosaccharides in wt% relative to the total amount of detected monosaccharides; procedure shown in chapter 2.2.7; n = 3 for daughter, n = 2 for mature, n = 2 for coenobia; error bars indicate standard deviation.

The recalcitrance fraction of *C. vulgaris* consisted of GlcN and GlcA throughout the entire life cycle (Figure 27). Daughter cell walls held 83 ± 8 % and 17 ± 8 % GlcN and GlcA, respectively. The recalcitrance fraction of mature cell walls was composed of 94 ± 0.8 % GlcN and 5.6 ± 0.8 % GlcA. Coenobial cell walls of 91 ± 4.3 % GlcN and 9 ± 4.3 % GlcA.

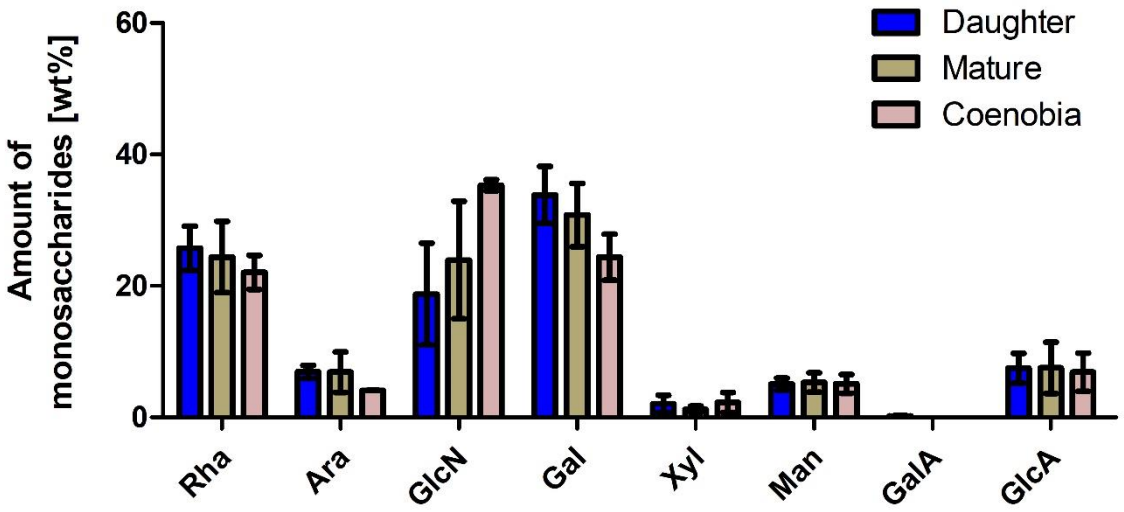

Figure 28: Monosaccharide composition of the cell walls of Chlorella vulgaris 211-11b. Cell population of daughter (■), mature (■) and coenobia (■); amount of individual monosaccharides in wt% relative to the total amount of detected monosaccharides; procedure shown in chapter 2.2.7; n = 3 for daughter, n = 3 for mature, n = 2 for coenobia; error bars indicate standard deviation.

C. vulgaris daughter cell walls consisted of 18 ± 5.5 % 31 ± 3.9 % and 24 ± 0.5 % GlcN, Gal and Rha, respectively (Figure 28). Additionally, Ara (6.9 ± 0.8 %), Man (5.1 ± 0.7 %), Xyl (2.1 ± 1.1 %) and GlcA (7.9 ± 1.2 %) were found. Interestingly, GalA was only detected in daughter cell walls (0.2 ± 0.1 %).

Mature cell walls consisted of 24 ± 6.3 %, 29 ± 5 %, 22.6 ± 3 % and 6.9 ± 2.2 % GlcN, Gal, Rha and Ara, respectively (Figure 28). Coenobia held 35 ± 0.5 %, 24 ± 2 %, 22 ± 1.5 % and 4.1 ± 0.01 % GlcN, Gal, Rha and Ara, respectively (Figure 28). The amount of GlcA was almost constant during the life cycle (mature 8.7 ± 4.2 %; coenobia 6.9 ± 1.7 %), which is also true for the proportions of Xyl (mature 1.2 ± 0.3 %; coenobia 2.3 ± 0.9 %) and Man (mature 5.3 ± 1.0 %; coenobia 5.1 ± 0.8 %) (Figure 28).

These results indicate that the hemicellulose fraction decreases during cell maturing, while the recalcitrance fraction, especially the proportion of GlcN, increases.

Parachlorella kessleri 211-11g

The composition of the hemicellulose fraction of *P. kessleri* is depicted below.

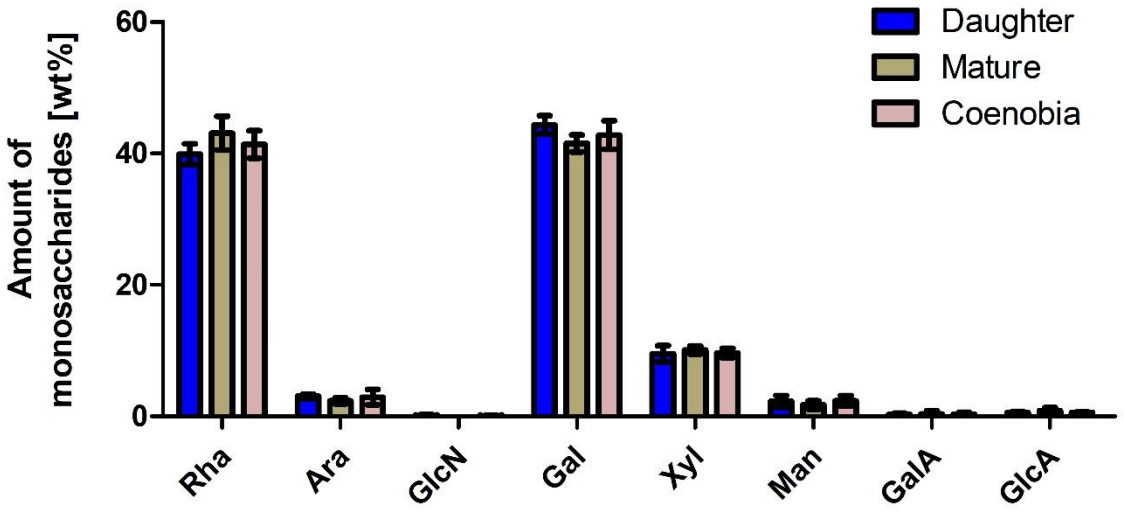

Figure 29: Cell wall monosaccharides of the hemicellulose fraction of Parachlorella kessleri 211-11g. Cell population of daughter (■), mature (■) and coenobia (■); amount of individual monosaccharides in wt% relative to the total amount of detected monosaccharides; procedure shown in chapter 2.2.7; n = 9 for daughter, n = 4 for mature, n = 9 for coenobia; error bars indicate standard deviation.

The hemicellulose fraction of *P. kessleri* daughter cells was mainly composed of Gal, Rha and Xyl with 44 ± 1.3 %, 39 ± 1.5 % and 9.5 ± 1.2 %, respectively (Figure 29). Only slight changes occurred during the life cycle. Mature cell walls contained 41 ± 1.1 %, 43 ± 2.2 % and 10 ± 0.5 % Gal, Rha and Xyl, respectively (Figure 29). Coenobia cell walls contained 43 ± 1.9 %, 41 ± 1.9 % and 9.6 ± 0.7 % Gal, Rha and Xyl, respectively. Additionally, Ara, GlcN, Man, GalA and GlcA (< 4 % each) were detected across all life cycle stages. No indication for the presence of Fuc was found.

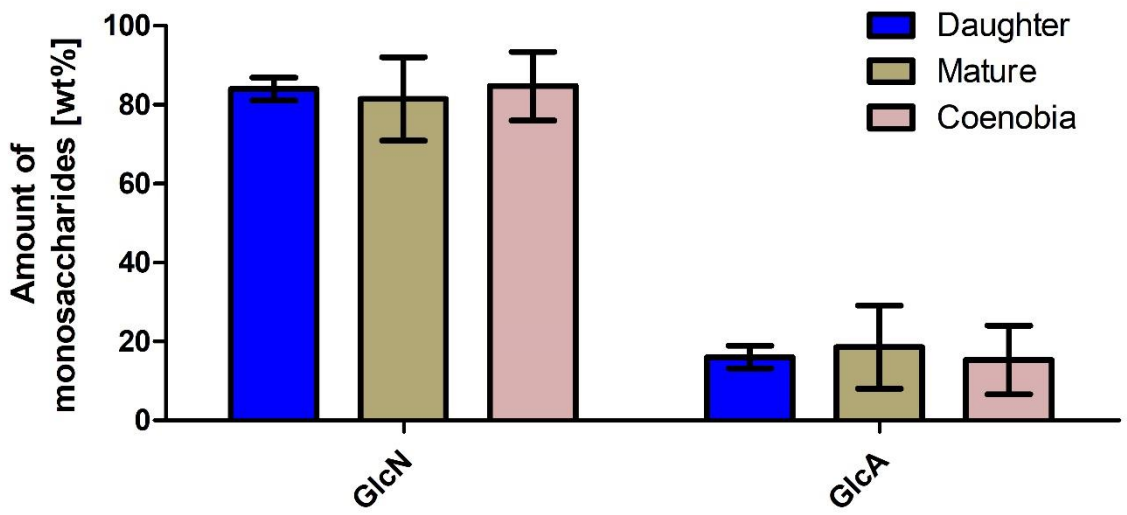

Figure 30: Monosaccharides of the recalcitrance fraction of Parachlorella kessleri 211-11g cell walls. Cell population of daughter (■), mature (■) and coenobia (■); amount of individual monosaccharides in wt% relative to the total amount of detected monosaccharides; procedure shown in chapter 2.2.7; n = 3 for daughter, n = 2 for mature, n = 3 for coenobia; error bars indicate standard deviation.

The recalcitrance fraction of *P. kessleri* consisted of GlcN and GlcA throughout the entire life cycle (Figure 30). The proportions only changed slightly. Daughter cell walls consisted of 84 ± 2.4 % GlcN and 16 ± 2.4 % GlcA, mature cells of 81 ± 7 % and 19 ± 7 % GlcN and GlcA, respectively, and coenobia of 85 ± 6 % and 15 ± 6 % GlcN and GlcA, respectively.

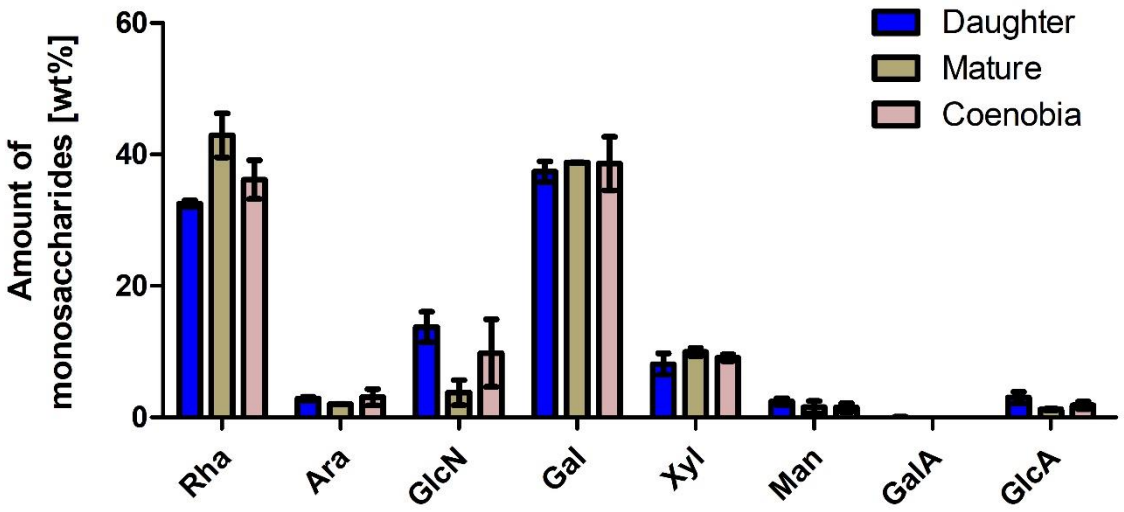

Figure 31: Monosaccharide composition of the cell walls of Parachlorella kessleri 211-11g. Cell population of daughter (■), mature (■) and coenobia (■); amount of individual monosaccharides in wt% relative to the total amount of detected monosaccharides; procedure shown in chapter 2.2.7; n = 3 for daughter, n = 2 for mature, n = 3 for coenobia; error bars indicate standard deviation.

Even though there were no huge differences in the proportions of each individual fraction, the combined monosaccharide composition of *P. kessleri* differs when the cell ages (Figure 31). Daughter cell walls consist of 37 ± 1.1 %, 32 ± 0.4 % and 13 ± 1.6 % Gal, Rha and GlcN, respectively. Additionally, Ara (2.9 ± 0.3 %), Man (2.4 ± 0.4 %) and GlcA (3.0 ± 0.7 %) were detected (Figure 31).

Especially the proportion of GlcN decreases as daughter cells mature. Mature cell walls consist of 38 ± 0.1 %, 43 ± 1.9 % and 3.8 ± 1.1 % Gal, Rha and GlcN, respectively (Figure 31). In coenobial walls 38 ± 2.9 % Gal, 36 ± 2.1 % Rha and 9.8 ± 3.6 % GlcN were detected. Additionally, the amount of GlcA in daughter cells was the highest, compared to the other life cycle stages (mature 1.2 ± 0.1 %; coenobia 1.8 ± 0.4 %). There were only minor changes between the other monosaccharides across the life cycle stages.

These results indicate that daughter cell walls consist mainly of recalcitrance cell wall, while the amount of hemicellulose increases during cell aging.

3.5 Autolysin

This chapter will show the results of the Autolysin extraction and the consecutive assays in closer detail for *C. sorokiniana* and *P. kessleri*. For *Chlorella vulgaris* we were not able to obtain cultures with more than 20 % coenobia, due to unsynchronous growth and unexpected cell divisions in the light-period. Therefore, no Autolysin results are available.

3.5.1 Endo-1,3-β-Glucanase activity

Based on the results of the histochemical analyses and on the monosaccharide composition of the cell walls, we supposed an endo-1,3-β-Glucanase activity of autologous Autolysin from our *Chlorellaceae*. We tested our hypothesis with a 1,3-β-Glucanase kit and the endo-1,3-β-Glucanase from *Trichoderma sp.* (EC 3.2.1.39) of Megazyme®.

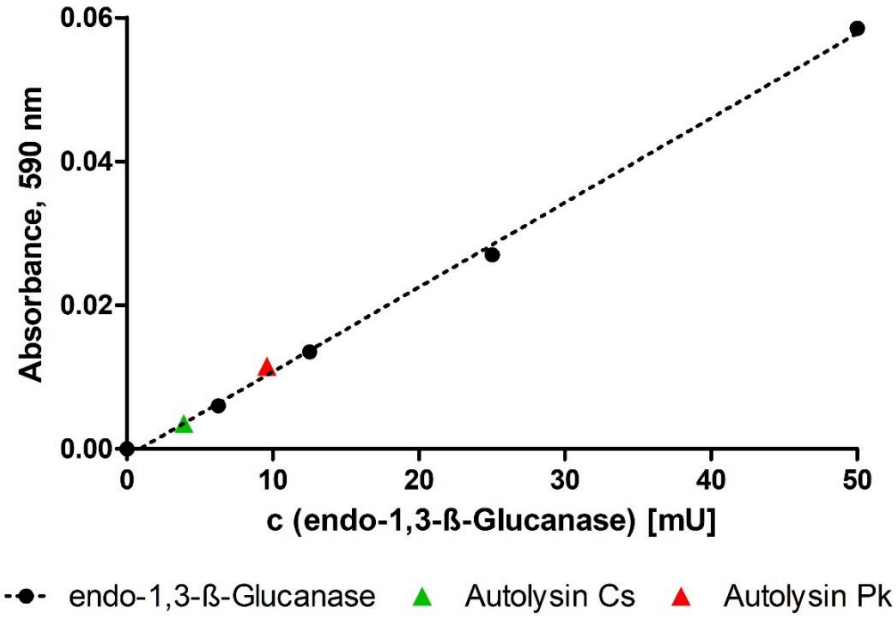

Figure 32: Activity of Autolysin from Chlorella sorokiniana 211-8k and Parachlorella kessleri 211-11g in endo-1,3-ß-Glucanase assay. Procedure described in chapter 2.2.9; endo-1,3-ß-Glucanase (Trichoderma sp., ●); Autolysin Cs (C. sorokiniana, ▲); Autolysin Pk (P. kessleri, ▲); x-axis: concentration of endo-1,3-ß-Glucanase in mU; y-axis: Absorbance at 590 nm.

Autolysin extracted from *C. sorokiniana* showed an endo-1,3-β-Glucanase activity of 3.9 mU (Figure 32). The initial culture had a cell count of 0.83 x 10^9 cells/mL, with a total volume of 100 mL. This results in an active Autolysin concentration of ~9.9 mU/10^9 cells.

The extract of *P. kessleri* showed a specific activity of 9.6 mU (Figure 32). With a total volume of 100 mL and a cell number of 1.76 x 10^9 cells/mL, yielding an Autolysin concentration of ~10.9 mU/10^9 cells.

3.5.2 Cell specific activity

As described in chapter 2.2.10, cultures of different strains and different life cycle stages were digested with Autolysin.

No clear activity was found for Autolysin from *C. sorokiniana* on mixed populations of *C. sorokiniana*. Even in enzymatic treatments with 8-fold concentrated Autolysin (Figure 33).

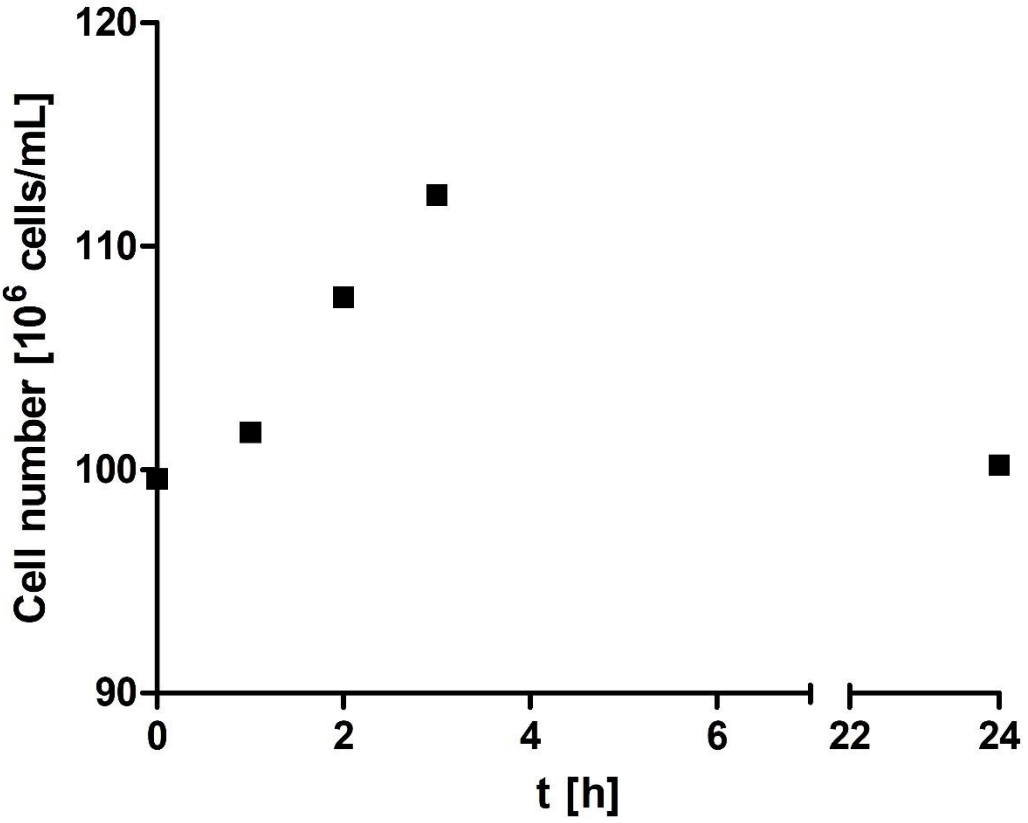

Figure 33: Cell number of Chlorella sorokiniana 211-8k treated with autologous Autolysin from Chlorella sorokiniana 211-8k. Procedure described in chapter 2.2.8, 8-fold concentrated Autolysin; x-axis: time in hours; y-axis: cell number in 10^6 cells per mL, counted with Neubauer counting chamber (improved).

The initial cell count of *C. sorokiniana* was 99.6 x 10^6 cells/mL (Figure 33). After 1 h, 101.6 x 10^6 cells/mL (102 %) were counted. The cell number continued to increase to 112 x 10^6 cells/mL (112 %), at 3 h. However, the cell count dropped to 100 x 10^6 cells/mL (100.6 %), after 24 h (Figure 33). One possible explanation for this increase and drop in the cell count could

be a premature release of daughter cells caused by Autolysin activity within the first 3 h, yet those premature autospores failed to mature and degraded. No cell leakages or unusual cell wall degradations were observed for daughter and mature cells, which indicated that the cell wall is resistant to Autolysin activity at this time point. Degradations of coenobia are not clearly attributable to the activity of extracellular Autolysin, as coenobial cell wall burst is a natural process during hatching.

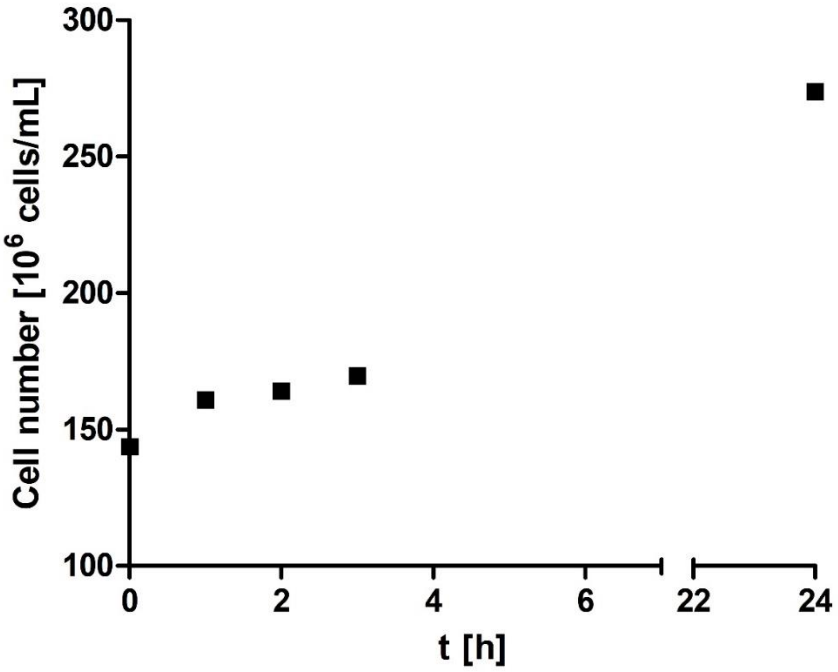

Figure 34: Cell number of Chlorella vulgaris 211-11b digested with Autolysin from Chlorella sorokiniana 211-8k. Procedure described in chapter 2.2.8; x-axis: time in hours; y-axis: cell number in 10^6 cells per mL, counted with Neubauer counting chamber (improved).

No cross-activity was found between Autolysin obtained from *C. sorokiniana* and coenobia of *C. vulgaris* (Figure 34). Within the first hour, the cell number of *C. vulgaris* increased from 143 x 10^6 cells/mL to 160 x 10^6 cells/mL (111 %) (Figure 34). In the next 2 h the cell number further increased by 5 x 10^6 cells/mL per hour to 170 x 10^6 cells/mL (118 %). After 24 h, including a dark period, the coenobia released their daughter cells and the cell number increased to 273 x 10^6 cells/mL (190 %,

Figure 34). No unusual signs of cell wall breakage or cell leakage were found in this culture (Figure 35).

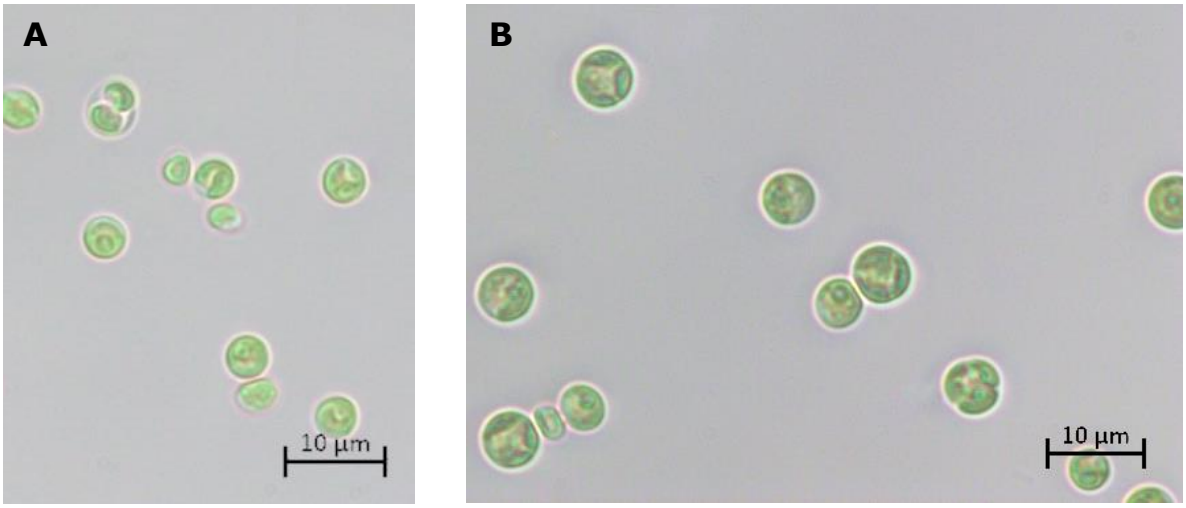

Figure 35: Cells of Chlorella vulgaris 211-11b treated with heterologous Autolysin from Chlorella sorokiniana 211-8k. Control (A) and treated cells after 1 h (B); procedure explained in chapter 2.2.10; examined with Axioplan 2 microscope with HAL 100 lamp and 100x magnification.

Likewise, Autolysin from *P. kessleri* showed no cross-activity on *C. vulgaris* cells. Over 24 h, the cell number remained relatively stable at 97 % of the initial cell concentration (data not shown).

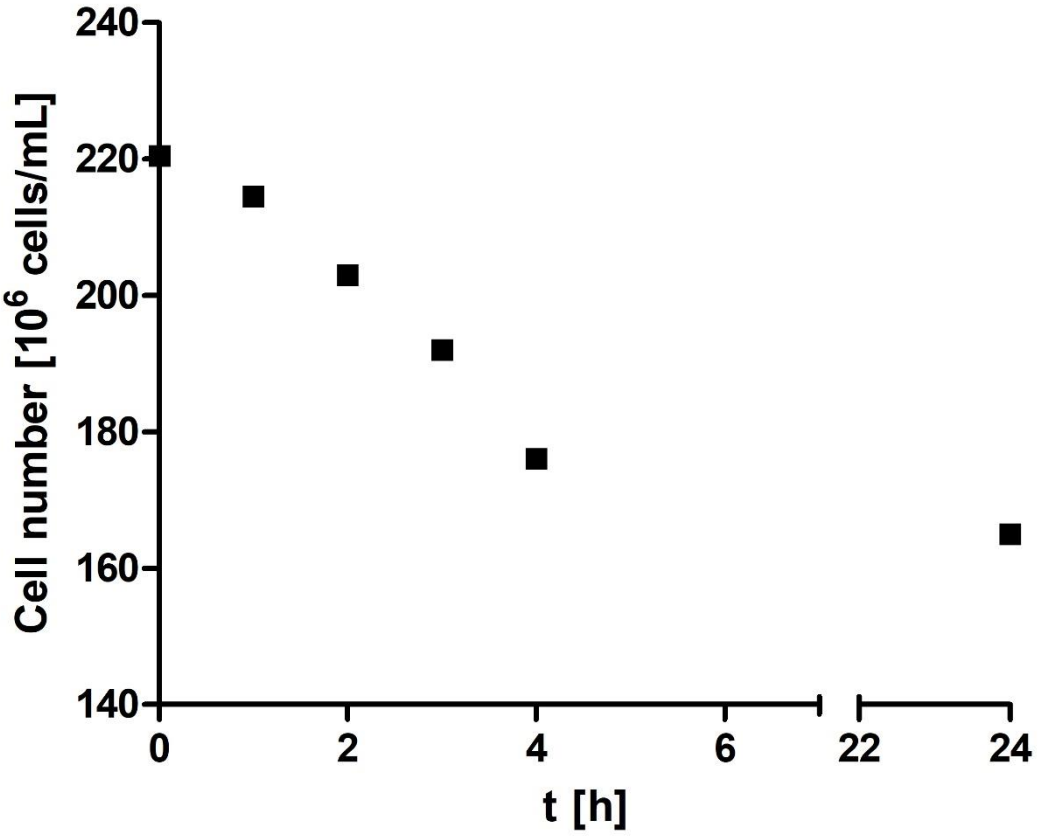

Figure 36: Cell number of Parachlorella kessleri 211-11g digested with Autolysin from Parachlorella kessleri 211-11g. Procedure described in chapter 2.2.8; x-axis: time in hours; y-axis: cell number in 10^6 cells per mL, counted with Neubauer counting chamber (improved).

Autolysin from *P. kessleri* showed a strong activity on its coenobia (Figure 36). The initial cell count of *P. kessleri* was 220 x 10^6 cells/mL (Figure 36). In 1 h, the cell number decreased to 214 x 10^6 cells/mL (97 %). The cell number continued to decrease to 176 x 10^6 (80 %) and 165 x 10^6 cells/mL (75 %) at 4 and 24 h, respectively. This hold could indicate a degradation of Autolysin or depletion of susceptible cells over time.

Microscopic images, taken during the treatment, indicate this enzymatic activity of the autologous Autolysin on *P. kessleri* cells (Figure 37).

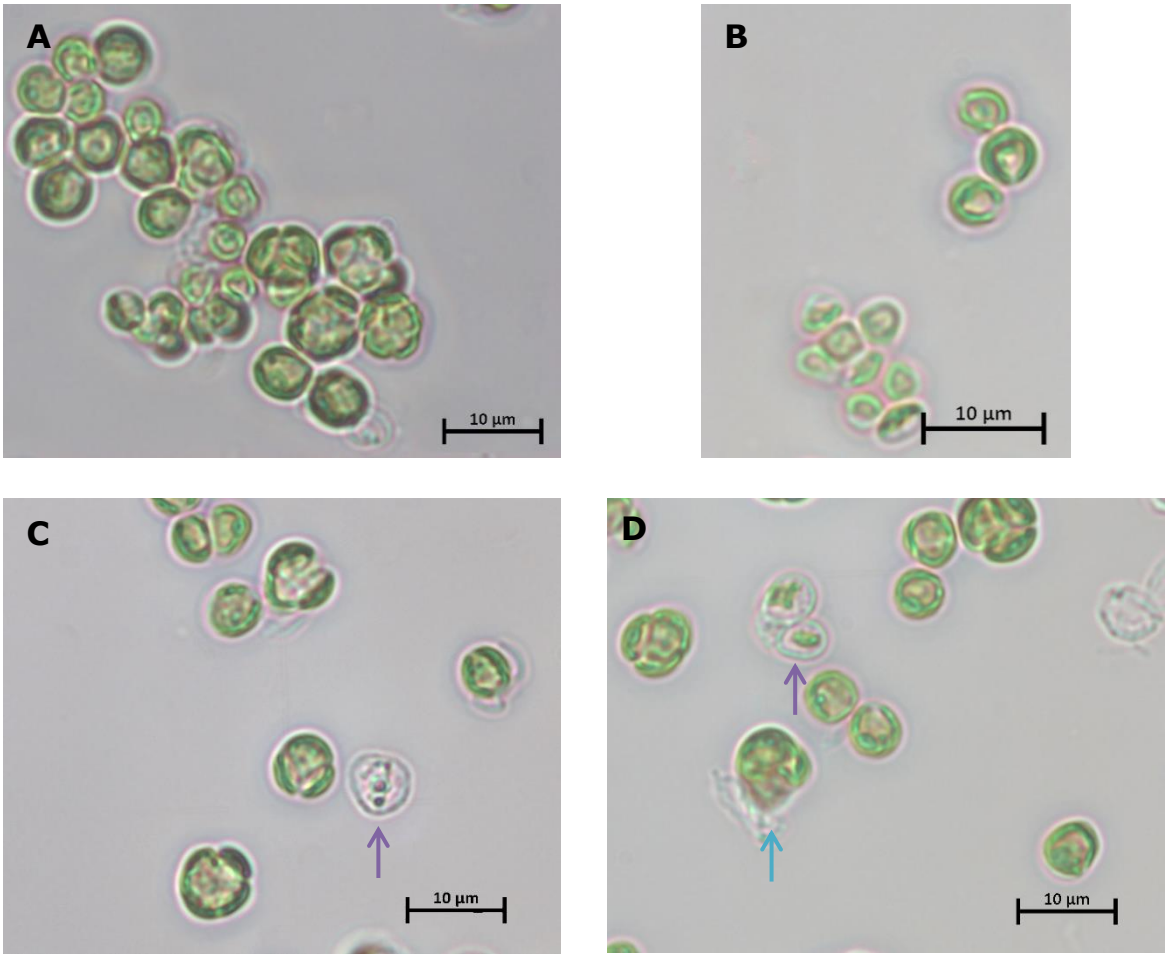

Figure 37: Microscopic images of Parachlorella kessleri 211-11g cells treated with autologous Autolysin. Pictures taken at 0 h (A) and after 1 h (B), 2 h (C) and 3 h (D); procedure explained in chapter 2.2.10; examined with Axioplan 2 microscope with HAL 100 lamp and 100x magnification; ghost cell (↑), leaking cell (↑).

The cells of *P. kessleri* clustered at the beginning of the digestion (Figure 37A). This is caused by the centrifugation during Autolysin extraction from the culture. After 1 h, young daughter cells were released (Figure 37B), which would result in a cell number increase. However, as shown before, the cell number already decreased by 3 % (Figure 36). This is a first hint for the activity of Autolysin. After 2 and 3 h of digestion, ghost cells were visible in the culture (Figure 37C/D, purple arrows). They are caused by degradation of the cell walls by Autolysin and leaking of the cell inner (Figure 37D, turquoise arrow). The supernatant of the Autolysin digestion was analyzed with the HPAEC-PAD, but no monosaccharides were detected. This either indicates that Autolysin digestion produces oligosaccharides, or that the concentration of monosaccharides was below the detection limit.

4 Discussion

4.1 Growth experiment

The three different *Chlorellaceae* strains were cultivated under the same growth conditions to obtain comparable results in this work. These conditions were specifically chosen to reliably harvest individual populations (daughter cells, mature cells and coenobia) and mimic industrial cultivation systems as close as possible on a laboratory scale. However, this implies that the strains are not grown under their inert optimal conditions.

Chlorella sorokiniana 211-8k is well-known for its temperature resilience. According to Wu and co-workers, the optimal growth temperature is 39 °C, with a generation time of only 8 h. Cultivated at 31 °C, the generation time was prolonged to 24 h (Wu, Tischner and Lorenzen, 1986). The growth behavior shown under our specific conditions indicates a generation time of *Chlorella sorokiniana* 211-8k of 72 h (Figure 5). This slow growth rate is likely to be caused by the low growth temperature (21 ± 1 °C), as temperature effects the entire metabolism. An increase or decrease in temperature of 10 °C can change the metabolic rate by at least two-fold (Bišová and Zachleder, 2014).

Additionally, the illumination intensity and cycle are critical factors for the growth performance. As mentioned above, the light intensity used in this work was 50 ± 10 µmol photons m^{-2} s^{-1} at light/dark periods of 16 : 8 h (chapter 2.2.1). Alternating light and dark periods is an important tool to synchronize alga cultures, which is close to their natural habitats (Bišová and Zachleder, 2014; Hlavová, Vítová and Bišová, 2016; Holdmann *et al.*, 2018). Abiusi and co-workers used an almost 10-times higher light intensity (500 µmol photons m^{-2} s^{-1}) to cultivate *C. sorokiniana* (Abiusi, Wijffels and Janssen, 2020), Malavasi and her group used 90 – 100 µmol photons m^{-2} s^{-1} (Malavasi *et al.*, 2017) and Holdmann and

co-workers cultivated their algae with a photon flux density between 100 and 1700 µmol m^{-2} s^{-1} (Holdmann *et al.*, 2018).

Our relatively low photon flux rate and growth temperature caused a higher generation time of *C. sorokiniana* cultures (Figure 5), than previously reported (Wu, Tischner and Lorenzen, 1986). On the one hand, this might have reduced the synchronicity and development of coenobia to ≤ 60 % in our cultures. On the other hand, *Chlorella* species have a rapid multiple fission cell cycle with consecutive nuclear divisions (M-phase) and a short multinuclear G3-phase (Bišová and Zachleder, 2014). We microscopically observed mainly coenobia of the four-nuclei type (2^2), but the cell number after daughter cell release (300 %) indicated two-nuclei types (2^1), too (Figure 5). These results differ to previous reported results under continuous light. Yamamoto found 89 and 11 % of 2^1 and 2^2 types, respectively, in his cultures (Yamamoto *et al.*, 2003).

The optimal growth temperature for *Chlorella vulgaris* is reported within the range of 25 – 30 °C (Converti *et al.*, 2009; Serra-Maia *et al.*, 2016). Photon flux rates are reported between 37.5 and 980 µmol m^{-2} s^{-1} (Khoeyi, Seyfabadi and Ramezanpour, 2012; Gong *et al.*, 2014; Safi *et al.*, 2014). This wide range might be caused by the use of different strains, however, the light intensity, as well as the temperature used in this work are low compared to other authors. An increase in both is likely to reduce the generation time of *C. vulgaris* (7 days, Figure 6), however it would as well shorten the time-window to harvest specific populations.

The highest amount of coenobia reached, was ≤ 50 %. This indicates a high diversity within the culture. Furthermore, as the cell number (265 %) suggests, the two-nuclei (2^1) type was mainly present in the culture (Figure 1Figure 6). As mentioned in chapter 3.5, the growth of *C. vulgaris* was not as predictable as the growth of the other two species. Cell divisions within the light phase occurred, as well as the development of distinct populations within one culture. This might be caused by the not optimized growth conditions and a higher sensitivity of *C. vulgaris*.

The optimal growth conditions for *Parachlorella kessleri* are 30 °C and 500 µmol m^{-2} s^{-1} (Zachleder *et al.*, 2021). The majority of coenobia were of the 2^2 type, which is also indicated by the daughter cell number (334 %). Autosporulation up to 2^3 was reported for *P. kessleri* 211-11g (Krienitz *et al.*, 2004). As it is true for the other species, the culture conditions used in this work are not optimized for *P. kessleri*. An increase in both, light intensity and temperature would increase the metabolic rate, resulting in faster growth, but reducing the time-window for harvesting the individual populations.

Yet, aim of this work was not to culture the strains towards high growth rates, but to generate industry-related conditions for the cell wall formation. As mentioned before, microalgae tend to change their cell wall compositions, depending on the specific growth conditions (Liang, Sarkany and Cui, 2009; Safi *et al.*, 2014). Therefore, we cultivated under photoautotrophic conditions, diurnal light regime, atmospheric CO_2 supply and ambient temperature. And used glass column reactors bubbled with ambient air, rather than Erlenmeyer flask of lower shear force. Thus, our histochemical and biochemical results of the cell wall composition are more transferable to the industrial cultures than most lab cultures.

4.2 Histochemistry

The application of various *in-vivo* staining methods can provide important information about the cell wall composition, components and its integrity. Thus, we tested specific dyes at the three different life cycle stages of our Chlorellales, presented by young daughters, mature cells and coenobia.

Evans Blue

Evans Blue (EB) stains the cytoplasm and nucleus in blood cells with a degraded plasma membrane (Yao *et al.*, 2018). Additionally, it can be used for plant cell viability tests (Gaff and Okong'o-ogola, 1971). Our results showed that EB is also applicable to both *Chlorella* species, as it selectively stained dead cells and cell wall debris (Table 4). In contrast, *P. kessleri* cells were EB negative throughout, indicating the absence of specific protein targets for EB.

Interestingly, the cell walls of *C. sorokiniana* daughter cells are stained by EB as well. This could either indicate proteinous components in the cell wall of young daughter cells (which are lost during maturation) or extracellularly bond residual proteins. The presence of proteins integrated in the cell walls of *Chlorella* is reported independent of the life cycle point (Baudelet *et al.*, 2017). However, this would result in a positive cell wall staining throughout. The specific staining of young daughter cell walls is in line with the results of Loos and Meindl, who postulated the bounding of enzymes to autospores of *Chlorella fusca* (now: *Scenedesmus vacuolatus* SAG 211-8b). These enzymes are assumed to be responsible for coenobial cell wall breakage during daughter cell release (i.e. the autologous Autolysin) (Loos and Meindl, 1985). Thus, the EB positive result for daughter cell walls might be a first indication for Autolysin in *C. sorokiniana*.

Calcofluor White

In line with previous works, cell walls of both of our *Chlorella* species stained Calcofluor White (CFW) positive, throughout (Table 4) (Kloareg, Quatrano and Marine, 1987; Reinecke *et al.*, 2018). This is a clear indication for the presence of 1-3-β- or 1-4-β-linked polysaccharides in their cell walls. Our results of *P. kessleri* vary (Table 4). The cell walls of mature cells and coenobia were CFW negative, but daughter cell walls were CFW positive. Additionally, cell wall debris and intra-coenobial autospores with readily formed cell walls were positive (Figure 9). This indicates the presence of β-linked polysaccharides in *P. kessleri* cell walls. These are CFW accessible during the early cell wall development, such as in autospores and daughter cells, as well as in cell wall debris. During the maturation process, the cell wall structure and composition changes and the polysaccharides become inaccessible for the CFW. Yamamoto reported an increase in hemicellulose and thickness of the maturing daughter cell wall (Yamamoto, Kurihara and Kawano, 2005). A comparable increase in hemicellulose fraction over time was found by Takeda and Hirowaka for *C. ellipsoidea* IAM C-27 (now: *Chlorella vulgaris* Beijerinck NIES-2170 (Hatano *et al.*, 1992)) (Takeda and Hirokawa, 1978).

Moreover, the intra-coenobial immature autospores were CFW negative (Figure 9, green arrows). This is in line with the results of Yamamoto and co-workers, stating that *P. kessleri* belongs to the "late type" of autospore cell wall synthesis (Figure 4) (Yamamoto, Kurihara and Kawano, 2005). Additionally, we found an increasing permeability of coenobial cell wall for CFW during their maturation. The coenobia were impermeable before autospore formation, but positive staining results for intra-coenobial ripe autospores indicate a cell wall weakening prior daughter cell release.

Ruthenium Red

Ruthenium Red (RR) dye, a hexavalent cation, stained the cells of both *Chlorella* species at all cell cycle stages (Table 4). Additionally, it induced

clustering of *C. sorokiniana* cells (Figure 10). Our findings are in line with previous works, showing that RR can stain uronic acids in *Chlorella* cell walls (Pieper *et al.*, 2012; Reinecke *et al.*, 2018). Additionally, we found that RR could penetrate the cell wall and stain cell content, except in daughter cells of *C. vulgaris* (Figure 10).

The cell walls of *P. kessleri* remained RR negative at all life cycle stages. But a RR positive region was located on the outer surface of the plasma membrane (Yamamoto, Kurihara and Kawano, 2005; Baudelet *et al.*, 2017). This region might cause a weak RR staining, but we could not produce a clear positive result (Figure 11).

One more, the (RR) dye induced clustering during staining of *C. sorokiniana* and *P. kessleri* cells. This could be caused by the cationic nature of RR, influencing the negatively charged cell walls (Shelef and Sukenik, 1984).

Astra Blue

Astra Blue (AB) is mainly used for lignin staining in plant materials (Kraus *et al.*, 1998; Vazquez-Cooz and Meyer, 2002; Montiel *et al.*, 2007), and secondly for staining of glycosaminoglycans (GAGs) (Blaies and Williams, 1981). GAGs are negatively charge polysaccharides due to the presence of sulphate ester and/or carboxyl groups of uronic acids (Song, Shang and Ratner, 2012). They consist of disaccharide building blocks with at least one deoxyamino sugar residue (e.g. N-acetylglucosamine). The presence of GAGs in *Chlorella* cell walls was confirmed by Kapaun and Reisser (Kapaun and Reisser, 1995). In line, AB stained the cell walls of our three *Chlorellaceae* strains at all life cycle stages (Table 4). Cell wall debris and dead cells were AB positive, too. The latter might be caused by unspecific binding of AB to negatively charged cell components.

Safranin

Safranin (S) is commonly used as a counter stain to AB, as it stains lignin in plant cell walls (Vazquez-Cooz and Meyer, 2002). In a first approach, we evaluated its suitability for the staining of Chlorophyta cell walls, by direct application without previous AB staining. First trials resulted in clustering and S negative cells in our three strains, throughout (Table 4). The cells of *P. kessleri* completely bleached under the standard staining conditions (Figure 13).

In line with Soukup, we modulated particular conditions, such as pH value temperature and incubation times (Soukup, 2014). We gained positive staining results for *C. vulgaris* and *P. kessleri* after the washing step was altered to water instead of ethanol/hydrochloric acid. Yet, *C. vulgaris* cells were unspecific stained throughout the entire life cycle, including dead cells and cell wall debris (Figure 14). *C. sorokiniana* cells remained S negative throughout, but clustered, as did the other species. This might be caused by S influencing the negatively charged cell walls (Shelef and Sukenik, 1984). In *P. kessleri* only young daughter cells and autospores stained S positive (Figure 14).

According to Shephard and Mitchell, S can be used for the GAGs staining like the AB (Shepard and Mitchell, 1976). This cross-reactivity might explain the S positive staining results in *C. vulgaris* and *P. kessleri*. While the negative result for *C. sorokiniana* indicate further differences in the cell wall composition, such as lower amount or less accessible uronic acid residues in the cell walls.

Combined Astra Blue and Safranin

Sequential AB-S staining was tested on our algal strains as described in chapter 2.2.2. Again, the cells of *P.* kessleri bleached in the standard ethanol-HCl washing step and water was used instead. *C. sorokiniana* clustered, as it did in S dye alone, but showed negative results for sequential staining (Figure 15). Interestingly, in *C. vulgaris* the mature and

coenobial cells were negative for sequential staining, but the cell wall debris were purple colored. This indicates that both dyes are overlapping. After the cell wall rupture, the AB can bind to the interior cell wall resulting in positive results for the cell wall debris. However, since S alone was washed away in our previous approach, we assume that either the binding of S to its target is weaker than of AB, or both dyes are binding to the same target, which causes steric hindrance. This is a clear indication for the presence of uronic acids and the late increase in covering hemicellulose in the cell wall of *C. vulgaris*.

In *P. kessleri* sequential staining showed similar results than S alone. As mentioned, AB staining of *P. kessleri* showed weak positive results, which can now be overlayed by stronger S staining.

Summarizing we can conclude that *C. sorokiniana* daughter cell walls are stained by a protein specific dye (EB), indicating the presence of extracellular proteins (e.g. Autolysin) at this life cycle stage. The presence of 1-3-β- or 1-4-β-linked polysaccharides in the cell walls was confirmed by CFW staining throughout the entire life cycle. Likewise, uronic acids, likely as part of GAGs, were indicated by RR and AB staining in all three cell populations.

C. vulgaris viability tests can be conducted with the EB dye. In line with other works, 1-3-β- or 1-4-β-linked polysaccharides were found in the cell wall staining throughout the entire cell cycle. Additionally, uronic acids were confirmed by RR, AB and S in all three cell populations. The S results depended strongly on the applied staining procedure.

The staining behavior of *P. kessleri* differed remarkably to both *Chlorella* species. It was EB negative throughout. Only cell walls of daughter cells, intra-coenobial autospores and debris were CFW positive, indicating the presence of β-linked polysaccharides which become inaccessible for CFW in mature cells. Additionally, *P. kessleri* was AB and S positive, but RR negative. Overall, our findings highlight the strain-specific temporal and spatial susceptibility towards the tested histochemical dyes and the underlying cell walls alterations of these Chlorellaceae.

To confirm our results of the histochemical analyses, a quantitative cell wall monosaccharide analysis of the different populations and strains was performed. Prerequisite was the establishment of a reliable cell disruption procedure.

4.3 Disruption techniques

Three different disruption methods were tested in *C. sorokiniana*, namely sonication (5 and 30 min), manually grinding in liquid nitrogen and hydrolysis in 1 mol/L NaOH. The efficiency was evaluated by automated cell count (Coulter Counter), microscopy, and measurement of cell wall related monosaccharides release after dAIR production.

Sonication is a common disruption method in microalgae (Lee, Lewis and Ashman, 2012; Safi *et al.*, 2014; Ward, Lewis and Green, 2014; de Carvalho *et al.*, 2020). After 30 min treatment, our automated cell count indicated a high degree of cell destruction (Figure 17), and 89 % of the cells stained EB positive (Figure 18). The 5 min treatment yielded just 17 % of EB positive cells. Yet, HPAEC-PAD detected after our dAIR preparation for both treatments almost the same total amount of monosaccharides. These findings indicate that 30 min of sonication were sufficient to disrupt the cell wall, but not to increase the monosaccharide debonding. In comparison, the hydrolysis in 1 mol/L NaOH yielded three-fold more monosaccharides.

The high efficiency of the chemical-based cell disruption was confirmed by the automated cell count, detecting only 19 % intact cells (Figure 20). However, the microscopic observations found no viable cells (Figure 21). Thus, the automated cell count of 19 % was false-positive for clumped cell debris and damaged cells.

The grinding in liquid nitrogen is a common disruption method for plant materials and microalgae (Burden, 2012). In *C. vulgaris* the addition of quartz sand is very efficient (Zheng *et al.*, 2011). Our results obtained in this study for *C. sorokiniana* differ. The microscopic observation found damaged cells, but the monosaccharide release was lower than in the

sonication treatment. Overall, the mechanical methods failed to increase the monosaccharide release prior the dAIR preparation.

Thus, the alkali catalyzed hydrolysis was chosen as a pre-treatment for the monosaccharide analyses, due to its higher monosaccharide release.

4.4 Monosaccharide composition

The results of the monosaccharide compositions were separated into two different fractions according to the existing literature (Baudelet *et al.*, 2017; de Carvalho *et al.*, 2020). To my best knowledge, the monosaccharide composition of these analyzed strains were reported by Takeda only (Takeda, 1988a, 1988b, 1991).

Chlorella sorokiniana 211-8k

The monosaccharide composition of the hemicellulose fraction of *C. sorokiniana* detected in this work differs to the composition reported by Takeda (Takeda, 1988a). Takeda found Gal and Rha (30 % each), Xyl and Man (10 % each), Ara (5 %) and Glc (2 %) and unknown carbohydrates (13 %). Later he reported the presence of 11.9 % uronic acids in the cell walls (Takeda, 1991).

The major hemicellulose component of our strain was Gal (60, 54 and 53 % in daughter, mature and coenobia). Additionally, 22, 28 and 28 % Rha were found in daughter, mature and coenobia, respectively.

The highest fraction of Man was found in daughter cell walls 7.7 % (mature: 4.8 %; coenobia: 4.6 %), and the lowest amount of 3.5 % Xyl (mature: 4.3 %; coenobia: 5.9 %). All life cycle stages are below the fractions found by Takeda. Finally, 1.7, 2.4 and 3.2 % Ara were found in daughter, mature and coenobia, which is again lower than the 5 % found by Takeda.

The results for Glucose are not mentioned in this work, as it was not possible to distinguish between Glc from starch and Glc from cell wall

polysaccharides. Takeda mentioned a small fraction of Glc in the hemicellulose of *C. sorokiniana*. Additionally, he found 13 % of unknown polysaccharides, which could be the later identified uronic acids. However, he mentioned that *C. sorokiniana* was Ruthenium Red negative, what contradicts the presence of high amounts of uronic acids (Pieper *et al.*, 2012). The recalcitrance fraction consisted of GlcN (for daughters) and GlcN + GlcA (for mature and coenobia). The existence of GlcN was also reported by Takeda.

The differences could be due to the technical evolution of detection methods. Additionally, as mentioned earlier, the cell wall composition differs, depending on the growth conditions (Liang, Sarkany and Cui, 2009; Safi *et al.*, 2014). Takeda used a 5 cm thick flat vessel system with 8 L of media, 16 : 8 h light:dark regimen with a light intensity of 276 µmol m^{-2} s^{-1} (Takeda and Hirokawa, 1979). The differences in the cultivation could cause the different cell wall monosaccharide compositions as various robust cell wall types were naturally selected.

The total monosaccharide composition (Figure 25), i.e. the combination of hemicellulose and recalcitrance cell wall, was not shown by Takeda. In our strain, the three main monosaccharides were Gal, GlcN and Rha throughout the entire life cycle.

GlcN is especially present in daughter cell walls (38 ± 7 %), while only 17 ± 2.8 % were found in mature cells. This is most likely caused by an increase in hemicellulose fraction, instead of decrease in recalcitrance cell wall, which was also reported for *Chlorella ellipsoidea* IAM C-27 (now: *Chlorella vulgaris* Beijerinck NIES-2170) (Takeda and Hirokawa, 1978). Additionally, this is supported by the fact that a total of 0.2 ± 0.01 g monosaccharides per g biomass before hydrolyzation were found in daughter cells, while mature cells showed 0.5± 0.15 g/g and coenobia 0.4 ± 0.05 g/g (Appendix, Figure 38). However, the amount of GlcN was almost constant throughout (0.08 ± 0.01, 0.08 ± 0.01 and 0.09 ± 0.001 g/g in daughter cells, mature cells and coenobia, respectively (Appendix, Figure 38)).

In line with the positive CFW results, this could indicate that GlcN is a part of 1,3-β- or 1,4-β-linked polysaccharides, as there were no CFW intensity differences detected across the life cycle stages. Most likely GlcN (as N-acetylglucosamine) is part of GAGs, in combination with GlcA. This would be in line with the positive results for RR and AB. According to Kapaun and Reisser, N-acetylglucosamine is degraded to glucosamine during 6 mol/L HCl hydrolysis (Kapaun and Reisser, 1995). We could not detect GlcA in daughter cell walls, which might be caused by technical error. Positive RR and AB staining of daughter cells argues for the presence of uronic acids in the cell wall.

The hemicellulose fraction is most likely based on polysaccharides with Gal-Rha backbones but there is no reliable histochemical method present to identify hemicellulose. This gap can be filled by specific antibodies against polysaccharides (Soukup, 2014), which would provide very important information about the hemicellulose composition *in-vivo*.

Chlorella vulgaris 211-11b

Takeda reported a hemicellulose fraction of *Chlorella vulgaris* 211-11b consisting of Glc (45 %), Rha (20 %), Gal and Xyl (10 % each) and minor amounts of Ara and Man (Takeda, 1991).

As mentioned before, the results for Glc are not considered in this work. Contrary to Takeda, our detected amount of Gal was higher than the amount of Rha throughout the entire life cycle (daughter 40 ± 5.5 %, 34 ± 4.3 % Gal and Rha, respectively; mature 43 ± 6.1 %, 33 ± 6.6 % Gal and Rha, respectively; coenobia 38 ± 5.1 %, 33 ± 2.4 % Gal and Rha, respectively; Figure 26). Additionally, the proportion of Xyl was much lower in this work (< 5 % in all life cycle stages). Almost the same amounts of Ara and Man were found throughout, which is comparable to Takeda. Finally, 5.6 ± 1, 5.7 ± 0.7 and 7.2 ± 1.4 % GlcA were found in young daughters, mature cells and coenobia, respectively, which was to our best knowledge not mentioned by Takeda.

The recalcitrance cell wall consisted mainly of GlcN throughout, which is in line with the taxonomical classification by Takeda (Takeda, 1991). GlcA was the second component of the recalcitrance fraction. The presence of GlcA most likely corresponds to the positive results for RR (in line with (Takeda, 1991)), AB and S, as mentioned above.

When the total cell wall composition is considered, daughters contained less GlcN than mature cells and coenobia (18 ± 5.5, 24 ± 6.3 and 35 ± 0.5 %, respectively, Figure 28). However, the proportions, as well as the total amounts of Rha, Gal and Ara decreased during maturation (Figure 28 and Appendix, Figure 39). This could indicate the contrary to previously explained for *C. sorokiniana* and previously reported for *Chlorella ellipsoidea* IAM C-27 (now: *Chlorella vulgaris* Beijerinck NIES-2170) (Takeda and Hirokawa, 1979)

Our data suggest an increase in recalcitrance components in the cell walls over time, while the amount of hemicellulose related monosaccharides decreases. Consequently, *C. vulgaris* develops more robust cell walls, as the cells age.

This is comparable to the findings of Corre and co-workers. They found for *Chlorella vulgaris* fo. *tertia* (Fott and Novakova (CCAP 211/8k), now: *Chlorella vulgaris* fo. *tertia* CCAP 211/11D similar to *Chlorella sorokiniana* UTEX 261) that the cells become more resistant to detergents as they aged. Algaenan is mentioned as the main reason for the rigidity (Corre, Templier and Largeau, 1996). The existence of algaenan, a highly aliphatic structure found in many different independent algal species, consisting of C30 – 40 mono - or di - unsaturated ω - hydroxy fatty acids that are linked to one another by ether, ester, and glycosidic bonds (Blokker *et al.*, 1998; Burczyk *et al.*, 2014; Alhattab, Kermanshahi-Pour and Brooks, 2019), can neither be confirmed nor disproved in this work. However, the monosaccharide composition evolves towards a more resistant cell wall during the life cycle.

The high standard deviations for the amount of released monosaccharides [g/g] are an indication for high diversities within biological replicates of one strain (Appendix, Figure 39). Besides that, the chemical-

based disruption method could as well be insufficient for the rigid cell walls of *C. vulgaris*.

Parachlorella kessleri 211-11g

Takeda reported the hemicellulose fraction of *P. kessleri* 211-11g consisting of Gal (40 %), Rha (30 %), almost equal amounts of Man, Xyl, Ara and Glc (7 % each) and traces of Fuc (2 %). The recalcitrance fraction consisted of GlcN (Takeda, 1991).

In our strain almost equal amounts of Gal and Rha were detected across all life cycle stages (daughter 44 ± 1.3 and 39 ± 1.5 % Gal and Rha, respectively; mature 41 ± 1.1 and 43 ± 2.2 % Gal and Rha, respectively; coenobia 42 ± 1.9 % and 41 ± 1.9 % Gal and Rha, respectively, Figure 29). Slightly higher amounts of Xyl were found in our analysis compared to Takeda (daughter 9.5 ± 1.2 %; mature 10.1 ± 0.5 %; coenobia 9.6 ± 0.7 %). And lower amounts of Man and Ara (< 4 % each, for all life cycle stages).

Interestingly, traces of both uronic acids were detected at all life cycle stages (< 1 %). No indication for Fuc was found, which is contrary to the results reported previously (Takeda, 1991). The recalcitrance cell wall consisted of GlcN (in line with (Takeda, 1991)) and GlcA independent of the life cycle stage (Figure 30).

When both fractions are combined, daughter cells contained the highest amount of GlcN (13.8 ± 1.9 %), while mature cells contained 3.8 ± 1.3 % GlcN (Figure 31). Opposite to this, daughter cells hold the lowest amount of Rha (32 ± 0.4 %; mature 42 ± 2.4 %). Interestingly, the percentage of Gal was almost constant as the cell ages, which is also true for the other components of the cell wall. However, the absolute amounts of Rha, Gal and Xyl increased during maturation (daughter 0.186 ± 0.023, 0.214 ± 0.035 and 0.047 ± 0.014 g/g Rha, Gal and Xyl, respectively: mature 0.347 ± 0.059, 0.311 ± 0.036 and 0.080 ± 0.007 % Rha, Gal and Xyl, respectively (Appendix, Figure 40)).

These results are in line with the positive CFW staining of daughter cell walls and readily formed autospores within the coenobia. As mentioned above, GlcN is most likely a component of 1,3-β- or 1,4-β-linked polysaccharides, which seem to be much more prominent in daughter cell walls, than in mature. However, as it is true for *C. sorokiniana*, it is unlikely that the GlcN containing polysaccharides are degraded over time (which would be energy ineffective (Dunker and Wilhelm, 2018)). More likely, the proportion of hemicellulose, based on a Rha-Gal-containing polysaccharide increases. This is in line with the absolute proportion of monosaccharides [g/g] found in this work (Appendix, Figure 40).

Only traces of uronic acids were found in the cell walls across all cell cycle stages, which explains the RR negativity mentioned above. However, AB stains the cell walls of *P. kessleri*. This either shows that the binding of AB to its negative charged target (most likely the uronic acids) is stronger than RR, or there are differences in the specificity.

One especially important aspect needs to be considered when analyzing the data. The new daughter cell wall synthesis of *Chlorella* begins short after hatching (Němcová and Kalina, 2000; Yamamoto *et al.*, 2004; Baudelet *et al.*, 2017). Consequently, to exactly distinguish between *Chlorella* daughter, mature and coenobia cell walls is almost impossible. For *Parachlorella kessleri* it is not that severe, as the daughter cell wall synthesis begins late (Yamamoto, Kurihara and Kawano, 2005). However, coenobia contain daughter cell walls and coenobia cell walls as well. This explains the increase in GlcN and the decrease in Rha fraction, compared to mature cell walls (Figure 31).

Additionally, when daughter cells were harvested, coenobia cell wall debris were present in the cultures. The cultures were routinely washed with water to remove as much residues as possible, but this procedure is unlikely to result in 100 % success. Thus, the data can be influenced by residues of different life cycle stages. One possible option to improve the purity of each stage would be cell sorting prior harvest. The rather low amounts of coenobia shown during the growth experiments indicate a diversity within

the culture. This could further distort the results. And finally, due to technical issues with the HPAEC-PAD, a large quantity of samples was not considered in the analyses shown above. This leads to unbalanced quantities and a (statistical) evaluation that should be viewed with reservation.

4.5 Autolysin

Based on the monosaccharide analyses and the histochemistry, we supposed an endo-1,3-β-Glucanase activity of the autologous Autolysin from our three strains. Indeed, this specific activity of autologous Autolysin from *C. sorokiniana* and *P. kessleri* was confirmed with the standard kit from Megazyme® (Figure 32). *C. sorokiniana* showed an Autolysin concentration of ~9.9 mU/10^9 cells and *P. kessleri* ~10.9 mU/10^9 cells. This differs to previously reported Autolysin activities of other species. Protease activity was reported for Autolysin from *Chlamydomonas reinhardtii* (Jaenicke and Waffenschmidt, 1981; Kubo *et al.*, 2009). And the Autolysin activity of *Chlorella fusca* (now: *Scenedesmus vacuolatus* SAG 211-8b) was closely related to endo-mannanase activity (Loos and Meindl, 1985).

No cross-activities were found across the three strains, which is in line with previously reported results for autolytic extracts of *P. kessleri* (Araki and Takeda, 1992b) and other species (Schlösser, Sachs and Robinson, 1976; Schlösser, 1981). Araki and Takeda postulated the species specificity of Autolysin as a reliable taxonomic marker in the genus *Chlorella* (Araki and Takeda, 1992b).

We found hints for the activity of autologous Autolysin on coenobia of *C. sorokiniana* (Figure 33). The increase of the cell count to 112 %, after 3 h, and decrease to 100 %, after 24 h, might be caused by the release of premature daughter cells, which failed to mature. Another possible explanation could be cell death caused by sub-optimal conditions during the Autolysin treatment. However, due to the resilience of *Chlorella* it is unlikely that an incubation in MES buffer (20 mmol/L) results in cell death within 24 h. No signs of unusual cell wall degradations were found for daughter and mature cells. This indicates the life cycle specificity of Autolysin, which was also mentioned by other authors (Schlösser, Sachs and Robinson, 1976; Schlösser, 1981). Degradation of coenobia is a natural process during hatching, caused by intracellular Autolysin (Schlösser, 1981). Thus, the microscopic observations of degraded coenobia during Autolysin treatment were no clear indications for the activity of extracellular Autolysin. It would

be interesting to isolate the young daughter cells, released during treatment. This could be done by cell sorting, based on the size differences between coenobia and daughter (Figure 5). Testing their viability or analyzing their cell wall structure, would be a strong indication for or against the activity of extracellular Autolysin. Additionally, there could be more enzymes than the endo-1,3-β-Glucanase with autolytic activities. Further analyses of the genomic data could present other possible candidates.

Autologous Autolysin from *P. kessleri* showed a strong activity on its coenobia (Figure 36). The cell count during treatment decreased by 20 and 25 % after 4 and 24 h, respectively. This could be caused by degradation of coenobia and release of (premature) daughter cells (Figure 37B). Contrary to *C. sorokiniana*, autospores of *P. kessleri* are not enveloped by a cell wall during autospore synthesis. The cell wall synthesis begins late, after autospore formation (Figure 4) (Yamamoto, Kurihara and Kawano, 2005). This, and the cell number implies that a presumable premature release of daughter cells (without their readily formed cell walls) is most likely resulting in cell death. After 2 and 3 h, ghost cells were visible in the culture. Judging by their cell size, they likely derived by cell wall degradation and leaking of cell content in coenobia and mature cells (Figure 37C/D, purple and turquoise arrows).

Conclusively, our Autolysin results for *C. sorokiniana* and *P. kessleri* deliver interesting options for protoplast formation (formation of cells without their cell walls). Further work is needed to optimize the Autolysin treatment, regarding its temperature and pH-optimum and buffer-system. Additionally, finding optimized conditions that also stabilizes premature daughter cells or mature cells with degraded cell walls would be an important step towards reliable autologous protoplast formation. Premature daughter cells presumably contain weaker cell walls in *C. sorokiniana,* and weaker or even absent cell walls in *P. kessleri*. Stabilizing protoplasts in *Chlorella* is usually achieved with osmotic stabilizers, such as sorbitol (Kumar *et al.*, 2018) or mannitol (Honjoh *et al.*, 2003). A combination of osmotic stabilizers and optimized Autolysin treatment could efficiently open the cell walls for genome engineering.

5 Conclusion and Outlook

Basic histochemical procedures have been applied to three different *Chlorellaceae* cultured under the same, industry-related conditions. The different dyes delivered important insights into the *in-vivo* cell wall composition, as well as they highlighted differences between the species. A detailed cell wall monosaccharide composition analysis at three different life cycle stages (represented by young daughters, mature cells and coenobia) provided another important tool for *in-vitro* cell wall analysis.

The cell walls of *Chlorella sorokiniana* 211-8k change during maturation. Young daughter cells contained higher proportions of recalcitrance cell wall fraction (glucosamine and glucuronic acid) than mature cells. The hemicellulose fraction was most likely based on a galactose and rhamnose containing polysaccharide. The amount of hemicellulose fraction increased, as the cells mature, while the absolute amounts of recalcitrance cell wall remained constant. Calcofluor White staining across all life cycle stages indicated the presence of 1,3-β- or 1,4-β-linked polysaccharides. Additionally, the presence of glucosamine, uronic acids and the positive results of Ruthenium Red and Astra Blue staining indicated glycosaminoglycan in the cell walls.

In contrast, the cell wall of *Chlorella vulgaris* 211-11b becomes more resistant during maturation. The recalcitrance fraction increased, while the hemicellulose fraction decreased. Like *C. sorokiniana*, *C. vulgaris* cells were CFW, RR and AB positive throughout, indicating the presence of similar polysaccharides in the cell wall of both *Chlorella* species. However, the positive results after modified S staining differed to *C. sorokiniana*. They were most likely related to the high amounts of uronic acids detected in the cell wall of *C. vulgaris*.

The cell wall of *Parachlorella kessleri* 211-11g incorporated increasingly hemicellulose components during maturation. This was especially supported by the CFW positive results for young daughter cells and autospores with readily formed cell walls. In contrast, mature cells and coenobia were CFW

negative. However, CFW positive cell wall debris indicated the presence of the β-linked polysaccharides across all life cycle stages. Interestingly, the cells were RR negative, but AB positive, indicating different specificities of the dyes, as well as the presence of other polysaccharides than in *Chlorella*. Additionally, *Parachlorella kessleri* cell walls were less resistant to solvent treatment than C*hlorella*.

The results of the histochemical staining need to be confirmed with more specific staining procedures, like *in-vivo* antibody staining. This would additionally fill the gap of missing hemicellulose specific dyes. These analyses would provide more precise data regarding the polysaccharide composition of the different life cycle stages. Furthermore, linkage-analyses of the cell wall related monosaccharides deepens the knowledge of the polysaccharide structure.

The successful Autolysin extraction of *C. sorokiniana* and *P. kessleri* provided an important step towards reliable autologous protoplast formation. An endo-1,3-β-Glucanase activity was shown for Autolysin of both strains. Future work is needed to examine the optimal conditions for autologous Autolysin digestion, as well as the enzymatic properties of Autolysin. Additionally, an activity comparison of the commercially available endo-1,3-β-D-glucosidase from *Trichoderma sp.* (EC 3.2.1.39, Megazyme®) and the autologous Autolysin on the species cell walls would deliver important information about the existence of other autolytic enzymes. The isolation and stabilization of the presumable premature released daughter cells with weakened or absent cell walls would be an optimal starting point for future work towards protoplast formation and genome editing.

6 Literature

Aach, H. G., Bartsch, S. and Feyen, V. (1978) 'Studies on Chlorella protoplasts - Demonstration of the protoplastic nature and the regeneration of the cell wall', *Planta*, 139(3), pp. 257–260. doi: 10.1007/BF00388638.

Abiusi, F., Wijffels, R. H. and Janssen, M. (2020) 'Oxygen Balanced Mixotrophy under Day-Night Cycles', *ACS Sustainable Chemistry and Engineering*. American Chemical Society, 8(31), pp. 11682–11691. doi: 10.1021/acssuschemeng.0c03216.

Alhattab, M., Kermanshahi-Pour, A. and Brooks, M. S. L. (2019) 'Microalgae disruption techniques for product recovery: influence of cell wall composition', *Journal of Applied Phycology*, pp. 61–88. doi: 10.1007/s10811-018-1560-9.

Araki, N. and Takeda, H. (1992a) 'Purification and properties of a lytic enzyme from the cell wall of Chlorella ellipsoidea C-87', *Physiologia Plantarum*, 85(4), pp. 710–718. doi: 10.1111/j.1399-3054.1992.tb04775.x.

Araki, N. and Takeda, H. (1992b) 'Species-specificity of the lytic activity of the cell wall in the genus Chlorella', *Physiologia Plantarum*, 85(4), pp. 704–709. doi: 10.1111/j.1399-3054.1992.tb04774.x.

Atkinson, A. W., Gunning, B. E. S. and John, P. C. L. (1972) 'Sporopollenin in the cell wall of Chlorella and other algae: Ultrastructure, chemistry, and incorporation of 14C-acetate, studied in synchronous cultures', *Planta*. Springer-Verlag, 107(1), pp. 1–32. doi: 10.1007/BF00398011.

Bachmann (1921) 'Über die Geschwindigkeit der photochemischen Kohlensäurezersetzung in lebenden Zellen', *Naturwissenschaften*, 9(20), pp. 397–398. doi: 10.1007/BF01486468.

Baudelet, P. H. *et al.* (2017) 'A new insight into cell walls of Chlorophyta', *Algal Research*. Elsevier, 25(June), pp. 333–371. doi: 10.1016/j.algal.2017.04.008.

Bišová, K. and Zachleder, V. (2014) 'Cell-cycle regulation in green algae dividing by multiple fission', *Journal of Experimental Botany*, pp. 2585–2602. doi: 10.1093/jxb/ert466.

Blaies, D. M. and Williams, J. F. (1981) 'A simplified method for staining mast cells with astra blue', *Biotechnic and Histochemistry*, 56(2), pp. 91–94. doi: 10.3109/10520298109067288.

Blokker, P. *et al.* (1998) 'Cell wall-specific ω-hydroxy fatty acids in some freshwater green microalgae', *Phytochemistry*, 49(3), pp. 691–695. doi: 10.1016/S0031-9422(98)00229-5.

Blumreisinger, M., Meindl, D. and Loos, E. (1983) 'Cell wall composition of chlorococcal algae', *Phytochemistry*, 22(7), pp. 1603–1604. doi: 10.1016/0031-9422(83)80096-X.

Burczyk, J. *et al.* (2014) 'Polyamines in cell walls of chlorococcalean microalgae', *Zeitschrift fur Naturforschung - Section C Journal of Biosciences*, 69 C(1–2), pp. 75–80. doi: 10.5560/ZNC.2012-0215.

Burden, D. (2012) 'Guide to the Disruption of Biological Samples', *Random Primers*, 25(12), pp. 1–25.

Canelli, G., Murciano Martínez, P., Austin, S., *et al.* (2021) 'Biochemical and Morphological Characterization of Heterotrophic Crypthecodinium cohnii and Chlorella vulgaris Cell Walls', *Journal of Agricultural and Food Chemistry*, 69. doi: 10.1021/acs.jafc.0c05032.

Canelli, G., Murciano Martínez, P., Maude Hauser, B., *et al.* (2021) 'Tailored enzymatic treatment of Chlorella vulgaris cell wall leads to effective disruption while preserving oxidative stability', *Lwt*. Elsevier Ltd, 143(February), p. 111157. doi: 10.1016/j.lwt.2021.111157.

de Carvalho, J. C. *et al.* (2020) 'Microalgal biomass pretreatment for integrated processing into biofuels, food, and feed', *Bioresource Technology*. Elsevier, 300(October 2019), p. 122719. doi: 10.1016/j.biortech.2019.122719.

Champenois, J., Marfaing, H. and Pierre, R. (2014) 'Review of the taxonomic

revision of Chlorella and conseqeunces for its food uses in Europe', *Journal of Applied phycology*, pp. 1845–1851. doi: 10.1007/s10811-014-0431-2.

Cho, H. S. *et al.* (2013) 'Effects of enzymatic hydrolysis on lipid extraction from Chlorella vulgaris', *Renewable Energy*. Elsevier Ltd, 54, pp. 156–160. doi: 10.1016/j.renene.2012.08.031.

Claes, H. (1971) 'Autolyse der Zellwand bei den Gameten yon Chlamydomonas reinhardii', *Archiv für Mikrobiologie*, 78(180–188).

Coelho, D. *et al.* (2019) 'Novel combination of feed enzymes to improve the degradation of Chlorella vulgaris recalcitrant cell wall', *Scientific Reports*, 9(1), pp. 1–11. doi: 10.1038/s41598-019-41775-0.

Conte, M. V. and Pore, R. S. (1973) 'Taxonomic implications of Prototheca and Chlorella cell wall polysaccharide characterization', *Archiv für Mikrobiologie*, 92(3), pp. 227–233. doi: 10.1007/BF00411203.

Converti, A. *et al.* (2009) 'Effect of temperature and nitrogen concentration on the growth and lipid content of Nannochloropsis oculata and Chlorella vulgaris for biodiesel production', *Chemical Engineering and Processing: Process Intensification*, 48(6), pp. 1146–1151. doi: 10.1016/j.cep.2009.03.006.

Corre, G., Templier, J. and Largeau, C. (1996) 'Influence Of Cell Wall Composition On The Resistance Of Two Chlorella Species (Chlorophyta) To Detergents', *Journal of Phycology*, 590(April), pp. 584–590.

Darienko, T. *et al.* (2010) 'Chloroidium, a common terrestrial coccoid green alga previously assigned to Chlorella (Trebouxiophyceae, Chlorophyta)', *European Journal of Phycology*, 45(1), pp. 79–95. doi: 10.1080/09670260903362820.

Daroch, M., Geng, S. and Wang, G. (2013) 'Recent advances in liquid biofuel production from algal feedstocks', *Applied Energy*. Elsevier Ltd, 102, pp. 1371–1381. doi: 10.1016/j.apenergy.2012.07.031.

Dunker, S. and Wilhelm, C. (2018) 'Cell wall structure of coccoid green algae as an important trade-offbetween biotic interference mechanisms and

multidimensional cell growth', *Frontiers in Microbiology*. Frontiers, 9(APR), p. 719. doi: 10.3389/fmicb.2018.00719.

Echeverri, D. *et al.* (2019) 'Microalgae protoplasts isolation and fusion for biotechnology research', *Revista Colombiana de Biotecnología*, 21(1), pp. 71–82. doi: 10.15446/rev.colomb.biote.v21n1.80248.

Foster, C. E., Martin, T. M. and Pauly, M. (2010) 'Comprehensive compositional analysis of plant cell walls (Lignocellulosic biomass) part I: Lignin', *Journal of Visualized Experiments*. MyJoVE Corporation, (37). doi: 10.3791/1745.

Fott, B. and Nováková, M. (1969) 'A monograph of the genus Chlorella. The freshwater species', in Fott, B. (ed.) *Studies in Phycology*. Prague: Academia, pp. 10–74.

Fukada, K., Inoue, T. and Shiraishi, H. (2006) 'A posttranslationally regulated protease, VheA, is involved in the liberation of juveniles from parental spheroids in Volvox carteri', *Plant Cell*, 18(10), pp. 2554–2566. doi: 10.1105/tpc.106.041343.

Gaff, D. F. and Okong'o-ogola, O. (1971) 'The use of non-permeating pigments for testing the survival of cells', *Journal of Experimental Botany*, 22(3), pp. 756–758. doi: 10.1093/jxb/22.3.756.

Gerken, H. G., Donohoe, B. and Knoshaug, E. P. (2013) 'Enzymatic cell wall degradation of Chlorella vulgaris and other microalgae for biofuels production', *Planta*. Springer-Verlag, 237(1), pp. 239–253. doi: 10.1007/s00425-012-1765-0.

Gerlach, D. (1977) *Botanische Mikrotechnik (2. Aufl.)*. Stuttgart: Georg Thieme Verlag.

Gong, Q. *et al.* (2014) 'Effects of light and pH on cell density of Chlorella vulgaris', *Energy Procedia*, 61, pp. 2012–2015. doi: 10.1016/j.egypro.2014.12.064.

Görs, M. *et al.* (2010) 'Quality analysis of commercial Chlorella products used as dietary supplement in human nutrition', *Journal of Applied*

Phycology, 22(3), pp. 265–276. doi: 10.1007/s10811-009-9455-4.

Guiry, M. D. and Guiry, G. M. (2021) *AlgaeBase*, *World-wide electronic publication, National University of Ireland, Galway*. Available at: http://www.algaebase.org (Accessed: 28 July 2021).

Hatano, S. *et al.* (1992) 'Preparation of protoplasts from chiorella ellipsoidea C-27', *Plant and Cell Physiology*, 33(5), pp. 651–655.

Hlavová, M., Vítová, M. and Bišová, K. (2016) 'Synchronization of green algae by light and dark regimes for cell cycle and cell division studies', in *Methods in Molecular Biology*. Humana Press Inc., pp. 3–16. doi: 10.1007/978-1-4939-3142-2_1.

Holdmann, C. *et al.* (2018) 'Keeping the light energy constant — Cultivation of Chlorella sorokiniana at different specific light availabilities and different photoperiods', *Algal Research*, 29(March), pp. 61–70. doi: 10.1016/j.algal.2017.11.005.

Honjoh, K. I. *et al.* (2003) 'Preparation of protoplasts from Chlorella vulgaris K-73122 and cell wall regeneration of protoplasts from C. vulgaris K-73122 and C-27', *Journal of the Faculty of Agriculture, Kyushu University*, 47(2), pp. 257–266.

Huzisige, H. and Ke, B. (1993) 'Dynamics of the history of photosynthesis research', *Photosynthesis Research*, 38(2), pp. 185–209. doi: 10.1007/BF00146418.

Jaenicke, L. and Waffenschmidt, S. (1979) 'Matrix-lysis and release of daughter spheroids in volvox carteri - a proteolytic process', *FEBS Letters*, 107(1), pp. 250–253. doi: 10.1016/0014-5793(79)80507-4.

Jaenicke, L. and Waffenschmidt, S. (1981) 'Liberation of Reproductive Units in Volvox and Chlamydomonas: Proteolytic Processes', *Berichte der Deutschen Botanischen Gesellschaft*, 94(1), pp. 375–386. doi: 10.1111/j.1438-8677.1981.tb03413.x.

Kapaun, E. and Reisser, W. (1995) 'A chitin-like glycan in the cell wall of a Chlorella sp. (Chlorococcales, Chlorophyceae)', *Planta*. Springer-Verlag,

197(4), pp. 577–582. doi: 10.1007/BF00191563.

Khoeyi, Z. A., Seyfabadi, J. and Ramezanpour, Z. (2012) 'Effect of light intensity and photoperiod on biomass and fatty acid composition of the microalgae, Chlorella vulgaris', *Aquaculture International*, 20(1), pp. 41–49. doi: 10.1007/s10499-011-9440-1.

Kloareg, B., Quatrano, R. S. and Marine, D. B. (1987) 'Isolation of Protoplasts from Zygotes of fucus distichus (l.) powell (phaeophyta)', *Plant Science*. Elsevier, 50(3), pp. 189–194. doi: 10.1016/0168-9452(87)90073-2.

Kraus, J. E. *et al.* (1998) 'Astra blue and basic fuchsin double staining of plant materials', *Biotechnic and Histochemistry*, 73(5), pp. 235–243. doi: 10.3109/10520299809141117.

Krienitz, L. *et al.* (2004) 'Phylogenetic relationship of Chlorella and Parachlorella gen. nov. (Chlorophyta, Trebouxiophyceae)', *Phycologia*, 43(5), pp. 529–542. doi: 10.2216/i0031-8884-43-5-529.1.

Kubo, T. *et al.* (2009) 'The chlamydomonas hatching enzyme, sporangin, is expressed in specific phases of the cell cycle and is localized to the flagella of daughter cells within the sporangial cell wall', *Plant and Cell Physiology*, 50(3), pp. 572–583. doi: 10.1093/pcp/pcp016.

Kumar, M. *et al.* (2018) 'Rapid and efficient genetic transformation of the green microalga Chlorella vulgaris', *Journal of Applied Phycology*. Journal of Applied Phycology, 30(3), pp. 1735–1745. doi: 10.1007/s10811-018-1396-3.

Lee, A. K., Lewis, D. M. and Ashman, P. J. (2012) 'Disruption of microalgal cells for the extraction of lipids for biofuels: Processes and specific energy requirements', *Biomass and Bioenergy*. Pergamon, pp. 89–101. doi: 10.1016/j.biombioe.2012.06.034.

Liang, Y., Sarkany, N. and Cui, Y. (2009) 'Biomass and lipid productivities of Chlorella vulgaris under autotrophic, heterotrophic and mixotrophic growth conditions', *Biotechnology Letters*. Springer Netherlands, 31(7), pp.

1043–1049. doi: 10.1007/s10529-009-9975-7.

Loos, E. and Meindl, D. (1982) 'Composition of the cell wall of Chlorella fusca', *Planta*, 156(3), pp. 270–273. doi: 10.1007/BF00393735.

Loos, E. and Meindl, D. (1984) 'Cell wall-lytic activity in Chlorella fusca', *Planta*, 160, pp. 357–362.

Loos, E. and Meindl, D. (1985) 'Cell-wall-bound lytic activity in Chlorella fusca: function and characterization of an endo-mannanase', *Planta*, 166(4), pp. 557–562. doi: 10.1007/BF00391282.

Malavasi, V. *et al.* (2017) 'Deep genomic analysis of the Chlorella sorokiniana SAG 211-8k chloroplast', *European Journal of Phycology*. Taylor & Francis, 52(3), pp. 320–329. doi: 10.1080/09670262.2017.1287959.

Matsuda, Y. *et al.* (1995) 'Purification and characterization of a vegetative lytic enzyme responsible for liberation of daughter cells during the proliferation ofChlamydomonas reinhardtii', *Plant and Cell Physiology*, 36(4), pp. 681–689. doi: 10.1093/oxfordjournals.pcp.a078809.

McCullough, W. and John, P. C. L. (1972) 'A Temporal control of the de novo synthesis of iso- citrate lyase during the cell cycle of the eucaryote ChZorella pyrenoidosa', *Biochimica et Biophysica Acta*, 296, pp. 287–296.

Mercola, J. and Klinghardt, D. (2001) 'Mercury toxicity and systemic elimination agents', *Journal of Nutritional and Environmental Medicine*, 11(1), pp. 53–62. doi: 10.1080/13590840020030267.

Montiel, G. *et al.* (2007) 'Transcription factor Agamous-like 12 from Arabidopsis promotes tissue-like organization and alkaloid biosynthesis in Catharanthus roseus suspension cells', *Metabolic Engineering*, 9(2), pp. 125–132. doi: 10.1016/j.ymben.2006.10.001.

Müller, J. *et al.* (2005) 'Distinction between multiple isolates of Chlorella vulgaris (Chlorophyta, Trebouxiophyceae) and testing for conspecificity using amplified fragment length polymorphism and ITS rDNA sequences', *Journal of Phycology*, 41(6), pp. 1236–1247. doi: 10.1111/j.1529-8817.2005.00134.x.

Muys, M. *et al.* (2019) 'High variability in nutritional value and safety of commercially available Chlorella and Spirulina biomass indicates the need for smart production strategies', *Bioresource Technology*. Elsevier Ltd, 275, pp. 247–257. doi: 10.1016/j.biortech.2018.12.059.

Němcová, Y. and Kalina, T. (2000) 'Cell wall development, microfibril and pyrenoid structure in type strains of Chlorella vulgaris, C. kessleri, C. sorokiniana compared with C. luteoviridis (Trebouxiophyceae, Chlorophyta)', *Algological Studies/Archiv für Hydrobiologie, Supplement Volumes*, 100(March), pp. 95–105. doi: 10.1127/algol_stud/100/2000/95.

Nickelsen, K. (2007) 'Otto Warburg's first approach to photosynthesis', *Photosynthesis Research*, 92(1), pp. 109–120. doi: 10.1007/s11120-007-9163-3.

Pieper, S. *et al.* (2012) 'A new arabinomannan from the cell wall of the chlorococcal algae Chlorella vulgaris', *Carbohydrate Research*. Elsevier Ltd, 352, pp. 166–176. doi: 10.1016/j.carres.2012.02.007.

Reinecke, D. L. *et al.* (2018) 'Polyploid polynuclear consecutive cell-cycle enables large genome-size in Haematococcus pluvialis', *Algal Research*. Elsevier, 33(December 2017), pp. 456–461. doi: 10.1016/j.algal.2018.06.013.

Safi, C. *et al.* (2013) 'Influence of microalgae cell wall characteristics on protein extractability and determination of nitrogen-to-protein conversion factors', *Journal of Applied Phycology*. Springer Netherlands, 25(2), pp. 523–529. doi: 10.1007/s10811-012-9886-1.

Safi, C. *et al.* (2014) 'Morphology, composition, production, processing and applications of Chlorella vulgaris: A review', *Renewable and Sustainable Energy Reviews*, 35(October 2017), pp. 265–278. doi: 10.1016/j.rser.2014.04.007.

Schlösser, U. (1966) 'Enzymatisch gesteuerte Freisetzung von Zoosporen bei Chlamydomonas reinhardii Dangeard in Synchronkultur', *Archiv für Mikrobiologie*, 54(2), pp. 129–159. doi: 10.1007/BF00408711.

Schlösser, U. G. (1981) 'Algal Wall-Degrading Enzymes - Autolysines', in Tanner, W. (ed.) *Plant Carbohydrates II*. Springer-Verlag Berlin Heidelberg, pp. 333–351.

Schlösser, U. G., Sachs, H. and Robinson, D. G. (1976) 'Isolation of protoplasts by means of a "species-specific" autolysine in Chlamydomonas', *Protoplasma*, 88(1), pp. 51–64. doi: 10.1007/BF01280359.

Serra-Maia, R. *et al.* (2016) 'Influence of temperature on Chlorella vulgaris growth and mortality rates in a photobioreactor', *Algal Research*, 18, pp. 352–359. doi: 10.1016/j.algal.2016.06.016.

Shaw, G. (1971) *the Chemistry of Sporopollenin*, *Sporopollenin*. ACADEMIC PRESS INC. doi: 10.1016/b978-0-12-135750-4.50017-1.

Shelef, G. and Sukenik, A. (1984) 'Microalgae Harvesting and Processing : A Literature Review', p. 65. doi: http://dx.doi.org/10.2172/6204677.

Shepard, N. and Mitchell, N. (1976) 'The localization of proteoglycan by light and electron microscopy using Safranin O. A study of epiphyseal cartilage', *Journal of Ultrasructure Research*, 54(3), pp. 451–460. doi: 10.1016/S0022-5320(76)80029-9.

Song, E. H., Shang, J. and Ratner, D. M. (2012) 'Polysaccharides', *Polymer Science: A Comprehensive Reference, 10 Volume Set*, 9, pp. 137–155. doi: 10.1016/B978-0-444-53349-4.00246-6.

Soukup, A. (2014) 'Selected Simple Methods of Plant Cell Wall Histochemistry and Staining for Light Microscopy', *Methods in Molecular Biology*, 1080(August), pp. 67–76. doi: 10.1007/978-1-62703-643-6.

Takeda, H. (1988a) 'Classification of Chlorella strains by cell wall sugar composition', *Phytochemistry*, 27(12), pp. 3823–3826. doi: 10.1016/0031-9422(88)83025-5.

Takeda, H. (1988b) 'Classification of Chlorella Strains by Means of the Sugar Components of the Cell Wall', *Phytochemistry*, 27(12), pp. 3823–3826.

Takeda, H. (1991) 'Sugar Composition of the Cell Wall and the Taxonomy of Chlorella (Chlorophyceae)', *Journal of Phycology*, pp. 224–232. doi:

10.1111/j.0022-3646.1991.00224.x.

Takeda, H. and Hirokawa, T. (1978) 'Studies on the cell wall of Chlorella I. Quantitative changes in cell wall polysaccharides during the cell cycle of Chlorella ellipsoidea', *Plant and Cell Physiology*, 19(5), pp. 591–598. doi: 10.1093/oxfordjournals.pcp.a075894.

Takeda, H. and Hirokawa, T. (1979) 'Studies on the cell wall of chlorella II. Mode of increase of glucosamine in the cell wall during the synchronous growth of chlorella ellipsoidea', *Plant and Cell Physiology*, 20(5), pp. 989–991. doi: 10.1093/oxfordjournals.pcp.a075894.

Vazquez-Cooz, I. and Meyer, R. W. (2002) 'A differential staining method to identify lignified and unlignified tissues', *Biotechnic & Histochemistry*, 77(5–6), pp. 277–282. doi: 10.1080/bih.77.5-6.277.282.

Voiniciuc, C. *et al.* (2019) 'Mechanistic insights from plant heteromannan synthesis in yeast', *Proceedings of the National Academy of Sciences of the United States of America*, 116(2), pp. 522–527. doi: 10.1073/pnas.1814003116.

Ward, A. J., Lewis, D. M. and Green, F. B. (2014) 'Anaerobic digestion of algae biomass: A review', *Algal Research*. Elsevier, 5, pp. 204–214. doi: 10.1016/J.ALGAL.2014.02.001.

Wood, P. J., Fulcher, R. G. and Stone, B. A. (1983) 'Studies on the specificity of interaction of cereal cell wall components with Congo Red and Calcofluor. Specific detection and histochemistry of (1→3),(1→4),-β-D-glucan', *Journal of Cereal Science*. Academic Press Inc. (London) Limited, 1(2), pp. 95–110. doi: 10.1016/S0733-5210(83)80027-7.

Wu, J.-T., Tischner, R. and Lorenzen, H. (1986) 'Semi-circadian Oscillation of Cell Productivity in Synchronous Chlorella Culture', *Biochemie und Physiologie der Pflanzen*. VEB Gustav Fischer Verlag Jena, 181(7), pp. 475–480. doi: 10.1016/s0015-3796(86)80038-5.

Yamada, T. and Sakaguchi, K. (1981) *Protoplast Induction in Chlorella Species*, *Agric. Biol. Chem.*

Yamada, T. and Sakaguchi, K. (1982) 'Comparative studies on Chlorella cell walls: Induction of protoplast formation', *Archives of Microbiology*. Springer-Verlag, 132(1), pp. 10–13. doi: 10.1007/BF00690809.

Yamamoto, M. *et al.* (2003) 'Relationship between presence of a mother cell wall and speciation in the unicellular microalga Nannochloris (Chlorophyta)', *Journal of Phycology*, 39(1), pp. 172–184. doi: 10.1046/j.1529-8817.2003.02052.x.

Yamamoto, M. *et al.* (2004) 'Regeneration and maturation of daughter cell walls in the autospore-forming green alga Chlorella vulgaris (Chlorophyta, Trebouxiophyceae)', *Journal of Plant Research*, 117(4), pp. 257–264. doi: 10.1007/s10265-004-0154-6.

Yamamoto, M., Kurihara, I. and Kawano, S. (2005) 'Late type of daughter cell wall synthesis in one of the Chlorellaceae, Parachlorella kessleri (Chlorophyta, Trebouxiophyceae)', *Planta*. Springer-Verlag, 221(6), pp. 766–775. doi: 10.1007/s00425-005-1486-8.

Yao, L. *et al.* (2018) 'Evans Blue Dye: A Revisit of Its Applications in Biomedicine', *Contrast Media and Molecular Imaging*. doi: 10.1155/2018/7628037.

Zachleder, V. *et al.* (2021) 'Supra-Optimal Temperature: An Efficient Approach for Overaccumulation of Starch in the Green Alga Parachlorella kessleri', *Cells*, 10(7), p. 1806. doi: 10.3390/cells10071806.

Zheng, H. *et al.* (2011) 'Disruption of chlorella vulgaris cells for the release of biodiesel-producing lipids: A comparison of grinding, ultrasonication, bead milling, enzymatic lysis, and microwaves', *Applied Biochemistry and Biotechnology*. Humana Press Inc, 164(7), pp. 1215–1224. doi: 10.1007/s12010-011-9207-1.

Zuorro, A. *et al.* (2019) 'Use of cell wall degrading enzymes to improve the recovery of lipids from Chlorella sorokiniana', *Chemical Engineering Journal*. Elsevier B.V., 377. doi: 10.1016/j.cej.2018.11.023.

7 Appendix

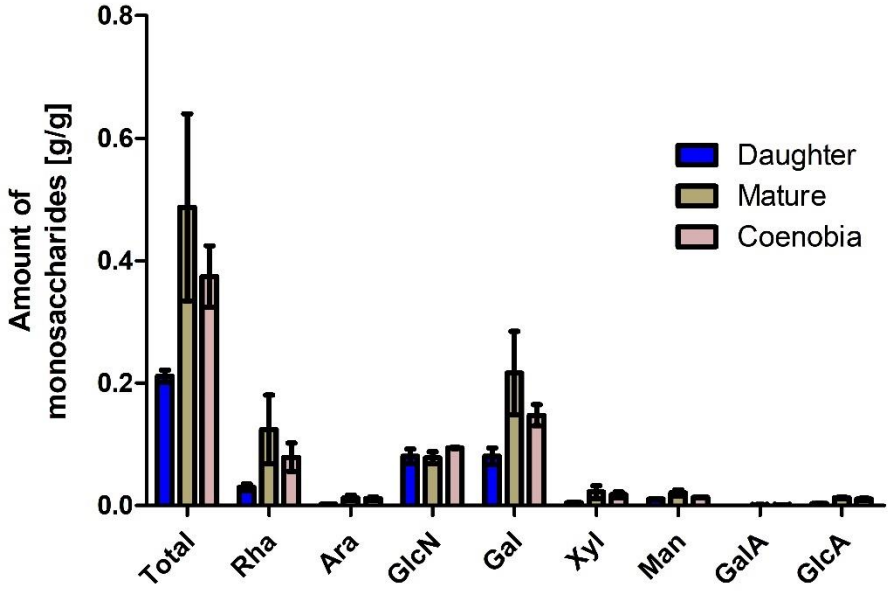

Figure 38: Monosaccharide composition of the cell walls of Chlorella sorokiniana 211-8k. Comparison of daughter (blue), mature (brown) and coenobia (pink) cell walls; amount of monosaccharides in g per g initial biomass prior hydrolyzation; total = sum of the individual monosaccharides; isolation procedure shown in chapter 2.2.7; n = 2 for daughter, n = 3 for mature, n = 2 for coenobia; error bars indicate standard deviation.

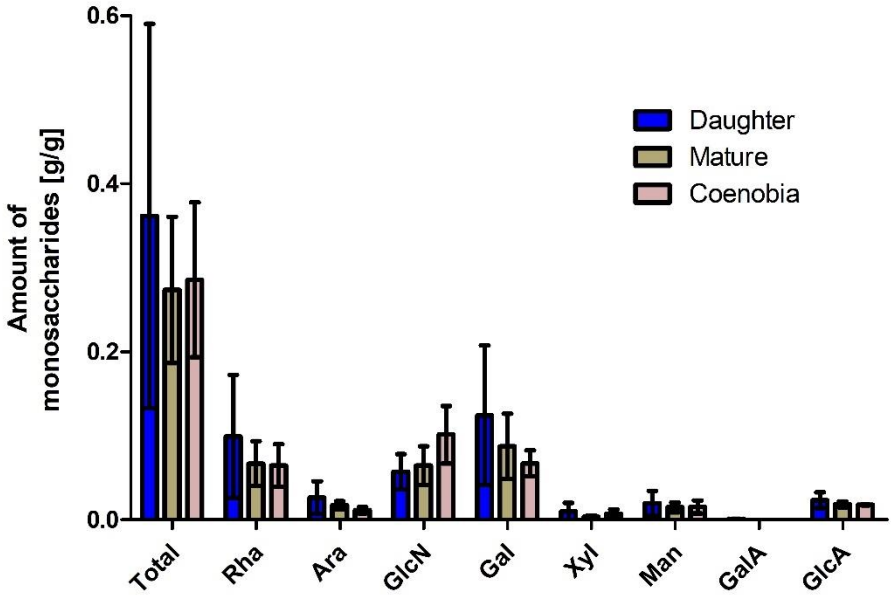

Figure 39: Monosaccharide composition of the cell walls of Chlorella vulgaris 211-11b. Comparison of daughter (blue), mature (brown) and coenobia (pink) cell walls; amount of monosaccharides in g per g initial biomass prior hydrolyzation; total = sum of the individual monosaccharides; isolation procedure shown in chapter 2.2.7; n = 3 for daughter, n = 3 for mature, n = 2 for coenobia; error bars indicate standard deviation.

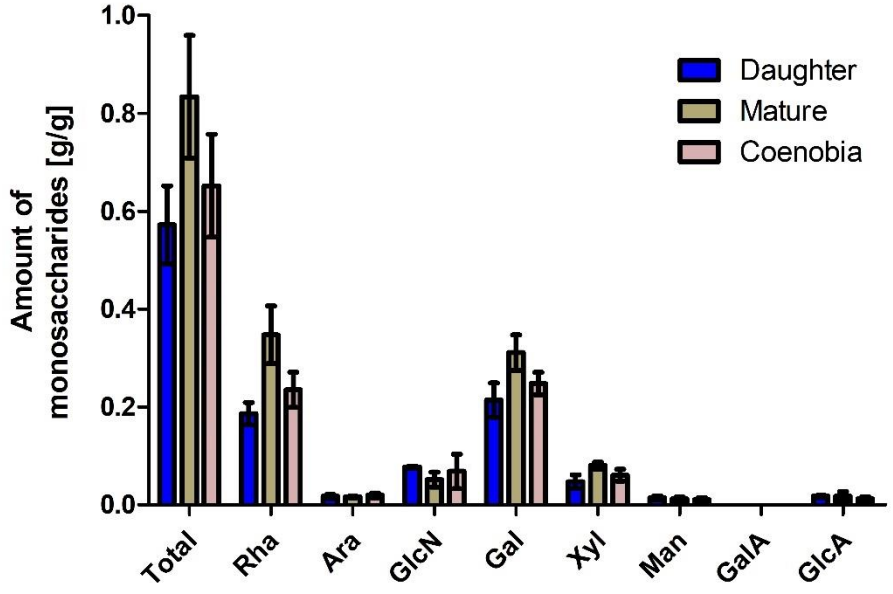

Figure 40: Monosaccharide composition of the cell walls of Parachlorella kessleri 211-11g. Comparison of daughter (blue), mature (brown) and coenobia (pink) cell walls; amount of monosaccharides in g per g initial biomass prior hydrolyzation; total = sum of the individual monosaccharides; isolation procedure shown in chapter 2.2.7; n = 3 for daughter, n = 2 for mature, n = 3 for coenobia; error bars indicate standard deviation.